Durham E-Theses

Radiochemical studies of pine structure in chain yields from neutron-induced fission

John Sellars

"Radiochemical Studies of Fine Structure

in Chain Yields from Neutron-induced Fission"

THESIS

presented in candidature for the degree

of

DOCTOR OF PHILOSOPHY

in the

UNIVERSITY OF DURHAM

by

JOHN SELLARS, B.Sc.(Dunelm).

DEDICATION

To my mother and father

ACKNOWLEDGEMENTS

MEMORANDUM

The work described in this thesis was carried out at the Londonderry Laboratory for Radiochemistry, University of Durham, between October 1963 and December 1964, and at the University of Kent at Canterbury, between January 1965 and May 1967 under the supervision of Dr. S.J. Lyle, Lecturer in Radiochemistry.

This thesis contains the results of some original research by the author; no part of the material offered has previously been submitted by the candidate for a degree in this or any other University. Where use has been made of the results and conclusions of other authors in relevant studies, care has always been taken to ensure that the source of information is clearly indicated, unless it is of such a general nature that indication is impracticable.

ABSTRACT

The cumulative fission yields of several mass
chains have been determined radiochemically relative
to those of mass-99 and -97 for fission of uranium-
238 and thorium-232 induced by both 3- and 14.8-MeV
neutrons. The yields of mass chains 133 and 135
produced in these fissioning systems were calculated
from measurements of xenon-133 and -135. Yields of
mass chains 131 to 134 resulting from 14.8-MeV
neutron-induced fission of uranium-238 were calculated
from measurements of the iodine isotopes in the decay
chains.

An end-window gas-flow β-proportional counter was
used to count the solid sources; gas Geiger-counters
were used to count the xenon samples. Computer
techniques were employed to analyse the decay data.

Fine structure was observed in the mass-yield
curves around masses 133-135 for fission of uranium-
238 at both neutron bombarding energies; it was also
observed for fission of thorium-232 at the lower but
not at the higher excitation energy. The results are
discussed in relation to other relevant experimental
data and theoretical models.

CONTENTS

CHAPTER 1

The Fission Phenomenon

1.1. Introduction

Since the practical feasibility of nuclear
fission was first demonstrated by Hahn and
Strassmann[1] in 1939, much experimental data has been
collected about the many facets of this phenomenon.
As yet, a theory embracing all aspects of fission is
lacking although qualitative explanations have been
proposed for many of the outstanding features.

The most probable fission process is that
resulting in the splitting of a nucleus into two
fragments of comparable mass; divisions into three or
four fragments of comparable mass have been observed,
but the cross-sections for such modes of fission are
several orders of magnitude less than that for binary
fission. The best-established type of ternary fission
is that in which an energetic α-particle is emitted in
coincidence with two heavy fragments; the cross-section
for this process is roughly 2.5×10^{-3} times that for
binary fission[2].

The compound nucleus theory, propounded by Bohr
and Wheeler[3] in 1939 and based on the proposition
that the fission process is independent of the mode of

formation of the excited nucleus, appears to hold for low to moderate excitation energies; the excitation energy is determined by the kinetic energy of the bombarding particle and the binding-energy released when the particle is absorbed into the nucleus. Fission induced by high energy particles cannot be completely described by the compound nucleus theory. It has been demonstrated that, even at moderate excitation energies, angular momentum contributions from the bombarding particle have an appreciable effect on the fission process[4]. At high excitation energies the effect is magnified. Particle-emission before fission and spallation processes, also become feasible at high excitation energies.

Subsequent to the fission process, the initial fragments de-excite by radioactive decay to stable nuclides. The fragments are neutron-rich and, hence, unstable towards neutron-emission and β-emission. Initially the fragments de-excite by neutron-emission[5]; this occurs roughly within 4×10^{-14} seconds of the fission event[6]. The number of neutrons emitted per fission event is normally between two and five. As the excitation energy of the fissioning nucleus is

increased, the number of prompt neutrons emitted increases[7]. As a direct result, the β-decay chains of fragments resulting from high energy fission are shorter than those resulting from low energy fission.

The fragments, after emission of prompt neutrons, de-excite to relatively low-lying nuclear states by γ-emission. Prompt γ-rays are emitted with a half-life of about 1 mμsec[5]; γ-rays of energies up to about 7-MeV have been observed[8]. The resulting nuclides decay mainly by β- and γ-emission to stable nuclides. Delayed neutrons have been observed, these being emitted with half-lives ranging up to one minute; this phenomenon has been attributed to nuclides decaying with appreciable half-lives to excited levels in daughter-products where neutron-emission is energetically feasible.

The energy balance for the fission process may be represented by the equation

$$\substack{A\\Z}M = \substack{A1\\Z1}M^* + \substack{A2\\Z2}M^* + Em$$

where $\substack{A1\\Z1}M^*$ and $\substack{A2\\Z2}M^*$ are the masses of the primary fission fragments produced from a nucleus of mass $\substack{A\\Z}M$; Em is the kinetic energy of the fragments.

The masses of the initial fragments may be represented by

$$_{Z1}^{A1}M^* = {}_{Z1}^{A3}M + \nu.n + \sum_{i=o}^{i=A1+1-A3} E_{(A1-i)} + E_\gamma$$

where $_{Z1}^{A3}M$ is the mass of the fragment remaining after emission of prompt neutrons and prompt γ-rays from the initial fragment $_{Z1}^{A2}M^*$; ν and n are the number of prompt neutrons and the mass of the neutron respectively;

$$\sum_{i=o}^{i = A1 + 1 - A3} E_{(A1 - i)}$$

is the sum of the binding-energies of the neutron to the initial fragment and to the fragments remaining after emission of successive prompt neutrons; E_γ is the prompt γ-ray energy.

Inspection of the energy equation shows that, for a given mass division, there is a range of values for the nuclear charge of the fragments. Measurement of charge distribution is technically difficult because of the short half-lives of the earlier members of the mass chains. Available data support the view that the range of values for the nuclear charge for a given mass is distributed about a certain probable value for the

charge in an approximately Gaussian manner.

For low to moderate excitation energies (i.e. less than 30-MeV), the charge distribution can be described by the Equal Charge Displacement Hypothesis originally proposed by Coryell, Glendenin and Edwards[9]; this postulates that the most probable charges for complementary fragments are equally far removed from the stable charges for the respective fragments.

At high excitation energies, the nuclear charge distribution changes rapidly with energy; the distribution does not conform to the hypothesis of Coryell et al[9]. There is indication that the charge divides in the same ratio as the mass so that the most probable charge is closer to a stable value in the heavy fragment than in the complementary light fragment[10]; a distribution of this nature is known as the Unchanged Charge Distribution. It is observed only at high excitation energies (in the region of 100-MeV or greater) whilst, at intermediate energies, the actual charge distribution cannot adequately be described by either postulate of charge distribution.

As suggested by Fong[11], the actual charge distribution is probably related to the energy equation;

as the masses of the fission fragments are not known, this cannot be checked. With the use of sophisticated techniques, such as measurement of prompt x-rays[12], a more detailed and accurate conception of the effect of excitation energy and nucleon shell-effects on the charge distribution may be realised.

The mass distribution of fission fragments has been investigated for many of the heavier nuclides in the periodic table; variation in mass distribution with excitation energy has also been examined.

A close study of the experimentally-determined mass distributions reveals several prevalent features. One such feature is the more probable division of a nucleus at low excitation energies into two fragments of unequal mass (asymmetric fission) than division into fragments of equal mass (symmetric fission); this is observed in the fission of uranium and heavier elements. As the excitation energy is increased, the probability of symmetric fission relative to asymmetric fission increases. At very high excitation energies, symmetric fission is predominant.

Elements, lighter than uranium but heavier than bismuth, exhibit essentially the same feature in the mass

distributions as those heavier than uranium. Under certain conditions, however, this group of elements displays a type of mass distribution peculiar to the group.

Mass distribution may be represented graphically as fission width (i.e. the probability of a fragment of a given mass being formed) against fragment mass, thus giving rise to the so-called mass-yield curves. Whereas the mass-yield curves of uranium and heavier elements exhibit two maxima, those of the group of elements between bismuth and uranium sometimes exhibit three maxima. Several examples of this type of mass distribution have been reported[13-18], although the majority of systems, in which such a distribution has been observed, are those involving charged particles of moderate energy (tens of MeV). Mass-yield curves exhibiting three maxima resulting from neutron-induced fission are few; evidence for three systems - fission of thorium-232[16] and protactinium-231[17] induced by 14-MeV neutrons and thorium-232[18] by fission-spectrum neutrons - has been reported.

Bismuth and lighter elements can be induced to undergo fission only at very high excitation energies; symmetric fission preponderates. Rhenium is the lightest

element for which a mass distribution has been investigated[19], although fission induced in copper has been observed[20].

The most salient feature of the observed mass distributions is the preferential formation of a particular heavy fragment during fission induced at low excitation energies; this phenomenon appears to be independent of the nature of the fissioning system. The mass ratio for the most probable division increases with the mass of the fissioning nucleus such that the most probable heavy fragment is virtually the same for all systems in which asymmetric fission is clearly discernible from symmetric fission. Only for the heavier nuclei such as fermium-254[21] has a slight shift towards heavier mass been reported.

It is now well-established that, although there is a fairly smooth variation of fission width with mass of the fragment, deviations from such a variation do occur. The more prominent deviations have been observed in mass regions where completed nucleon shells exist (around mass-134 and mass-84) but minor irregularities have been reported in mass regions far-removed from completed nucleon shells.

The best-established mass-yield curve, and
probably the most accurate, is that obtained from
the study of fission of uranium-235 by thermal
neutrons. The most recent investigations of this
system[22,23] report results quoted as being precise
to about one percent. These investigations have shown
that, as well as the irregularities at about mass-134
and mass-84, irregularities occur around masses 90,
100, 138 and 142.

The more prominent irregularities at about mass-134
have been observed for many systems, particularly those
in which fission is induced at low excitation energies.
The collated data on the irregularities will be discussed
in section 1.2. and also in Chapter 7.

In order that a more complete synopsis of the
fission process may be given, a brief mention of the
energy distribution between the initial fission fragments
will be made. Kinetic energy studies and prompt neutron
studies have shown that there is a disproportionate
distribution of excitation energy between the fragments;
the distribution is such that for symmetric divisions
the lighter fragments have the greater share of the
energy whilst, for very asymmetric divisions, the converse
occurs.

Vladimirski[24] has suggested that, during the fission process, the nucleus is unsymmetrically distorted so that the larger lobe tends to remain a constant size because of the energy associated with nucleonic states of high angular momentum. Such a hypothesis could rationalize the unequal energy distribution and also explain the constancy of the most probable heavy fragment.

Although the features discussed previously have been known for many years, a rigorous theory to explain these features has yet to be formulated. Determination of all of the parameters of the energy equation would almost certainly lead to a greater understanding of the fission phenomenon than is now available. It has been suggested that the energy associated with a pair of complementary fragments varies in such a manner that formation of fragments of unequal mass is favoured over fragments of equal mass. Fong[11,25] has developed this theory in analogy with the statistical theory of chemical equilibria.

The theory, developed by Bohr and Wheeler[3] in 1939, was based on a model of the fissioning nucleus behaving as a charged liquid drop; the energy changes associated with deformations were estimated assuming the

nucleus to act in an analogous manner to a charged drop of incompressible liquid. The theory has since been modified to allow for nuclear compressibility and charge distribution[26,27] and also dynamic effects[28,29]. The liquid-drop model, unlike that employed by Fong, does not allow for shell-effects in the mass surface. The liquid-drop theory can explain several features of the fission reaction; its main defect is the inability to rationalize the preference towards asymmetric fission at low excitation energies.

Only a brief outline of the information collected about the fission phenomenon has been proffered in this introduction. Several reviews are available which give more detailed accounts; that by Turner[30] summarizes the theoretical and practical work done prior to 1940; the research conducted during the Second World War is reported in the National Nuclear Energy Series[31]; the reviews by Halpern[32], Walton[33,34] and Hyde[35] report more recent work. There is also a recent review by Fraser and Milton[35a].

1.2. Purpose of this work

Many systems have been investigated in order
to ascertain the degree to which irregularities in
the mass-yield curves deviate from a smooth fission
width to mass relationship.

It has been suggested that, as the excitation
energy of the system is increased, the irregularities
become lessened so that in systems, other than those
endowed with low excitation energies, they are   not
discernible[32]. The results of Wahl[36] support this
view; the values of the fission yields (i.e. the fission
width represented as a fraction of the fission events
producing the pertinent fragment) at masses 131 - 135
resulting from fission of uranium-235 induced by 14-MeV
neutrons suggest that the irregularities in the mass-
yield curve are absent, or if present, occur to a much
lesser extent than those in the mass-yield curve
resulting from fission of the same nucleus induced by
thermal neutrons.

The results of Broom[37], obtained for cumulative
fission yields of masses 131 - 135 from neutron-induced
fission of thorium-232 at 3- and 14-MeV, add support to
this suggestion; the deviation at 14-MeV is less than
that at 3-MeV. The data of Kennett and Thode[38], for

fission induced in thorium-232 by fission-spectrum
neutrons, indicate the presence of irregularities
at masses 84 and 134; the extent of the deviation at
mass-134 is, however, less than that reported by
Broom at 3-MeV. The results of Kennett and Thode are
probably more precise than those of Broom; the former
employed mass-spectrometric techniques whereas the
latter used radiochemical methods.

Radiochemical methods are somewhat limited in
their application to the investigation of such a
phenomenon as the irregularities, or so-called fine
structure, in the mass-yield curves. The limitation is
set by the precision with which the nuclides under
investigation may be quantitatively determined and also
by the reliability with which corrections may be applied
so that cumulative fission-chain yields may be calculated
from experimental data.

The precision of the radiochemical method is
limited by the stability of the detecting equipment and
precision of the analysis of the experimental decay-curves;
the analysis is inherently dependent on the precision of
the half-lives of the components (this is normally only
about 1%) and, where applicable, the reliability with
which a parent-daughter relationship may be calculated.

The calculation of cumulative fission yields
from experimental data necessitates the application
of several correction terms; these are discussed in
detail in Chapter 4. The most critical and perhaps
the least accurately assessed correction terms are those
applied to allow for the independent yields of
succeeding members of the mass chain under investigation.
The correction terms are not normally accessible
experimentally, but rather they are either interpolated
from experimental data or calculated using a charge
distribution hypothesis. Whichever method is used,
uncertainties are introduced although these may be
limited by basing the determination on the later members
of a mass chain so that the corrections are kept small.
Calculation of the corrections to be applied is also
likely to be least reliable in the mass region where
completed nucleon shells exist.

The uncertainties, inherent in a radiochemical
method, may be obviated by employing mass-spectrometric
techniques to determine stable end-products of the mass
chains. Mass-spectrometric methods require quantities
of fission-product many times greater than that required
for radiochemical methods. Accumulation of sufficient
quantities is possible only for systems in which the
nuclide under investigation is fissioning spontaneously

or where long irradiation times are feasible; the latter are restricted to experiments in which a nuclear reactor is used as a source of neutrons.

To date, application of mass-spectrometric methods has revealed irregularities in the mass-yield curve in virtually every system investigated; the only exception is that for fission induced in uranium-233 by fission-spectrum neutrons[39]. The results do not reveal perceptible fine structure; the workers suggest that the uncertainties in their calculations may conceal small deviations but the deviations, if there are any, are minimal. Radiochemical investigation of fission induced in uranium-233 by thermal neutrons indicates the presence of fine structure at mass-133[40].

The greater portion of the data accumulated to date indicates that fine structure is most prominent at mass-134[37,38,41-48]. Evidence for its occurrence at other masses is very limited; there are data to indicate its presence at mass-132[49,50] and mass-133[40,51,52].

Several hypotheses have been postulated in attempts to rationalize the phenomenon of fine structure. That advanced by Glendenin[53] suggests that it is due to abnormal neutron-emission from fragments in which the neutron binding-energy is low due to neutron shell-effects.

The observed effect at about mass-134 would be attributable to the low neutron binding-energy in a nucleus containing 83 neutrons.

Pappas[54] has modified Glendenin's hypothesis; he suggests that the neutron binding-energy in nuclei containing 83, 85, 87 or 89 neutrons is low so that emission of a neutron from such nuclei is feasible.

A hypothesis of abnormal neutron-emission from certain fission fragments due to neutron shell-effects unavoidably predicts fine structure in the prompt neutron distribution curves; such structure was not observed by Stein[55] but the results investigated were of poor resolution. However, the work of Terrell[56] indicates irregularities in prompt neutron distribution curves for several systems.

Wiles and his co-workers[57] suggested that the fine structure may be caused by preferential formation during the fission process of fragments with nuclei in which the neutron binding-energy is high due to neutron shell-effects; nuclides such as tin-132, antimony-133, tellurium-134, iodine-135, xenon-136, caesium-137 and their respective complementary fragments would be expected to have unusually high independent yields. Fine structure, among the fragments complementary to

those of about mass-134, has been observed[23] but Farrar and Tomlinson[58] maintain that this is not conclusive evidence in support of this mechanism. The abnormal yields of tin-132 and antimony-133 from thermal-neutron fission of uranium-235, predicted by the mechanism, were not observed by Strom and his co-workers[59].

The work described in this thesis was directed towards improving and using the method of Silvester[45,60] for the determination of chain yields through radioactive xenon isotopes. The method developed limits the chains that can be investigated to two, namely those having masses 133 and 135. The method, however, ensures high precision in the analysis of the decay-curves and in the correction terms. Both xenon-133 and -135 are near to the end of their respective decay chains and the correction terms applied to account for the independent yields of succeeding members of the mass chains are hence small.

The systems investigated were neutron-induced fission of uranium-238 and thorium-232 at both 3- and 14-MeV. Data for neutron-induced fission of these nuclides have been obtained by mass-spectrometric methods[38,42] (fission-spectrum neutrons) and also by radiochemical

methods[37,45,49] (3- and 14-MeV neutrons). Comparison
of the data obtained in this work with those obtained by
other workers would, it was hoped, yield information
about the nature of the effect giving rise to fine
structure.

Some work was also carried out on the determination
of fission yields by measurement of radioactive iodine
isotopes produced during the fission process; this
work was initiated because of disagreement between
results obtained from measurements based on xenon
isotopes and those obtained by another worker[49] from
measurements based on iodine isotopes.

REFERENCES - CHAPTER 1

1. O. Hahn and F. Strassmann, Nature, 27, 11 (1939).

2. C.B. Fulmer and B.L. Cohen, Phys. Rev., 108, 370 (1957).

3. N. Bohr and J.A. Wheeler, Phys. Rev., 56, 426 (1939).

4. G.P. Ford and R.B. Leachman, Phys. Rev., 137, B826 (1965).

5. V.V. Skliarevskii, D.E. Fomenko and E.P. Stepanov, Soviet Phys. JETP, 5, 220 (1957).

6. J.S. Fraser, Phys. Rev., 88, 536 (1952).

7. B.D. Pate, J.S. Foster and L. Yaffe, Can. J. Chem., 36, 1691 (1958).

8. F.C. Maienschein, R.W. Peelle, W. Zobel and T.A. Love, Proceedings of the Second U.N. International Conference on the Peaceful Uses of Atomic Energy, 15, P/670 (1958).

9. C.D. Coryell, L.E. Glendenin and R.R. Edwards, Phys. Rev., 75, 337 (1949).

10. R.H. Goeckermann and I. Perlman, Phys. Rev., 76, 628 (1949).

11. P. Fong, Phys. Rev., 102, 434 (1956).

12. R.B. Leachman, Proceedings of the Second U.N. International Conference on the Peaceful Uses of Atomic Energy, 15, P/665 (1958).

13. R.C. Jensen and A.W. Fairhall, Phys. Rev., 109, 942 (1958).

14. R.C. Jensen and A.W. Fairhall, Phys. Rev., 118, 771 (1960).

15. R.B. Duffield, R.A. Schmitt and R.A. Sharp, Proceedings of the Second U.N. Conference on the Peaceful Uses of Atomic Energy, 15, P/678 (1958).

16. R. Ganapathy and P.K. Kuroda, J. inorg. nucl. Chem., 28, 2071 (1966).

17. M.G. Brown, S.J. Lyle and G.R. Martin, Radiochimica Acta, 6, 16 (1966).

18. R.H. Iyer, C.K. Mathews, N. Ravindran, K. Rengan, D.V. Singh, M.V. Ramaniah and H.D. Sharma, J. inorg. nucl. Chem., 25, 465 (1963).

19. R.D. Griffioen, Purdue University Thesis (1960). (Reported in reference 35).

20. D.W. Barr, Univ. Calif. Rad. Lab. Report UCRL-3793. (Reported in reference 35).

21. A. Smith, P. Fields, A. Friedman, S. Cox and R. Sjoblom, Proceedings of the Second U.N. International Conference on the Peaceful Uses of Atomic Energy, 15, P/690 (1958).

22. H. Farrar and R.H. Tomlinson, Nuclear Physics, 34, 367 (1962).

23. H. Farrar, H.R. Fickel and R.H. Tomlinson, Can. J. Phys., 40, 1017 (1962).

24. V.V. Vladimirskii, Soviet Phys. JETP, 5, 673 (1957).

25. P. Fong, Bull. Amer. Phys. Soc. Ser. II, 1, 303 (1956).

26. R.D. Hill, Phys. Rev., 98, 1272 (1955).

27. T.A.J. Maris, Phys. Rev., 101, 502 (1956).

28. D.L. Hill, Proceedings of the Second U.N. International Conference on the Peaceful Uses of Atomic Energy, 15, P/660 (1958).

29. D.R. Inglis, Annals of Physics, 5, 106 (1958).

30. L.A. Turner, Rev. Mod. Phys., 12, 1 (1940).

31. Radiochemical Studies: The Fission Products, Books 1-3, (McGraw-Hill Co., New York, 1951).

32. I. Halpern, Ann. Rev. Nuc. Sci., 9, 245 (1959).

33. G.N. Walton, Quart. Rev., 15, 71 (1961).

34. G.N. Walton, Prog. Nuc. Phys., 6, 193 (1957).

35. E.K. Hyde, The Nuclear Properties of the Heavy Elements, Vol. III (Prentice-Hall, 1964).

35a. J.S. Fraser and J.C.D. Milton, Ann. Rev. Nuc. Sci.,
     16, 379 (1966).

36. A.C. Wahl, Phys. Rev., 99, 730 (1955).

37. K.M. Broom, Phys. Rev., 133, B874 (1964).

38. T.J. Kennett and H.G. Thode, Can. J. Phys.,
     35, 969 (1957).

39. W. Fleming, R.H. Tomlinson and H.G. Thode,
     Can. J. Phys., 32, 522 (1954).

40. R. Ganapathy, T. Mo and J.L. Meason,
     J. inorg. nucl. Chem., 29, 257 (1967).

41. H.G. Thode and R.L. Graham, Can. J. Res.,
     25A, 1 (1947).

42. R.K. Wanless and H.G. Thode, Can. J. Phys.,
     33, 541 (1955).

43. H. Menke and G. Herrmann, Radiochimica Acta,
     6, 76 (1966).

44. F.T. Ashizawa and P.K. Kuroda, J. inorg. nucl. Chem.,
     5, 12 (1957).

45. R.H. James, G.R. Martin and D.J. Silvester,
     Radiochimica Acta, 3, 76 (1964).

46. H. Farrar, W.B. Clarke, H.G. Thode and
     R.H. Tomlinson, Can. J. Phys., 42, 2063 (1964).

47. J.W. Harvey, W.B. Clarke, H.G. Thode and
     R.H. Tomlinson, Can. J. Phys., 44, 1011 (1966).

48. J. Macnamara, C.B. Collins and H.G. Thode, Phys. Rev.,
     78, 129 (1950).

49. K.M. Broom, Phys. Rev., 126, 627 (1962).

50. J.L. Meason and P.K. Kuroda, Phys. Rev.,
     142, 691 (1966).

51. H.G. Richter and C.D. Coryell, Phys. Rev.,
     95, 1550 (1954).

52. J.B. Laidler and F. Brown, J. inorg. nucl. Chem.,
     24, 1485 (1962).

53. L.E. Glendenin, Phys. Rev., 75, 337 (1949).

54. A.C. Pappas, Laboratory for Nuclear Science, M.I.T. Technical Report No. 63 (Sept. 1953).

55. W.E. Stein, Phys. Rev., 108, 94 (1957).

56. J. Terrell, Phys. Rev., 127, 880 (1962).

57. D.R. Wiles, B.W. Smith, R. Horsley and H.G. Thode, Can. J. Phys., 31, 419 (1953).

58. H. Farrar and R.H. Tomlinson, Can. J. Phys., 40, 943 (1962).

59. P.O. Strom, D.L. Love, A.E. Greendale, A.A. Delucchi, D. Sam and N.E. Ballou, Phys. Rev., 144, 984 (1966).

60. D.J. Silvester, Ph.D. Thesis (Durham University, 1958).

CHAPTER 2

Experimental Techniques

2.1. Introduction

Radiochemical methods of determining absolute fission yields are subject to several limitations dependent essentially on the nature of the fission product under investigation. Restrictions imposed on a particular method result from sources of error inherent in the method; these are listed below.

(i) Errors may arise from fluctuations in the rate at which the target nuclide undergoes fission.

(ii) Systematic errors can result from the methods employed to quantitatively determine the fission product.

(iii) Inaccuracies in corrections are introduced by virtue of the nature of the distribution of members of the mass chain under investigation at the instant of fission.

Early radiochemical measurements of fission yields had uncertainties of 10% or more due mainly to instabilities in the equipment with which fission products were quantitatively determined and lack of reliable and detailed knowledge of the decay schemes. However, sophisticated techniques in conjunction with more intense sources of particles with which to induce

fission have permitted the reduction of errors in relative measurements to about 3-5%.

The techniques employed in this work were devised so as to reduce methodical uncertainties in relative measurements to a minimum, a limit of ~5% being set mainly by uncertainties in the analyses of decay curves; all other sources of uncertainty were estimated to be negligible by comparison.

Before an irradiation, a sample of the target nuclide was purified from daughter products when contamination of some fission products by daughter products was feasible. The sample in the form of a compressed pellet of either a nitrate or hydroxide compound was irradiated with neutrons produced using either a linear accelerator of the Cockcroft-Walton type (at the University of Durham) or an electrostatic accelerator (at the University of Kent at Canterbury). Throughout the irradiation the neutron flux was monitored; this enabled corrections to be made to account for changes in the fission rate within the sample.

Isolation of fission products was performed by virtue of differences in chemical and physical properties, the target sample being dissolved in the presence of known amounts of isotopic carriers to

facilitate this operation. Isotopic exchange between the inactive carriers and the fission products was ensured by well-tested procedures. Isolation methods were based on modified published radiochemical procedures.

In order to correlate results obtained with those of other workers, the yields of fission products were determined, where possible, relative to two reference nuclides; zirconium-97 and molybdenum-99.

Two radiometric methods were employed to determine the fission products under investigation; solid sources were counted using a calibrated end-window gas-flow β-proportional counter and gaseous samples using a calibrated Geiger-counter in which the sample constituted part of the filling. The counters do not specifically determine the isotope under observation, but as extensive information on the isolated radioactive isotopes was available there was normally no doubt about the genetics of the measured activities.

2.2. Target Materials

The target samples were prepared from analytical grade chemicals; uranium-238 targets from uranyl nitrate depleted in uranium-235; thorium-232 targets from thorium nitrate; uranium-235 targets, for use in calibration

experiments, from uranyl nitrate of natural isotopic composition.

It has been demonstrated[1] that, of the daughter products occurring in the decay-chain of uranium-238, only radon-222 is a possible source of contamination in xenon yield measurements. Radon is difficult to separate from xenon by conventional procedures due to similarities in their physical properties.

To minimize contamination from this source, the immediate precursor of radon-222 was removed from the target samples. This was effected by co-precipitation of radium-226, with barium sulphate from a solution of uranyl nitrate. Precipitation of uranium from the purified solution with sodium hydroxide or ammonium hydroxide gave samples of the corresponding polyuranate; this was the form in which uranium was irradiated at Durham. Evaporation of the purified solution produced uranyl nitrate hexahydrate crystals, the form in which uranium was irradiated at Canterbury.

The nature of the target sample was determined by the necessity of dissolving it in a closed system after irradiation. A chemical substance was therefore chosen so that after irradiation, dissolution could be easily

and speedily effected with minimal evolution of
gases other than those produced in the fission process.
The target nuclide under investigation was therefore
irradiated as hydrated basic oxide or hydroxide, or
as nitrate.

In order to calibrate the gas Geiger-counters,
encapsulated uranium oxide (UO_3) of natural isotopic
composition was irradiated in a thermal neutron flux.

Loss of fissiogenic gases by diffusion was avoided
by irradiating the target material in the form of a
compressed pellet or, as in the thermal irradiations,
sealed samples.

Preliminary experiments showed that xenon recovered
from systems containing unirradiated uranium samples had
negligible radioactive contamination.

Preliminary experiments failed to reveal any
contamination due to daughters produced naturally in the
decay of thorium-232. However, anomalous experimental
decay curves for radioactive xenon samples from fission
of thorium revealed the presence of radon-222 in some
samples of analytical grade thorium nitrate; this was
presumably due to the presence of thorium-230. The
concentration of thorium-230 would depend on the nature
of the ore from which the thorium was originally extracted.
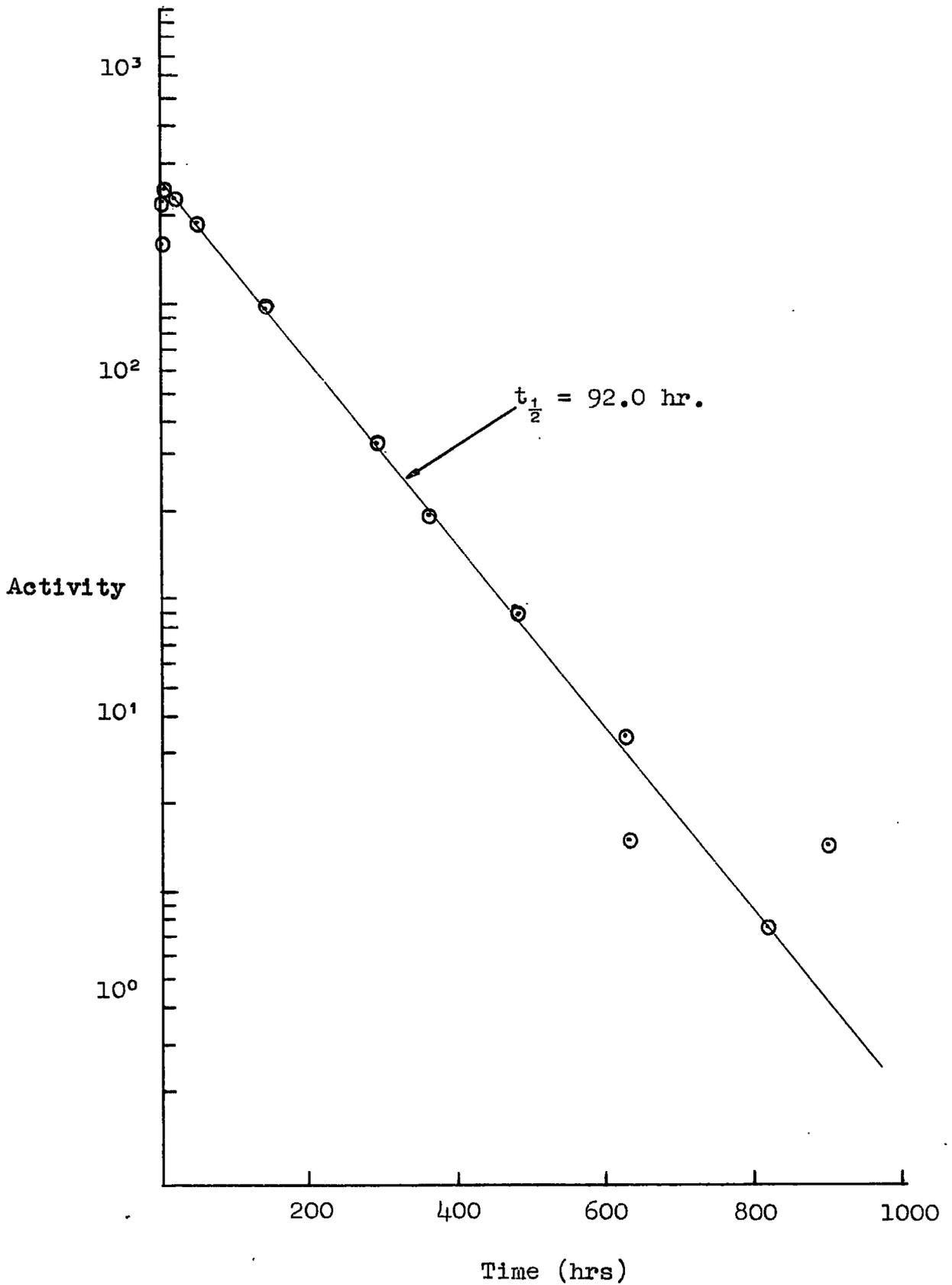
FIG. 2.1. Half-life of contaminant in thorium samples.

Figure 2.1 shows the activity in a xenon sample recovered from a system containing about six grams of unirradiated thorium nitrate; the activity was attributed to radon-222 and its daughter products.

Purification of thorium proved to be more difficult than that of uranium although the same purification procedure was performed in each case. Complete decontamination was not achieved and, as time did not allow for a revision of the purification scheme, target sample weights of thorium were kept to a minimum to limit this source of contamination. Even so, activities due to radon-222 were comparable to those due to xenon-133 produced by neutron-induced fission in thorium samples at 3-MeV.

Because of the similar half-lives of radon-222 and xenon-133, analyses of the experimental decay-curves could only be effected by means of computer calculations. With this procedure, uncertainties in the computed values of the activities of xenon-133 were still found to be quite high (about 10%) whereas the uncertainties in the computed values for the activities of xenon-135 were normally about 2%.

2.3. Neutron Sources

The production of the neutron fluxes used in this work was effected using the following nuclear reactions:

$$\begin{matrix}2\\H\\1\end{matrix} + \begin{matrix}3\\H\\1\end{matrix} \longrightarrow \begin{matrix}4\\He\\2\end{matrix} + \begin{matrix}1\\n\\0\end{matrix} \dots Q = 17.6\text{-MeV} \quad (1)$$

for 14-MeV neutrons, and

$$\begin{matrix}2\\H\\1\end{matrix} + \begin{matrix}2\\H\\1\end{matrix} \longrightarrow \begin{matrix}3\\He\\2\end{matrix} + \begin{matrix}1\\n\\0\end{matrix} \dots Q = 3.27\text{-MeV} \quad (2)$$
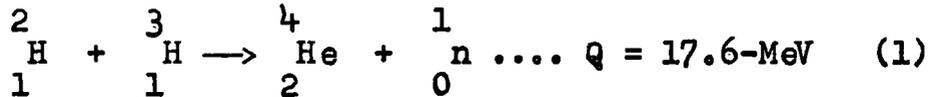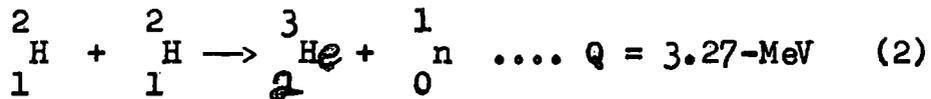
for 3-MeV neutrons.

The excitation function of reaction 1[2] is shown in Figure 2.2. The cross-section for the reaction rises to a resonance peak at about 5 barns for deuterons of about 110-keV incident energy striking the tritium nuclei. At this deuteron energy the neutrons produced are virtually monoenergetic and neutron emission is isotropic in the centre of mass coordinates[3]. The neutron energy is slightly dependent on the angle of emission relative to the incident deuteron beam (see Figure 2.3) but the variation is estimated to be less than 3% for a sample irradiated with 2Π-geometry.

For the second reaction, the excitation function increases with energy but has a value of only 70 milli-barns[4] at 400-keV, this being the maximum deuteron energy obtainable from the linear accelerator employed for
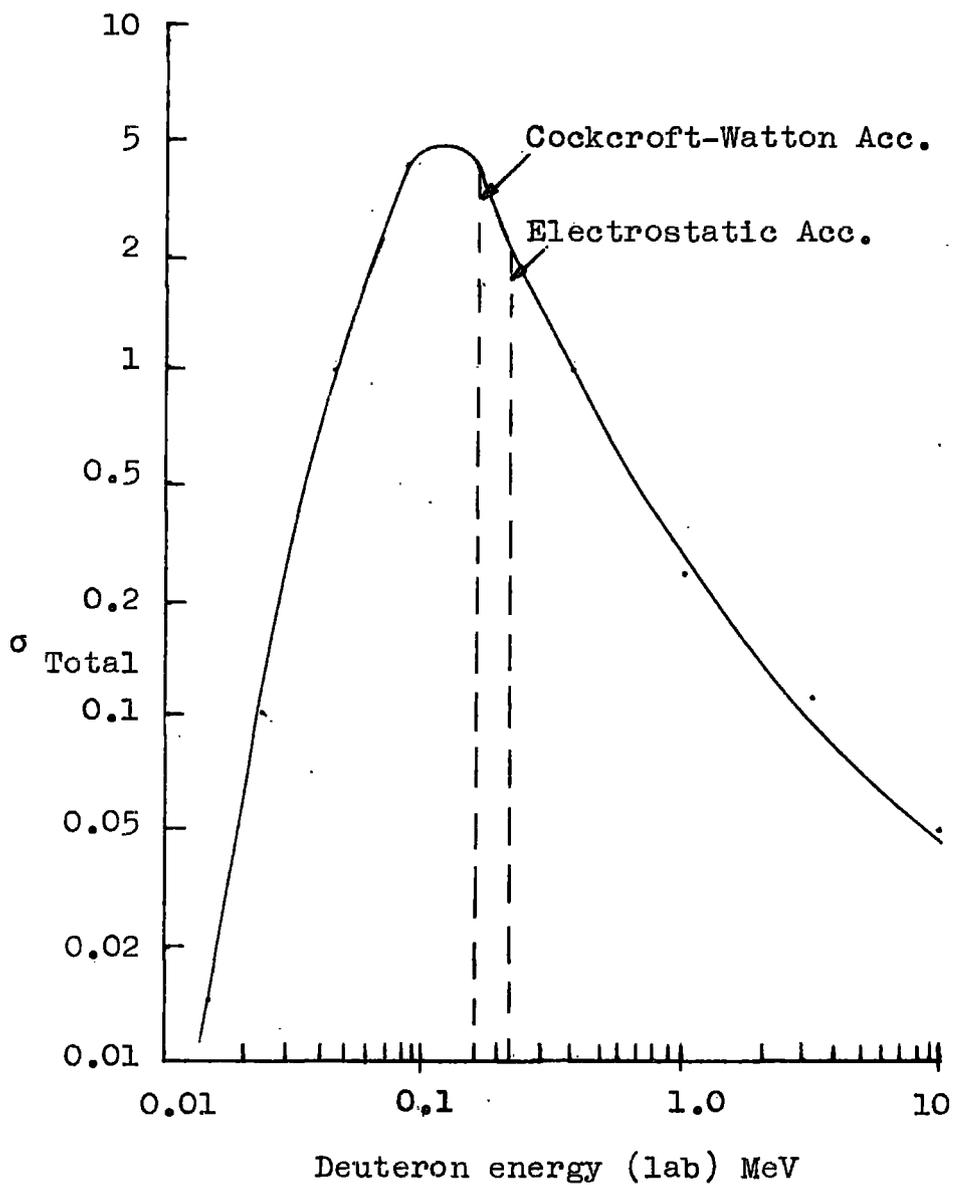
FIG. 2.2. Total cross-section of D,T reaction as a function of deuteron energy.[2]
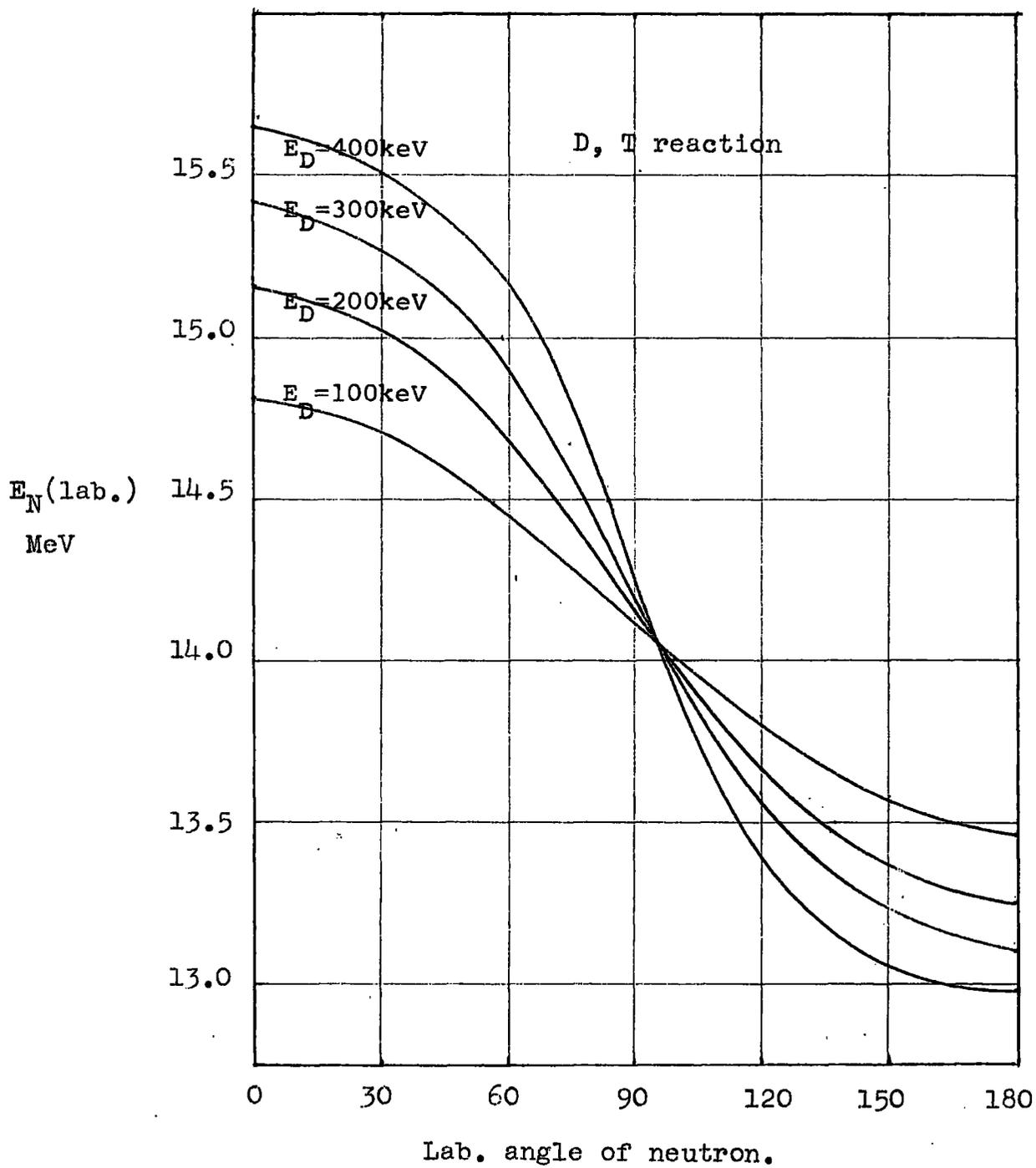
FIG. 2.3.   Neutron energy as a function of angle
of emission.

this investigation. The reaction is anisotropic[5];
neutrons are preferentially emitted in the forward and
backward direction. Variations of neutron energy with
laboratory angle for various incident deuteron energies
are shown in Figure 2.4.

Although the deuterons striking the tritium target
of the accelerator may be regarded as being monoenergetic,
the energy of the deuterons is degraded in penetrating
the tritium target material. The deuterons interacting
with the tritium nuclei have energies from zero up to the
incident deuteron energy. However, due to the resonance
peak in the excitation function, the spread in the
neutron energy is only about 4%.

The energy of neutrons, obtained under normal
irradiation conditions using a S.A.M.E.S. (Société
Anonyme de Machines Électrostatiques) 400 kV "T" type
electrostatic accelerator with an incident deuteron beam
of 200-keV, was estimated to be 14.8 ± 0.4-MeV. A S.A.M.E.S.
machine was used for irradiations carried out at
Canterbury. The Cockroft-Walton accelerator utilised at
Durham was capable of producing 150-keV deuterons which
in turn gave neutrons of energy 14.7 ± 0.2-MeV[6].

The neutrons produced by the second reaction are
not as well-defined as those produced by the first reaction.
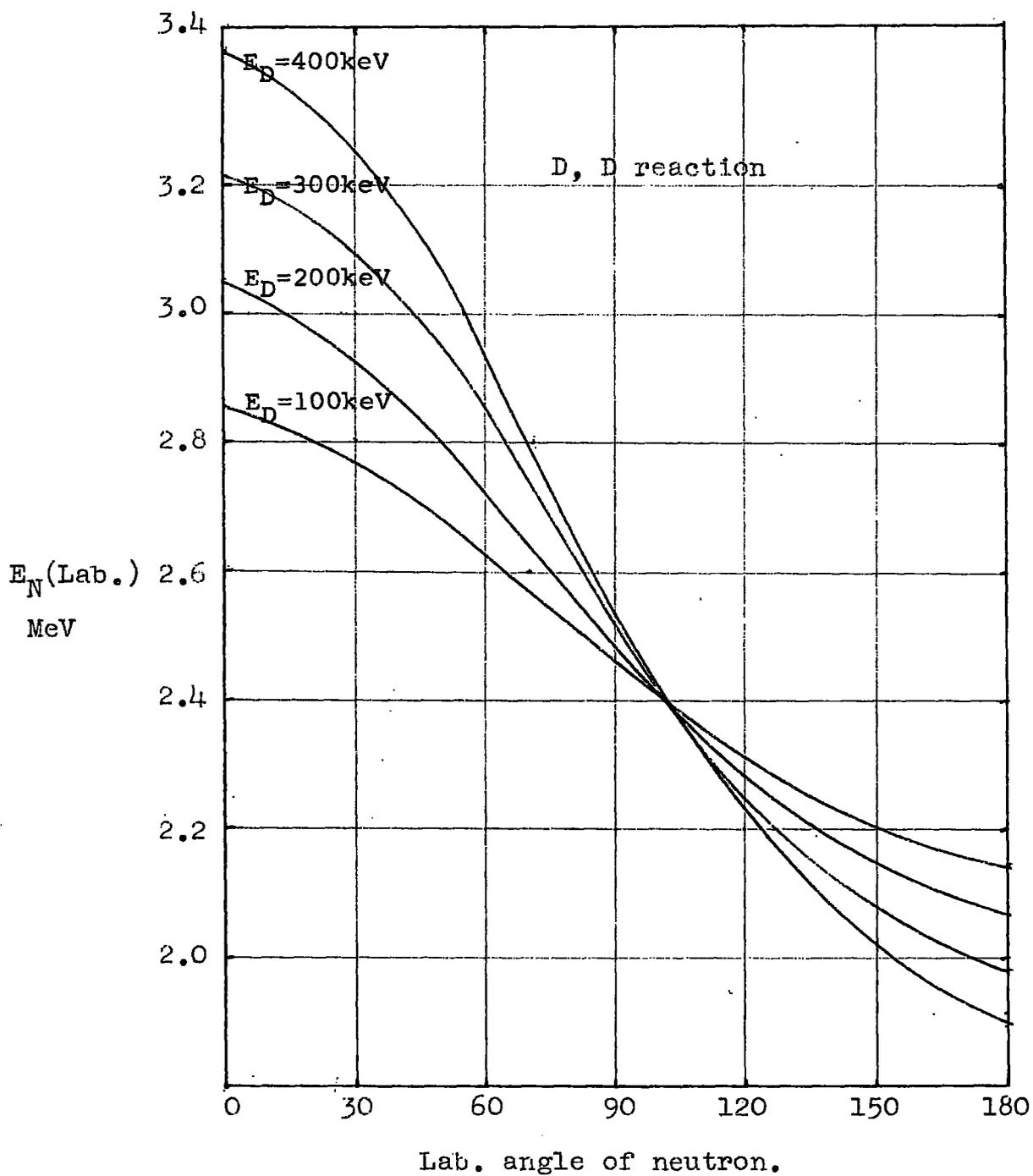
FIG. 2.4. Neutron energy as a function of angle
of emission.

This is due primarily to the lack of a resonance
peak in the excitation function of the second
reaction. The energy of neutrons produced under
normal irradiation conditions using the S.A.M.E.S.
accelerator at Canterbury with an incident deuteron
beam energy of 400-keV has been estimated to be
3.0 ± 0.4-MeV[7].

The fission cross-sections of the nuclides
investigated in this work do not show a significant
variation over the neutron energy limits at either 3-
or 14-MeV. The target samples were therefore positioned
as close as possible to the target of the accelerator so
as to obtain the maximum neutron flux through the sample.

The tritium and deuterium targets, in the form of
tritide and deuteride of titanium, were obtained from
the Radiochemical Centre at Amersham. They consisted of
titanium layers of about 1 mg/cm^2 thickness on a thin
copper backing of 2.5 cm diameter. When loaded with
tritium or deuterium, an atomic ratio of target atoms to
titanium atoms equal to or greater than one is obtained;
this corresponds to a gas concentration of about
0.23 ml/cm^2 of surface area at N.T.P. For convenience
each disc was divided into four segments, which were
bombarded separately.

The target segments were soldered on to water-cooled metal blocks; thermal energy in the range of 200 to 400 watts is dissipated during an irradiation and good thermal contact between the target segment and the metal block is essential to minimize evaporation of target hydrogen atoms.

The target assemblies, used at Canterbury, are illustrated in Figure 2.5; these were situated at the centre of an irradiation chamber in order to reduce the flux of neutrons scattered by surrounding materials. The sample to be irradiated was attached to the end of the target block by rubber bands.

Under normal operating conditions, the S.A.M.E.S. machine produced a deuteron beam current of 600 to 1000 μamps and neutron fluxes from new tritium targets of 10^{10} to 10^{11} neutrons per second. Fluxes of 10^8 to 10^9 neutrons per second were obtainable from new deuterium targets. At Durham, using the Cockcroft-Walton machine neutron fluxes of about 10^9 to 10^{10} neutrons per second were obtained from new tritium targets.

Deuterium inevitably accumulates in the target segment in the course of bombardments. This prolongs the life of the deuterium targets but shortens the useful life of tritium targets due to production of lower-

Deuteron
beam

Copper target
block

Tritium
target

Cooling water

D, T target block

Deuteron
beam

Aluminium
target block

Deuterium
target

Cooling water

D, D target block
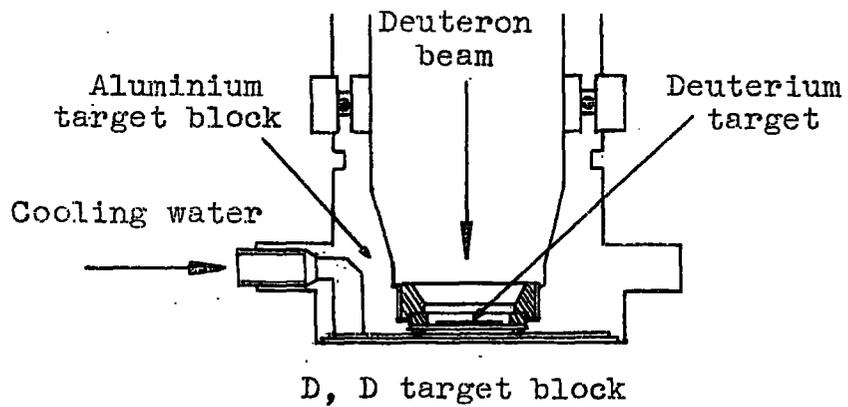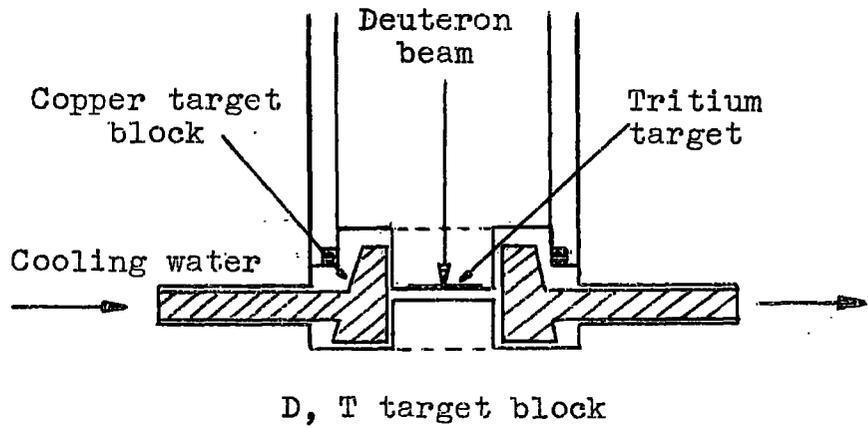
FIG. 2.5. Target assemblies for S.A.M.E.S.
machine.

energy neutrons; this causes a broadening of the
neutron energy spectrum. It was estimated that the
flux of lower energy neutrons due to deuterium in the
tritium targets became appreciable (i.e. about 5% of
the total neutron flux) after about 8000 μamp-hours
and normally the tritium targets were not used after
this life-time.

In the course of an irradiation, the neutron flux
is not constant due to variations in the deuteron beam
current and surface evaporation of target atoms.
Deposition of decomposed pump oil accumulates on the
target segment and this also reduces the neutron flux.

During irradiations the neutron flux was monitored
using a proton-recoil plastic scintillator placed in a
fixed position relative to the source. The discriminator
bias of the scintillation counter was set so that neutrons
of energy lower than those under investigation were not
recorded. Corrections applied to account for variation
in the neutron flux through the target sample are
discussed in Chapter 4.

2.4. Separation Procedures

In this work, fission yields were determined
relative to the two reference nuclides, zirconium-97 and
molybdenum-99. Both nuclides have high fission widths

for the systems under investigation and the half-
lives are suitable as separation procedures were
not normally carried out until about twenty hours
after the end of the irradiations in which the xenon
isotopes were studied. Longer periods between
irradiation and separation occurred when iodine
isotopes were studied; molybdenum-99 only was used as
the reference in this part of the work.

2.4(a). Zirconium

The decay chain of mass-97[8] is set out below.

$$17.0 \text{ hr } {}^{97}Zr \xrightarrow{.94} 60 \text{ sec } {}^{97m}Nb \xrightarrow{} 74 \text{ min } {}^{97}Nb \xrightarrow{} \text{Stable } {}^{97}Mo$$
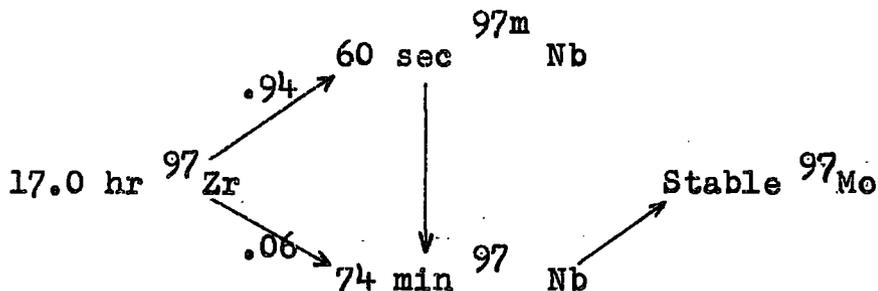
Several other radioactive zirconium isotopes are
produced during the fission process; zirconium-93
(10^6 yr), zirconium-95 (65 d), zirconium-99 (1.6 sec).
Only zirconium-95 was detected in the sources prepared
during this work but the activity attributable to this
nuclide was normally less than 1% of that of zirconium-
97.

Zirconium carrier was prepared as a solution of
zirconyl nitrate in dilute nitric acid. The procedure

of Belcher, Sykes and Tatlow[9] was used to
standardize the solution gravimetrically, the
zirconium being precipitated as the tetramandelate.
The carrier solution was checked about every six months
and, within experimental error, the concentration of
zirconium was found to remain constant.

The method used in the isolation of zirconium from
a fission-product mixture was that described by Hahn
and Skonieczny[10].

Separation method

1.   The irradiated sample was dissolved in 5M nitric
acid solution containing 10 mg amounts of carrier
molybdenum and zirconium; during experiments in which
xenon isotopes were studied, this step was by necessity
carried out in a closed system (the apparatus is
described in detail in section 2.4(d).).

2.   Subsequent to the isolation of the xenon isotopes,
the solution was adjusted to 3M in hydrochloric acid
and 10 ml of 1M mandelic acid solution were added. The
solution was heated for about twenty minutes at 80-90°C
to precipitate zirconium tetramandelate. The precipitate
was separated by centrifugation and the supernate was
further treated to effect isolation of molybdenum.

3.   The precipitate was transferred to a polythene
centrifuge tube with washings of water and dissolved
with 40% hydrofluoric acid.   0.5 ml of lanthanum
nitrate solution (containing 10 mg/ml of lanthanum)
was added and the solution mixed with a polythene rod.
The precipitate of lanthanum fluoride was centrifuged
down.

4.   The lanthanum fluoride precipitation step was
repeated and the supernate remaining after centrifug-
ation was decanted into a clean polythene tube.

5.   1 ml of barium nitrate solution (containing
1 mg/ml of Ba^{2+}) was added to the supernate with
stirring.   The precipitate of barium fluorozirconate
was isolated by centrifugation.

6.   The precipitate was suspended in 2 ml of water and
dissolved by the addition of 1 ml of saturated boric
acid solution and 0.5 ml of 5M nitric acid.   1 ml of
barium nitrate solution was added followed by 1 ml of
40% hydrofluoric acid.   The precipitate of barium fluoro-
zirconate was separated by centrifugation.

7.   Dissolution, precipitation and centrifugation of
barium fluorozirconate was repeated.

8.   The precipitate was then suspended in 2 ml of water
and dissolved by addition of 1 ml of saturated boric

acid solution and 2 ml of 5M hydrochloric acid.
The solution was made alkaline with 6M sodium
hydroxide and the precipitate was separated by
centrifugation and washed with distilled water.

9. The zirconium hydroxide precipitate was
dissolved by addition of a mixture of 3 ml of
concentrated hydrochloric acid and 3 ml of water
and transferred to a glass centrifuge tube with
washings of water to make the solution volume up to
10 ml. 10 ml of 1M mandelic acid solution were added
and the mixture was heated at 80-90°C for twenty
minutes to precipitate zirconium tetramandelate.

10. The precipitate was collected on a glass-fibre
filter disc and washed with 10 ml of 5% mandelic acid-
2% hydrochloric acid solution. The precipitate was
then washed with ethanol and ether, and dried under
vacuum.

2.4(b). Molybdenum

The decay chain for mass-99 is as shown on the
following page[8].

$$10\text{sec} \, ^{99m}\text{Nb} \qquad\qquad 6.0\text{hr} \, ^{99m}\text{Tc}$$

$$\geqslant .50 \qquad\qquad \geqslant .52 \qquad .88$$

$$<1.6\text{sec} \, ^{99}\text{Zr} \qquad\qquad 66.7\text{hr} \, ^{99}\text{Mo} \qquad\qquad \text{stable} \, ^{99}\text{Ru}$$

$$\leqslant .36 \qquad\qquad .12$$

$$2.4\text{min} \, ^{99}\text{Nb} \qquad\qquad 2.1 \times 10^{5}\text{yr} \, ^{99}\text{Tc}$$
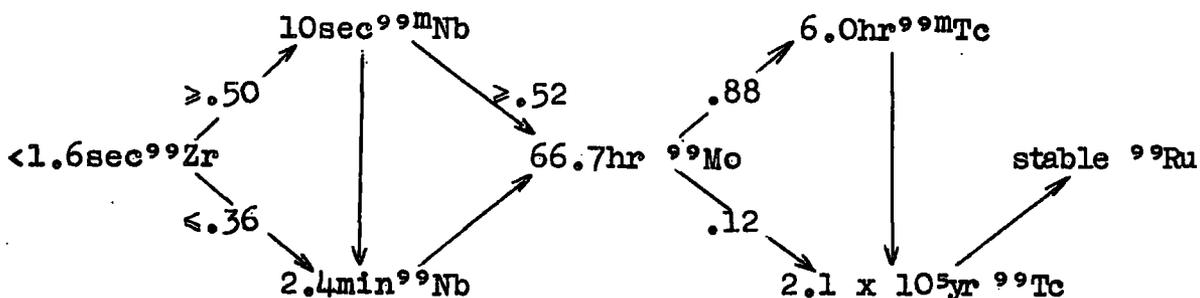
Other radioactive molybdenum isotopes produced during the fission process have short half-lives relative to that of molybdenum-99 and they were not detected in the sources prepared in the course of this work.

A carrier solution of molybdenum was prepared by dissolution of ammonium molybdate in water with addition of dilute hydrochloric acid and sodium bromate. The carrier solution used in the experiments performed to calibrate the gas Geiger-counters required the absence of chloride ions; a solution of molybdenum trioxide in 2M ammonium hydroxide was used for this purpose.

Both solutions were standardized gravimetrically by the method described by Vogel[11], the molybdenum being precipitated as the 8-hydroxyquinolate.

The ammoniacal solution of molybdenum was originally made up by weight and comparison with the gravimetric determination showed agreement to within

1%. The carrier solutions were restandardized about every six months and, within experimental error, the concentration of molybdenum in the solutions remained constant.

The method employed for isolation of molybdenum from bulk fission-products was a modification of that described by Scadden[12].

Separation method

1. The solution of the irradiated sample was adjusted to 1 to 2M in nitric acid and 5 ml of 2% alcoholic solution of α-benzoinoxime were added; precipitation of molybdenum was assumed to be complete after standing for five minutes at room temperature. The precipitate was isolated by centrifugation and washed with 10 ml of 1M nitric acid.

2. The precipitate was dissolved in hot concentrated nitric acid, diluted to about 30 ml with water and adjusted to 1 to 2M in nitric acid by addition of ammonium hydroxide solution. The molybdenum was re-precipitated with α-benzoinoxime. The precipitate was isolated by centrifugation and washed with 1M nitric acid.

3. Step 2 was repeated.

4. The molybdenum α-benzoinoxime complex was filtered through a Whatman No. 42 filter paper. The filter paper and precipitate were placed in a silica crucible and ignited at about 500°C in an electric furnace.

5. The ash remaining after ignition was dissolved in a few drops of concentrated sulphuric acid with warming. The volume was made up to 10 ml with water and the solution was transferred to a 50 ml glass centrifuge tube.

6. 1 ml of iron carrier solution (containing 1 mg/ml of Fe^{3+}) was added and, after stirring, ferric hydroxide was precipitated by the addition of ammonium hydroxide. The bulk of the precipitate was removed by centrifugation and the residual traces by filtration through a glass-fibre filter disc.

7. The solution was made just acid to methyl red with sulphuric acid. 5 ml of 2M ammonium acetate were added and the solution was heated to about 90°C. The molybdenum was precipitated by addition of 3% solution of 8-hydroxyquinoline in dilute acetic acid. Heating was continued until the precipitate coagulated; it was then centrifuged and washed with hot water.

8. The precipitate was collected on a glass-fibre filter disc, washed with hot water, ethanol and ether, and finally dried under vacuum.

2.4(c). Iodine

The decay chains[8], containing the iodine isotopes investigated in this work, are shown on the following page.

Analysis of a decay-curve obtained from a mixture of all of the iodine isotopes was considered to be difficult due to similarities and uncertainties in some half-lives. Under certain conditions, the concentration of some of the isotopes may be reduced to such an extent that the contributions from these isotopes to the total decay curve can be assumed to be negligible. The problem is thereby reduced to carrying out two separate and relatively simple measurements.

By allowing the irradiated sample to decay for about four days following the irradiation, the activity due to iodine-134 and -135 was negligible and the decay-curve obtained from iodine samples isolated after this time was assumed to contain contributions from iodine-131, -132 and -133.

Short "cooling" periods in conjunction with short irradiation times resulted in negligible contributions

131: 23 min ^{131}Sb
.07 → 30 hr ^{131m}Te
.93 → 24.8min ^{131}Te
↓ .19
→ 8.06d ^{131}I
.02 → 12d ^{131m}Xe
.98 → Stable ^{131}Xe
↓
Stable ^{131}Xe

132: 50 sec ^{132}Sn
→ 45 sec ^{132m}Sb
→ 3.1min ^{132}Sb
→ 77.7hr ^{132}Te → 2.28hr ^{132}I
↓
Stable ^{132}Xe

133: 2.6min ^{133}Sb
→ 52 min ^{133m}Te
→ 12.4 min ^{133}Te
↓ .13
→ 20.8hr ^{133}I
.02 → 54.2hr ^{133m}Xe
.98 → 5.27d ^{133}Xe
↓
Stable ^{133}Cs

134: <1.5 sec ^{134}Sb → 43min ^{134}Te → 52.8min ^{134}I → Stable ^{134}Xe

135: ~30 sec ^{135}Te → 6.75 hr ^{135}I
.27 → 15.7min ^{135m}Xe
.73 → 9.16 hr ^{135}Xe
↓
~10^{6}yr ^{135}Cs

from iodine-131 and -132. The decay-curves obtained
under these conditions were analysed for iodine-133, -134
and -135.

A standard carrier solution of iodine was prepared
by dissolving a weighed amount of dried analytical grade
potassium iodide in water. The recovery yield was
determined gravimetrically, the iodine being precipitated
as palladium(II) iodide. It has been demonstrated[13]
that the xenon daughters of radioactive iodine isotopes
are retained   in palladium iodide; the
experimental decay curves were therefore assumed to result
from iodine isotopes and their xenon daughters.

The method used to isolate iodine isotopes from mixed
fission products was based on that described by Meinke[14].

Separation method

1. The sample was dissolved in a dilute solution of
hydrochloric acid containing 10 mg amounts of carrier
molybdenum and iodine; this operation was performed in a
stoppered flask immediately after the end of the
irradiation.

2. The solution was made alkaline by addition of ammonium
hydroxide after adding sufficient tartaric acid to prevent
precipitation of uranium. 2 ml of hypochlorite solution
(2.5% W/v active chlorine) were added and the solution was
boiled to oxidize iodine to periodate. 5 ml of carbon

tetrachloride were added to the cooled solution which was then acidified with about 3 ml concentrated nitric acid. 2 ml of 1M hydroxylamine hydrochloride were then added and the iodine was extracted into the carbon tetrachloride layer; the time of extraction was taken as the time of separation of iodine isotopes from their precursors.

3. The carbon tetrachloride layer was shaken with 5 ml of water containing sulphur dioxide until both phases were colourless.

4. To the aqueous phase, 1 ml of 6M nitric acid and a few drops of 1M sodium nitrite were added. The iodine was extracted into 5 ml of carbon tetrachloride.

5. The extraction procedure was repeated. The carbon tetrachloride layer was shaken with 5 ml of water containing sulphur dioxide until both phases were colourless.

6. The solution was boiled to remove excess sulphur dioxide and iodine was precipitated from the aqueous layer by the addition of palladium(II) chloride solution. After standing for about 5 minutes the precipitate was collected by filtration, washed with water and methanol and then dried in an oven at 120°C.

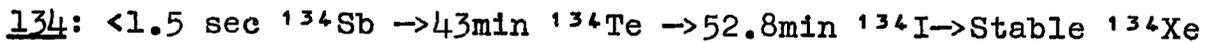The time of precipitation was taken as the zero time for the growth of xenon daughters from iodine precursors in the palladium iodide source.

2.4(d). Xenon

The decay chains[8] of the masses investigated are shown below:
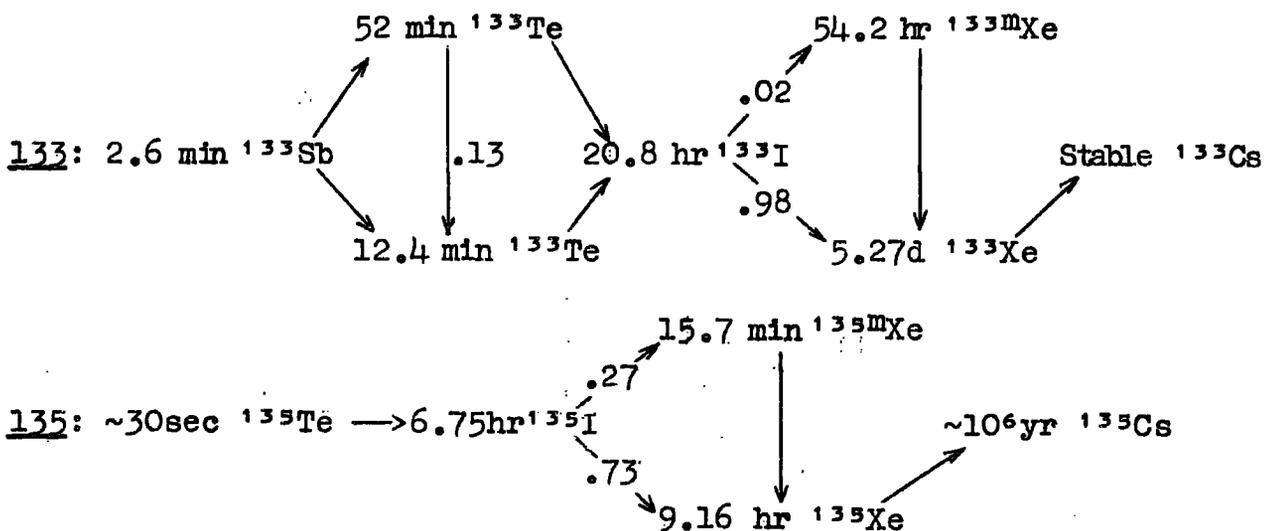
Information has not been found relating to the chemical environment of noble gases resulting from fission. It has been demonstrated, however, that xenon, resulting from β-decay of iodine isotopes chemically bound as iodates or periodates, is retained in appreciable amounts as molecules or ions in which the xenon atom is bonded to several oxygen atoms[15]. It has also been shown that the stability of the oxygen to xenon bond is such that treatment with a reducing agent is required to effect complete removal of xenon from solution[15].

Hall and Walton[16] found that iodine isotopes resulting from fission in the irradiation of uranyl iodate

occurred in several oxidation states. They further demonstrated that each iodine isotope exhibited an oxidation state peculiar to the genetics of the isotope. It would seem probable, therefore, that iodine isotopes resulting from fission induced in elements in chemical combination with oxygen atoms will exhibit a similar behaviour. An iodine isotope in combination with oxygen will decay to xenon with the possibility of a xenon oxide being formed.

At the time when this work was initiated, the information regarding stabilities of oxygenated xenon compounds was not available and no provision was made in the experimental procedure to ensure reduction of potential xenon compounds to elemental xenon. However, an experiment was latterly devised whereby a strong reducing agent (ascorbic acid) was present in the solution of mixed fission products resulting from neutron-induced fission of uranium-238 at 14-MeV; the calculated cumulative fission yields were, within experimental error, in agreement with experiments performed without the reducing agent. This seems to indicate either that there are minimal quantities of oxygenated xenon compounds produced from the iodine precursors, or that the solution of mixed fission products is an effective reducing agent.

Separation method

The vacuum system for isolating the xenon isotopes from bulk fission products is shown in Figure 2.6.

To minimize loss of xenon by diffusion out of the irradiated sample, the target sample was prepared as a compressed pellet. Immediately after the end of the irradiation, the sample was placed in a polythene container and positioned at the top of the dissolver vessel as shown in Figure 2.7.

The lower section of the vessel, containing carrier amounts of molybdenum and zirconium in about 30 ml of 5M nitric acid, was attached to the upper section by means of a B34 cone/socket connection lightly greased with silicone grease.

It ought to be mentioned at this point that in all taps and cone/socket connections in the main vacuum system silicone grease was used. Little difficulty was experienced in cleaning and regreasing operations and the wider working temperature range of silcone grease relative to that of Apiezon grease was the main factor in determining which to employ. Apiezon grease "N" was used only in greasing the taps of the dissolver vessel; complete decontamination was then easily effected by dissolution of the grease in benzene.
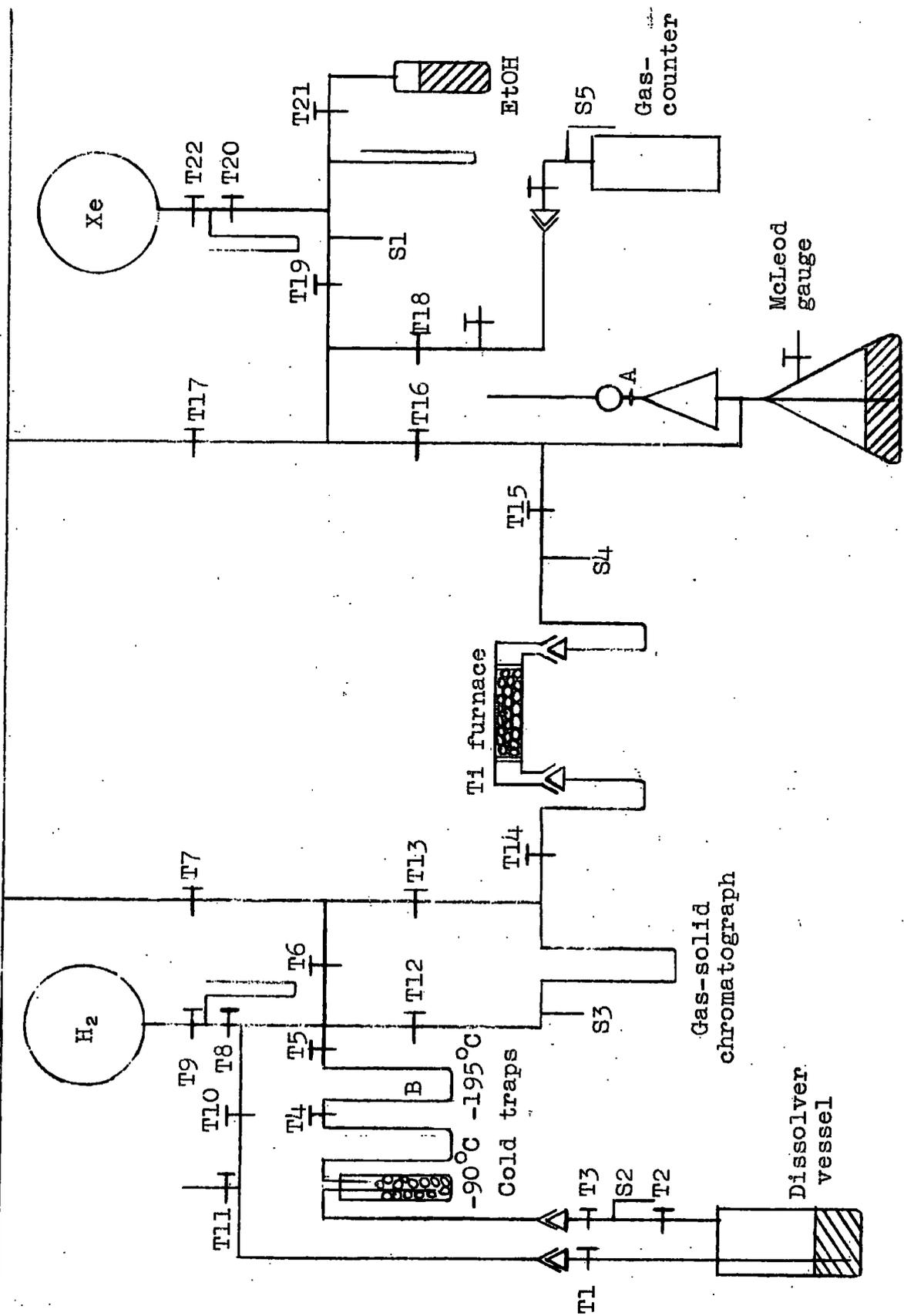
FIG. 2.6. Vacuum system for isolation of xenon isotopes.
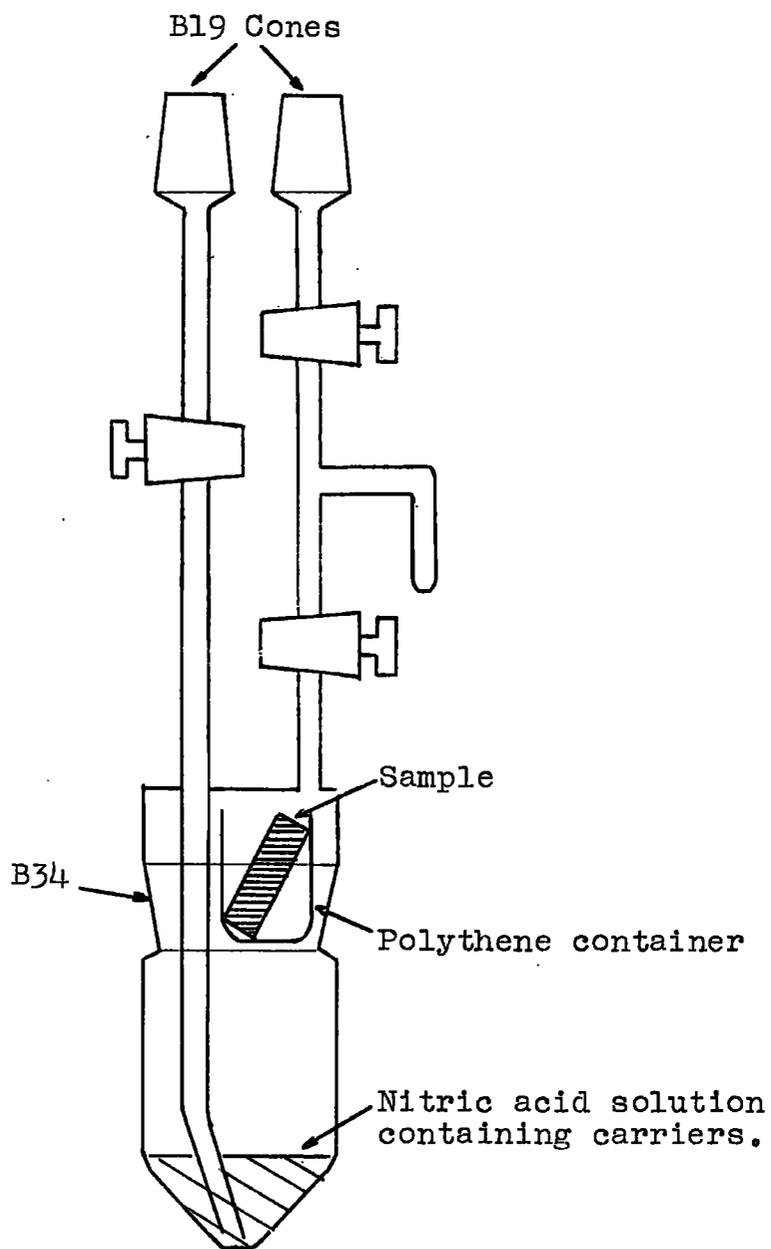
FIG. 2.7. Dissolver vessel.

The dissolver vessel was attached to the main vacuum system as illustrated in Figure 2.8 and partially evacuated so as to ensure a leak-proof connection around the B34 cone/socket. The cold-finger section S2 was then pumped down to vacuum.

Xenon was bled into the gas-measuring system from the reservoir. As a check against leakage of air into the reservoir, the carrier gas was condensed in side-arm S1 at -195°C; a vapour pressure over the condensed sample of about 5×10^{-3} torr as measured by the McLeod gauge was taken as an indication of purity. The vapour pressure over pure xenon at -195°C was calculated from data[17] available at other temperatures to be about 5×10^{-3} torr; (the major constituents of air have vapour pressures substantially higher than this at -195°C).

The gas was transferred to the modified McLeod gauge by means of the ground-glass valve at A; the valve consisted of an iron core within a pyrex envelope. When the greater part of the gas had been pumped into the section above the valve, the remaining traces in other sections of the system were removed to waste by pumping. The mercury level in the McLeod gauge was raised until the valve at A opened. The level of the mercury within the gauge was adjusted to an etched mark below the valve; the valve was retained in an "open" position by means of an external magnet.

High vacuum line
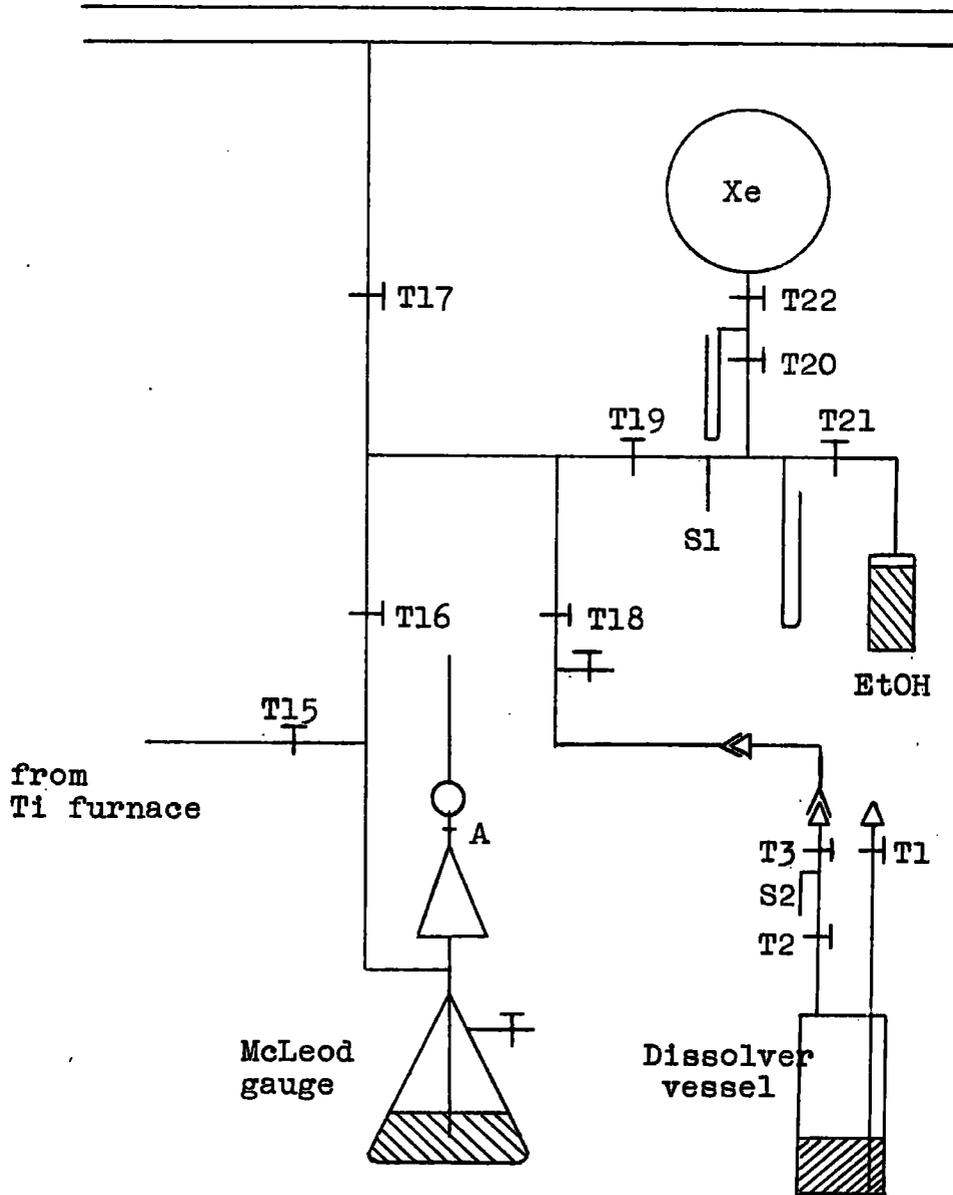
FIG. 2.8. Gas measuring section.

The difference between the mercury level in the evacuated section and that in the McLeod gauge was measured using a travelling microscope. The temperature was also noted. The volume of the section of gauge above the etched mark was estimated to be about 10 ml; the pressure of the gas contained in the section was normally about 20 cm(Hg) at about 20°C and this is equivalent to about 10 mg of xenon.

The carrier gas was transferred to the dissolver vessel by condensation in the side-arm S2 at -195°C. Maximum transference was assumed when the pressure of gas in this section had fallen to about 5×10^{-3} torr. The volume of the transference section was estimated to be about 300 ml; a residual pressure of 5×10^{-3} torr therefore represents an uncertainty of the quantity of xenon transferred of about 0.2 cm in about 20 cm or about 1%. There was a similar uncertainty in the quantity of xenon transferred to the gas Geiger-counter after recovery. However, this was not regarded as a serious source of error as the method by which calibration of the counters was effected, was similar to that of a normal run so that systematic errors of this type were eliminated provided the carrier gas pressures, before and after recovery, were comparable.

The dissolver vessel was detached from the vacuum system and the carrier xenon was allowed to diffuse into

the main section of the vessel. Several hours after the end of the irradiation - this was to allow the iodine precursors to decay appreciably - the sample was dissolved by tilting the vessel. Exchange between carrier xenon and fissiogenic xenon was effected by shaking to ensure efficient mixing of gaseous and aqueous phases.

After intermittent shaking for about thirty minutes, the dissolver vessel was attached to the vacuum system by means of two B14/19 adaptors as shown in Figure 2.6. Rotation of the lightly-greased adaptors about the vertical axis resulted in air-tight connections between the vessel and the vacuum system.

That section of the vacuum system to which the vessel was attached was partially evacuated. Opening tap T11 to atmosphere allowed about 20 ml of air to enter the system between taps T1 and T10; this quantity of air was used to flush the gases from the dissolver vessel. In preliminary experiments hydrogen was used as the flushing gas. However, as air was already present in the dissolver vessel due to the technique of introducing the irradiated sample, the use of hydrogen was considered unnecessary. The use of air as flushing agent did not produce any undesirable effects; indeed it proved useful in the calibration experiments. Dissolution of calibration samples produced

nitric oxide which was difficult to separate from
xenon by conventional means due to similar freezing
points. Introduction of air into the tap containing
the mixture of these gases and warming caused oxidation
of nitric oxide to nitrogen dioxide; the latter was
easily separated from xenon by condensation at -90°C.

The gases from the dissolver vessel were passed
through three cold traps; two traps at -90°C retained
iodine isotopes as well as acid spray and water; one trap
at -195°C retained xenon semi-quantitatively. So that
reliable corrections could be applied in the final
calculations, it was necessary that the isolation of the
xenon isotopes from iodine precursors be both rapid and
quantitative; this operation was effected in about one
minute.

The condensed solid in the trap at -195°C (trap B
in Figure 2.6) was pumped to remove the bulk of the
flushing gas after tap T4 was closed. The trap was
warmed to -90°C by means of an acetone bath at this
temperature and the evaporated gas was transferred to the
gas-solid chromatography section by condensation in side-
arm S3 at -195°C; residual traces of water etc. remained
in the trap.

The chromatography section consisted of about 1 gm
of 60 - 80 mesh charcoal activated with zinc chloride;

the charcoal was contained in a U-tube by copper gauze. The charcoal was outgassed prior to a determination by pumping for about six hours at 300°C. The heating was provided by a small electric furnace controlled by a variac.

The gas was passed into the chromatograph and adsorbed on the charcoal at -20°C, the U-tube being immersed in an acetone bath at this temperature. Removal of traces of fissiogenic krypton isotopes from the xenon gas was obtained by passage of a stream of hydrogen (about 50 ml at N.T.P.) through the column at -20°C and pumping. It has been shown that, at this temperature, there is the greatest difference in adsorption on charcoal between krypton and xenon[18].

The hydrogen used for this purpose was purified by passing hydrogen gas from a cylinder through a charcoal trap at -195°C into the reservoir.

The xenon was desorbed from the charcoal by heating the U-tube to about 200°C. Residual hydrogen was pumped away after condensing the xenon in side-arm S3 at -195°C; the temperature of the U-tube was held at about 200°C to prevent re-adsorption.

Side-arm S3 was warmed to room temperature and the evaporated xenon was passed through a column of 80 - 100 mesh titanium metal sponge at about 900°C; at this

temperature, non-noble gas impurities react with titanium[19]. The titanium furnace, illustrated in Figure 2.9, was outgassed prior to a determination by pumping at about 1000°C. During preliminary experiments it was observed that a vacuum of about 10^{-3} torr only was attainable in the furnace section while the temperature was held at about 1000°C. However, on cooling the furnace to room temperature, the pressure fell to about 10^{-5} torr. Consequently, the purification procedure was conducted by passing the xenon through the furnace at about 900°C, transference being effected by condensation of the gas in side-arm S4 at -195°C, followed by evaporation of the gas in the furnace section while the temperature of the latter was allowed to fall to room temperature.

The xenon was treated in the titanium furnace until the vapour pressure over a sample condensed at -195°C was about 5×10^{-3} torr. The recovered gas was measured in the McLeod gauge in a manner identical to that employed in determination of the pressure of the carrier xenon. The temperature was again noted to enable temperature corrections to be applied.

The gas was transferred to the gas Geiger-counter as shown in Figure 2.6 by condensation in side-arm S5 at -195°C. Inactive xenon and ethanol were added in
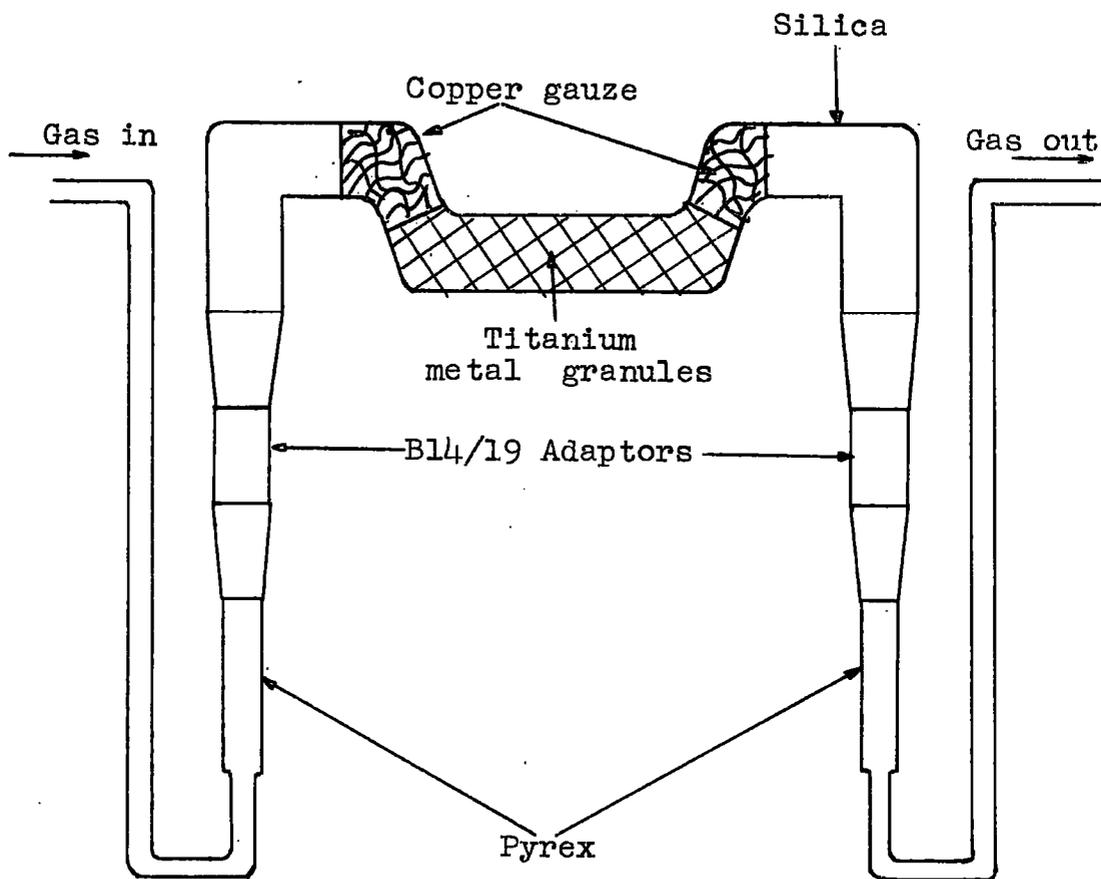
FIG. 2.9. Titanium furnace.

quantities such that the pressure of xenon and ethanol within the counter at room temperature was 5 cm (Hg) and 1 cm (Hg) respectively. The counter volumes were calibrated against the section of the system between taps T19, T20 and T21; correlation between the quantities of inactive xenon and ethanol, required to produce a counter-pressure of the desired value, and the manometer reading in the calibration section was hence straight-forward.

The ethanol used was of analytical grade, degassed by repeated freezing at -195°C and pumping. Preliminary experiments showed that ethanol purified by distillation over sodium metal did not perceptively improve counter-characteristics.

The counter was detached from the vacuum system and the decay of the active gas was followed for several weeks. Limitation on the length of time the decay was followed was due to deterioration of Geiger-action through leakage of air into the counter and necessary re-use of counters because of limited numbers. In all, three counters were used for quantitative determinations although there were several other counters available; these were used for qualitative experiments.

2.5. Counting Methods

2.5(a) Proportional counter

An end-window gas-flow β-proportional counter of the type used in this work is illustrated in Figure 2.10, together with its associated shelf-holder for source mounts. The cylindrical counter body was made of polished brass; the anode loop of 0.001" constantan wire was supported at the top of the counter body in a teflon insulator. The anode loop was soldered into a section of thin wall nickel tube (external diameter about 1 mm); the bottom of the loop (diameter about 10 mm) was adjusted to $\frac{3}{8}$" from the counter window.

Counter windows of several different materials have been used by workers at the Londonderry Laboratory for Radiochemistry at Durham, but the most satisfactory, to date, have been those made from 1 mg/cm^2 "Melinex" film stuck to a supporting ring by a solution of cellulose acetate in amyl acetate. "Melinex" is a strong polyester film aluminised on both surfaces; this excludes the need for evaporation of a conducting film on to the window material as was required for windows made from "V.Y.N.S." and "Milar".

The counter gas (90% argon and 10% methane) was dried over magnesium perchlorate before entering the
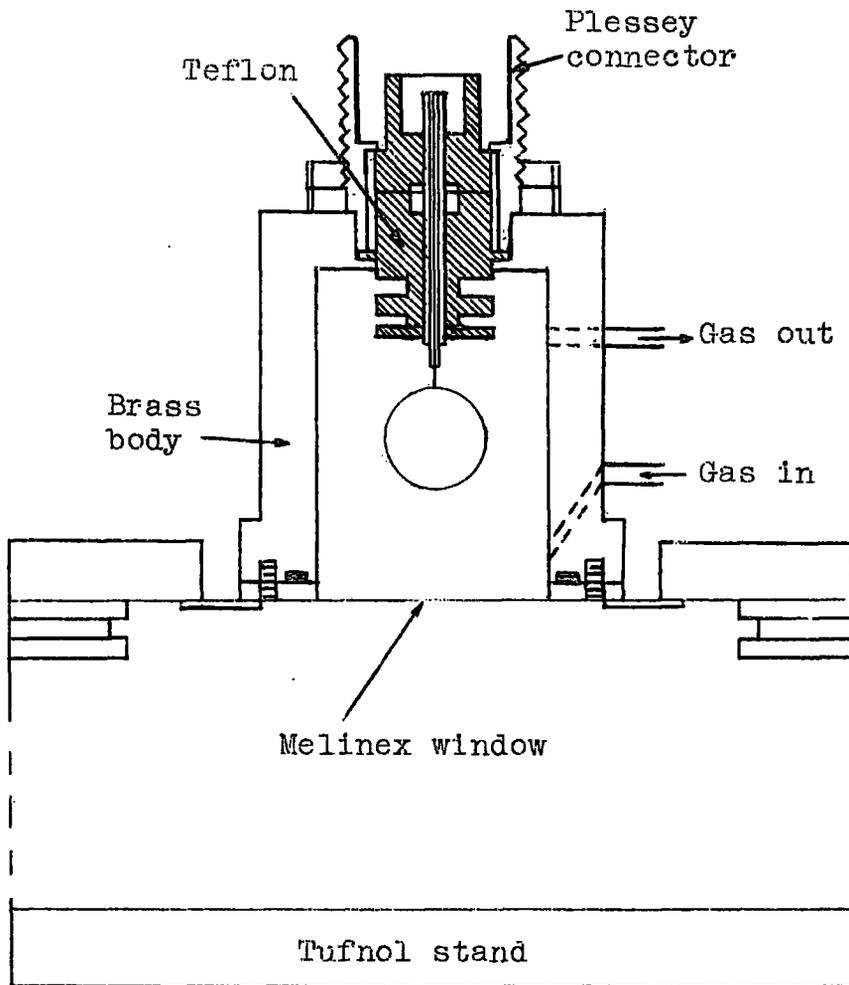
FIG. 2.10. End-window gas-flow proportional
counter.

counter at atmospheric pressure. The gas flow-rate, controlled by a needle valve, was normally held constant at around 40 ml/min. The variation in counter-efficiency was found to be slightly dependent on the flow-rate; between flow-rate limits of 20 ml/min and 60 ml/min, the variation was less than 0.1% per 1 ml/min.

The electronic equipment and gas flow arrangement is shown in Figure 2.11; operating conditions are listed below.

Gas flow-rate	40 ml/min
Amplifier	type 1217A
Preamplifier	type 1484A
Differentiation time	0.32 μsec
Integration time	0.32 μsec
Attenuation	10 dB
Scaler	type 1009D
Paralysis time	50 μsec
Discriminator level	15v

Under normal conditions, the counter exhibited a plateau centred at about 1.85 kV; the plateau was about 150v long with a slope of about 1-2% per 100v. The counter enclosed in a lead castle of 1.25" walls gave a background of 8 to 10 c.p.m. at an anode potential of 1.85 kV.

The shelf-holder, constructed from machined "tufnol" strips, was set up in a jig so that reproducible geometry could be obtained between shelf-holders. The solid sources, the preparation of which is described in section 2.5(b), were mounted on aluminium planchets and set in a hole
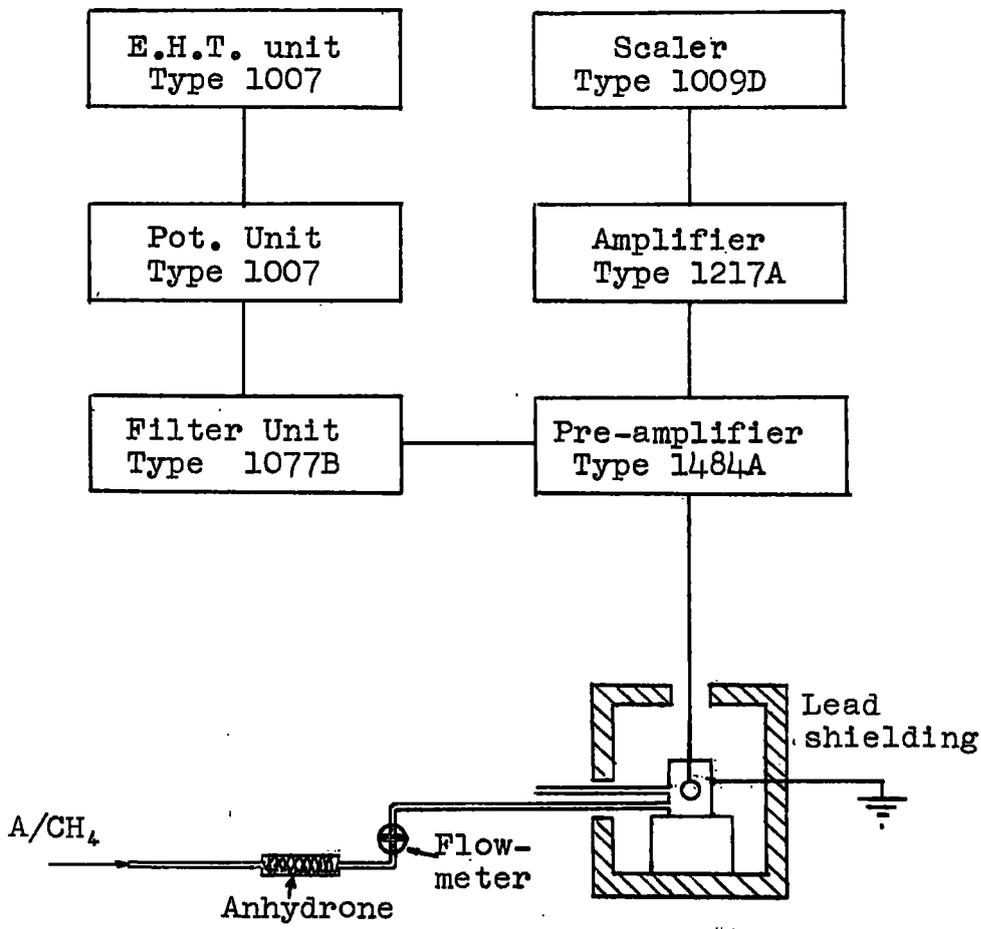
FIG. 2.11.   Electronic equipment associated
              with proportional counter.

machined in the centre of an aluminium shelf. The shelf was backed with 1 gm/cm^2 aluminium to ensure saturation backscatter for β-particles.

2.5(b). Preparation of solid sources

Sources were mounted on glass-fibre discs (Whatman GF/A). The discs were first washed with water, alcohol and ether and dried in a vacuum desiccator; they were then mounted on aluminium planchets and weighed on a Stanton semi-micro balance (Model MC1A).

A weighed glass-fibre disc was supported on a sintered polythene disc in a demountable (Hahn type) filter stick; the internal diameters of the sticks used by members of the laboratories both at Durham and at Canterbury were standardized at $\frac{5}{8}$", thus allowing sources of reproducible geometry to be obtained.

A slurry of the source material was filtered, washed with the relevant chemicals, and dried either in an oven or in a vacuum desiccator. The source was then placed on its aluminium planchet and weighed.

The balance was accurate to within 0.05 mg and source weights were normally in the range 10-30 mg; the recovery yield was therefore precise to within 0.5%.

2.5(c). <u>Calibration of the β-proportional counter</u>

The method described by Bayhurst and Prestwood[20] was employed for the purpose of calibrating the end-window proportional counter. The method centres around an experimentally-determined correlation between the counter efficiency for a particular nuclide and the β-spectra of that nuclide.

Several isotopes were chosen to act as calibrating nuclides by virtue of the simplicity of their β-spectra; the isotopes were calcium-45, tungsten-185, iodine-131, sodium-22, gold-198, sodium-24, yttrium-91, yttrium-90 and potassium-42.

High specific activity solutions of the calibrating nuclides were obtained from the Radiochemical Centre, Amersham, or by irradiation of an appropriate target nuclide in a nuclear reactor. Determination of the specific activity of each solution was effected by 4Πβ-counting or by 4Πβ/γ-coincidence counting methods where applicable; sodium-22 and gold-198 solutions were calibrated by the latter method. Calibrations were carried out by Williams of this laboratory[21].

A weighed aliquot of an active solution was added to a known weight of the relevant isotopic carrier solution. Precipitation of the element under consideration was effected by recommended procedures after ensuring isotopic

exchange and sources of various weights were prepared; this work was divided among several members of the laboratory.

The variation of counter efficiency with source weight was determined for source weights up to 50 mg for each calibrating nuclide. Examples of the observed variation are shown in Figure 2.12.

The average energy of the β-particles emitted during a nuclear transition can be estimated from the β-spectrum using a series of graphs from the original paper of Bayhurst and Prestwood[20]. A series of curves were constructed for several source weights of counter efficiency for β-particles emitted during a nuclear transition against the average energy of the β-particles. Figure 2.13 shows curves for sources of weights 10, 20 and 40 mg; the complete data for several source weights arelisted in Table 2.1.

The efficiency of the counter for a particular nuclide can then be estimated provided that the β-spectra of the nuclide are known and that no other particles are emitted. In calculating the counter efficiency for a nuclide, allowance was made for daughter products in transient equilibrium with the parent nuclide where the daughter products decayed by β-emission or by emission of a low energy γ-ray; the latter gives rise to conversion electrons.
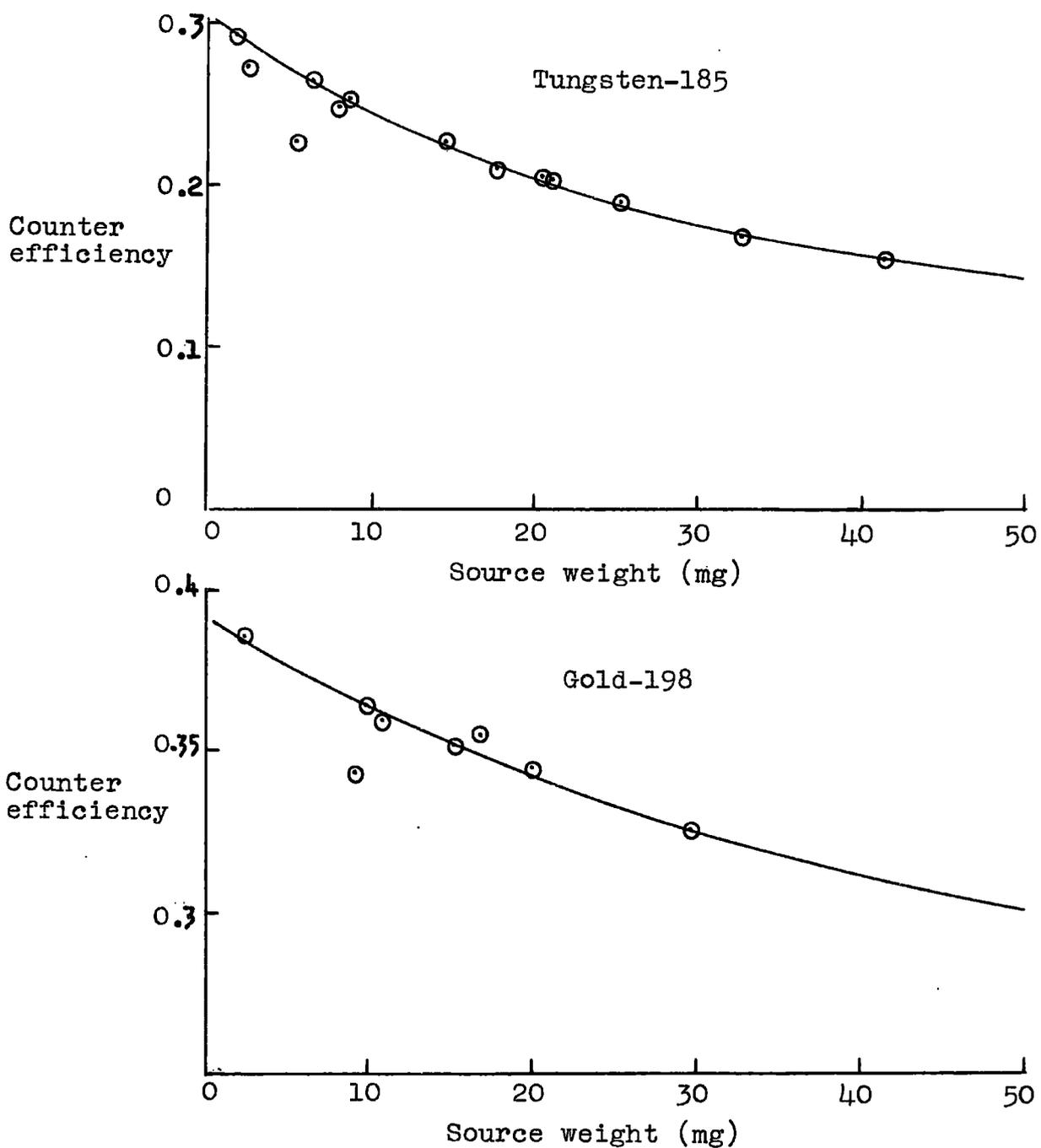
FIG. 2.12. Experimental counter efficiency curves.
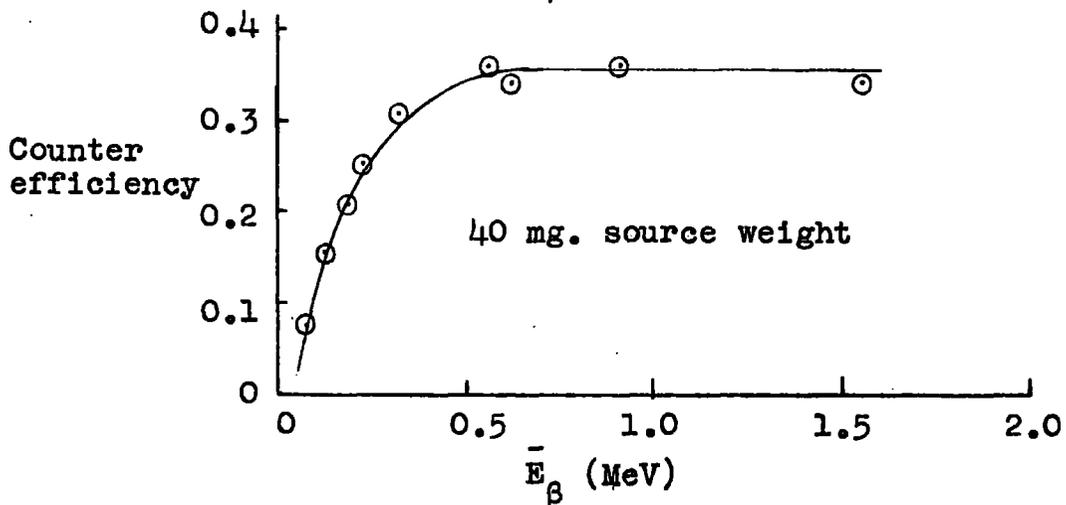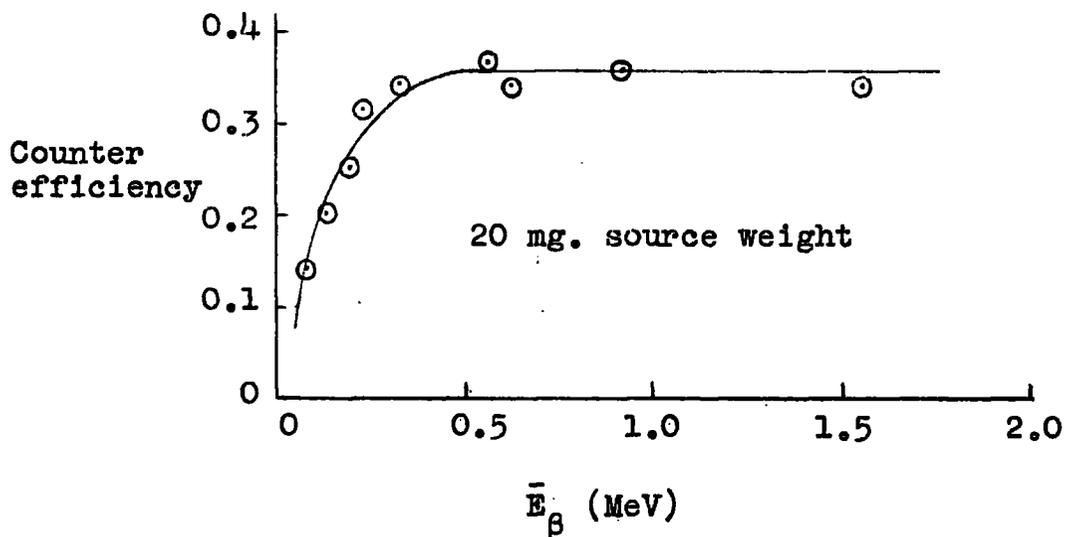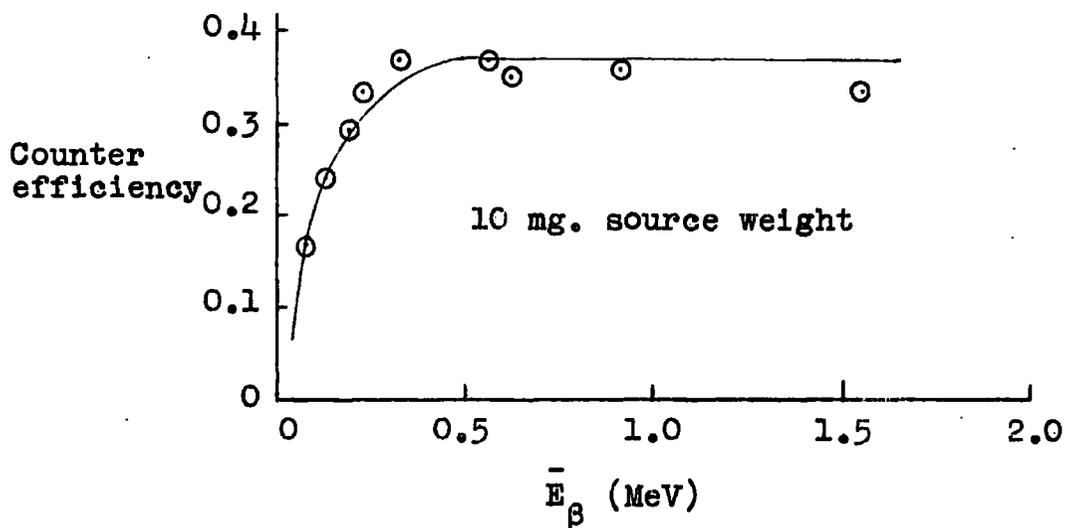
FIG. 2.13. Proportional counter calibration curves.

Table 2.1.

Nuclide	$E_\beta(\text{max})$ MeV	$\bar{E}_\beta$ MeV											
Calcium-45	0.254	0.076	source weight (mg)	1.12	2.45	2.84	4.05	9.50	12.67	19.75	29.04	52.58	
			efficiency	0.251	0.228	0.218	0.218	0.177	0.168	0.135	0.106	0.069	
Tungsten-185	0.428	0.127	source weight (mg)	1.81	2.31	5.48	8.04	8.77	17.74	20.51	25.24	41.51	53.56
			efficiency	0.291	0.274	0.227	0.249	0.253	0.210	0.205	0.189	0.155	0.129
Iodine-131	0.606	0.188	source weight (mg)	2.11	4.97	10.59	10.68	18.46	23.76	27.95	37.37	45.70	
			efficiency	0.289	0.308	0.289	0.280	0.264	0.241	0.222	0.211	0.206	
Sodium-22	0.542	0.225	source weight (mg)	1.91	3.74	6.24	8.62	11.35	16.91	19.12	28.62	34.39	45.81
			efficiency	0.345	0.327	0.343	0.349	0.336	0.326	0.323	0.297	0.288	0.262
Gold-198	0.963	0.321	source weight (mg)	2.32	9.15	9.86	10.75	15.03	16.67	19.90	29.41	61.85	
			efficiency	0.387	0.344	0.364	0.360	0.353	0.355	0.344	0.326	0.278	
Sodium-24	1.390	0.560	source weight (mg)	1.11	2.77	5.42	8.44	12.85	19.98	27.18	28.17	32.18	47.53
			efficiency	0.350	0.331	0.363	0.361	0.369	0.370	0.369	0.367	0.369	0.358
Yttrium-90	2.260	0.905	source weight (mg)	2.69	4.55	5.72	8.38	13.45	18.40	27.90	41.84	49.81	52.68
			efficiency	0.371	0.350	0.362	0.360	0.357	0.365	0.356	0.355	0.362	0.351
Yttrium-91	1.537	0.620	source weight (mg)	2.39	5.78	7.06	9.05	13.53	18.72	20.89	35.97	41.33	50.34
			efficiency	0.342	0.350	0.339	0.343	0.344	0.347	0.345	0.346	0.338	0.328
Potassium-42	3.58	1.55	source weight (mg)	1.40	4.01	7.68	10.42	15.29	18.86	20.51	21.35	24.98	49.18
			efficiency	0.360	0.346	0.331	0.344	0.340	0.343	0.341	0.340	0.346	0.355

Contribution from a daughter product in transient equilibrium with a parent nuclide is given by

$$\eta_T = \eta_P + \eta_D \cdot \frac{\tau_P}{\tau_P - \tau_D}$$

where η_T, η_P, η_D are the counter efficiencies for the mixture in transient equilibrium, the parent nuclide alone, and the daughter nuclide alone respectively; τ_P and τ_D are the half-lives of the parent and daughter nuclide respectively.

Estimation of the counter efficiency for daughter nuclide included contributions from conversion electrons where applicable. The fraction of low energy γ-rays giving rise to conversion electrons is given by $\alpha/(1+\alpha)$ where α is the conversion factor. The conversion electrons will be emitted with a discrete energy, E_{ce}, given by

$$E_{ce} = E_\gamma - BE$$

where E_γ is the γ-ray energy; BE is the binding-energy of the electron to the nucleus of the atom.

Conversion factors and decay-systematics were taken from the Nuclear Data Sheets[22]. No corrections were made for contributions from γ-rays; these were estimated to be very small (less than 1% of the total efficiency).

Calculated efficiency curves for molybdenum-99, zirconium-97, iodine-132, -133, -134, -135, xenon-133, -135

are shown in Figure 2.14. To complete the group of
nuclides investigated in this work, the experimentally-
determined curve for iodine-131 is shown in Figure 2.15.

2.5(d). Gas Geiger-counters

Two types of counter were used for measuring the
radioactive xenon isotopes; these are illustrated in
Figure 2.16.

The upper diagram illustrates a counter that was
constructed at Durham. The cathode was made of polished
passive-iron tubing. The anode wire of 100μ diameter
tungsten wire was held in perspex plugs by means of a
glass-bead at one end and a small tungsten rod at the
other end of the cathode; no guard tubes were incorporated
in this design.

The glass condensation section was attached to the
counter by means of a B7 cone sealed into one of the
persplex plugs with black wax. The counter was rendered
leak-proof by a thin film of black wax around the junctions.

As it was necessary to follow the decay of the active
gas within the counter for several days, a mercury seal
was attached as glass taps lightly greased with Apiezon
grease tended to leak air over such a period.

Rotation of the counter about the horizontal axis
caused the mercury to lie on the sintered glass plug.
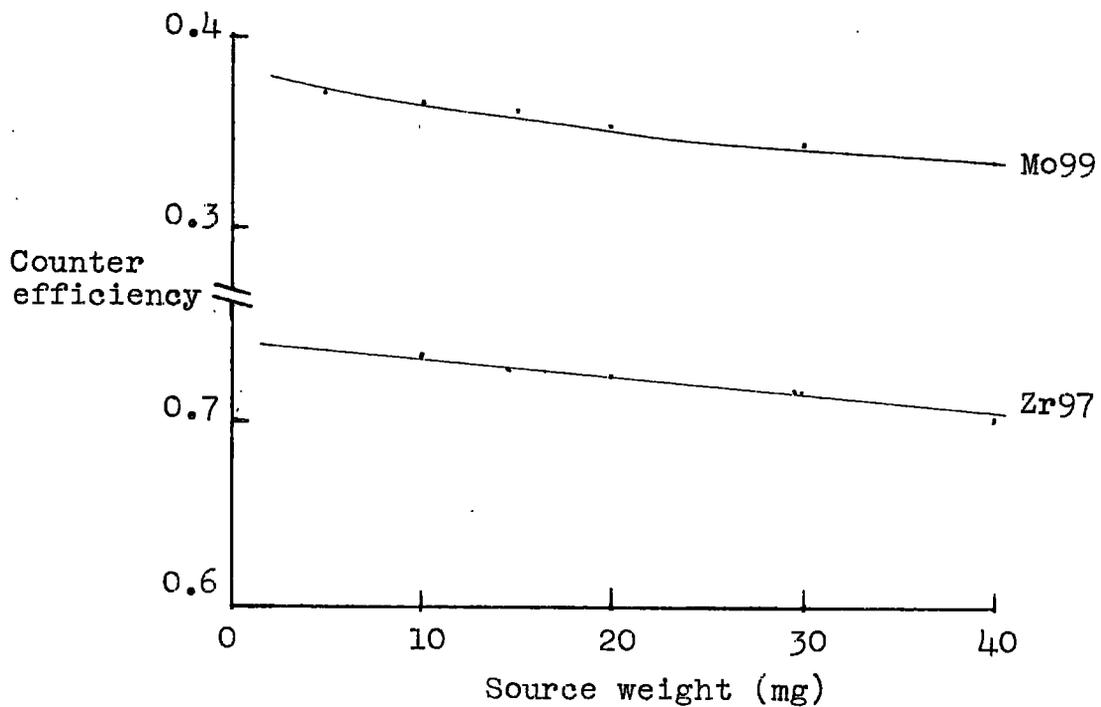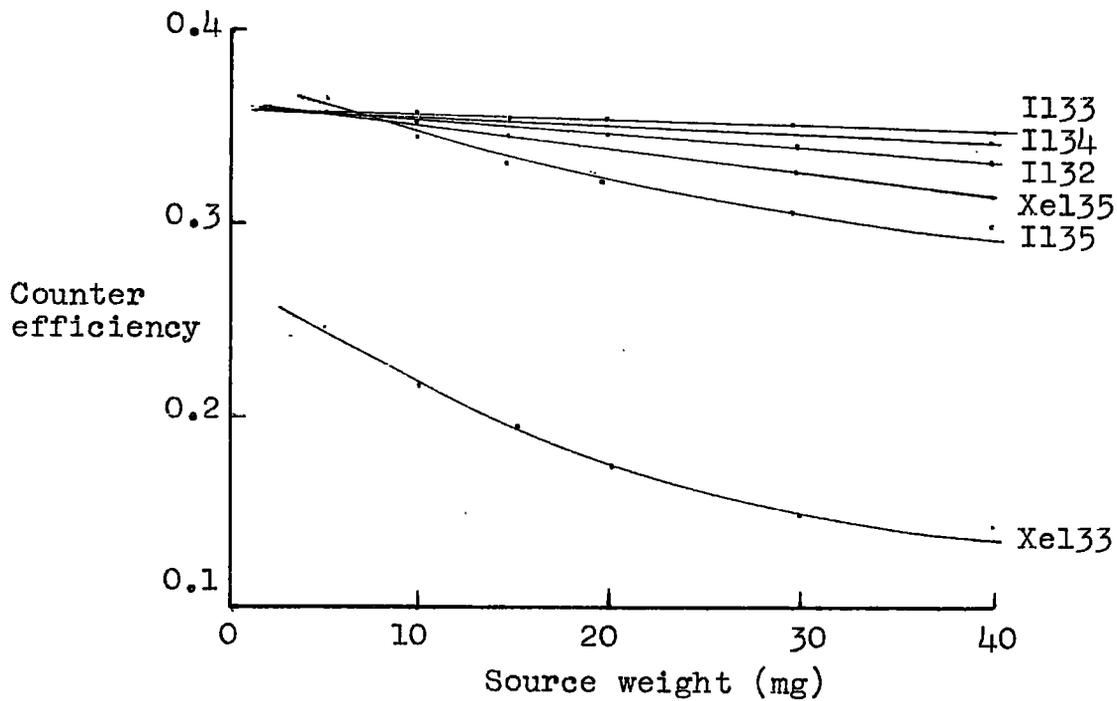
FIG. 2.14. Calculated counter efficiencies.
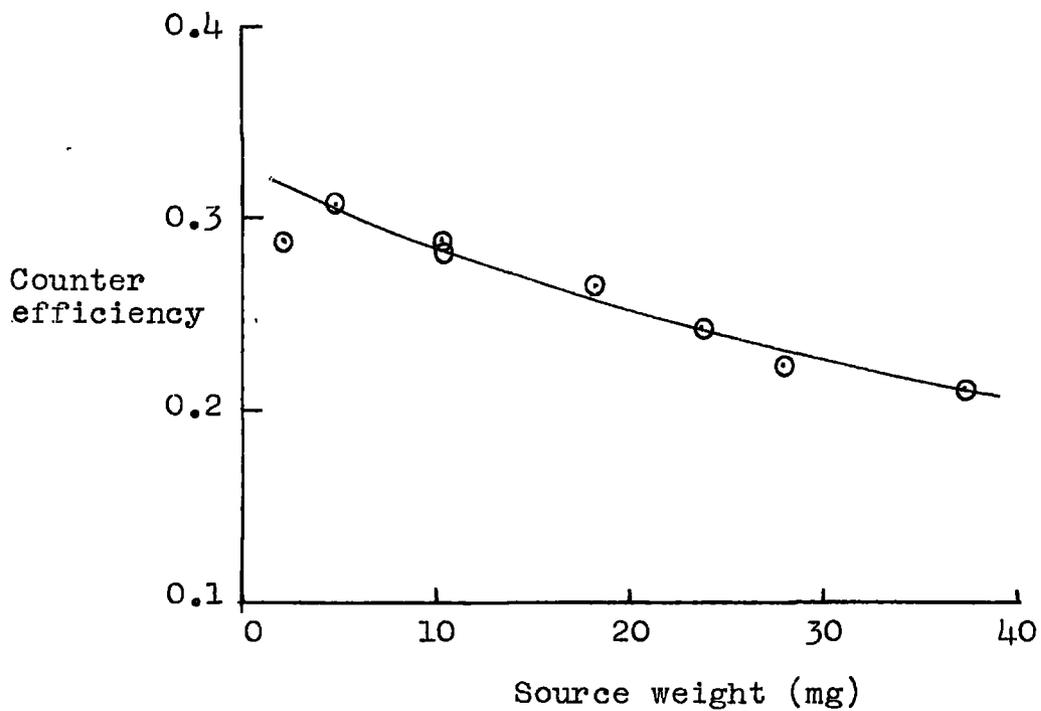
FIG. 2.15. Counter calibration curve for Iodine-131.
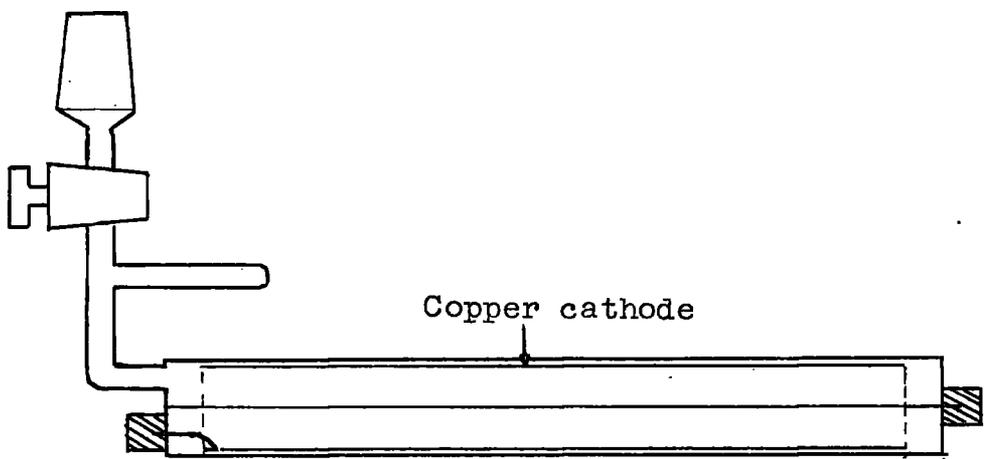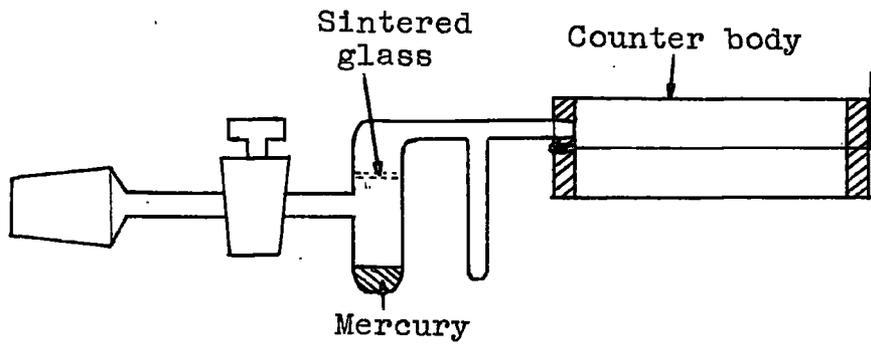
FIG. 2.16. Gas Geiger-counters.

Opening the attached tap to atmosphere produced a positive pressure on top of the mercury, thus preventing gas escaping from the counter.

The lower diagram in Figure 2.16 shows one of a series of counters constructed at Canterbury by modifying a commercial Geiger-counter (type G24 from Twentieth Century Electronics) by addition of a side-arm and glass tap; it was found that a glass tap lightly greased with silicone grease remained leak-proof for a sufficiently long period. The counter cathode was made of copper foil rolled into a cylinder. The anode was 100μ diameter tungsten wire sealed in the pyrex envelope.

The electronic equipment associated with the gas Geiger-counter was similar to that described by Silvester[1]; Figure 2.17 shows the electronic arrangement.

Optimum counter characteristics were obtained when the gas within the counter consisted of about 5 cm (Hg) xenon and about 1 cm (Hg) ethanol at room temperature; Figure 2.18 shows the characteristics observed at such pressures for the two types of counter. At higher pressures the plateaus deteriorated both in length and slope; the threshold voltage also increased.
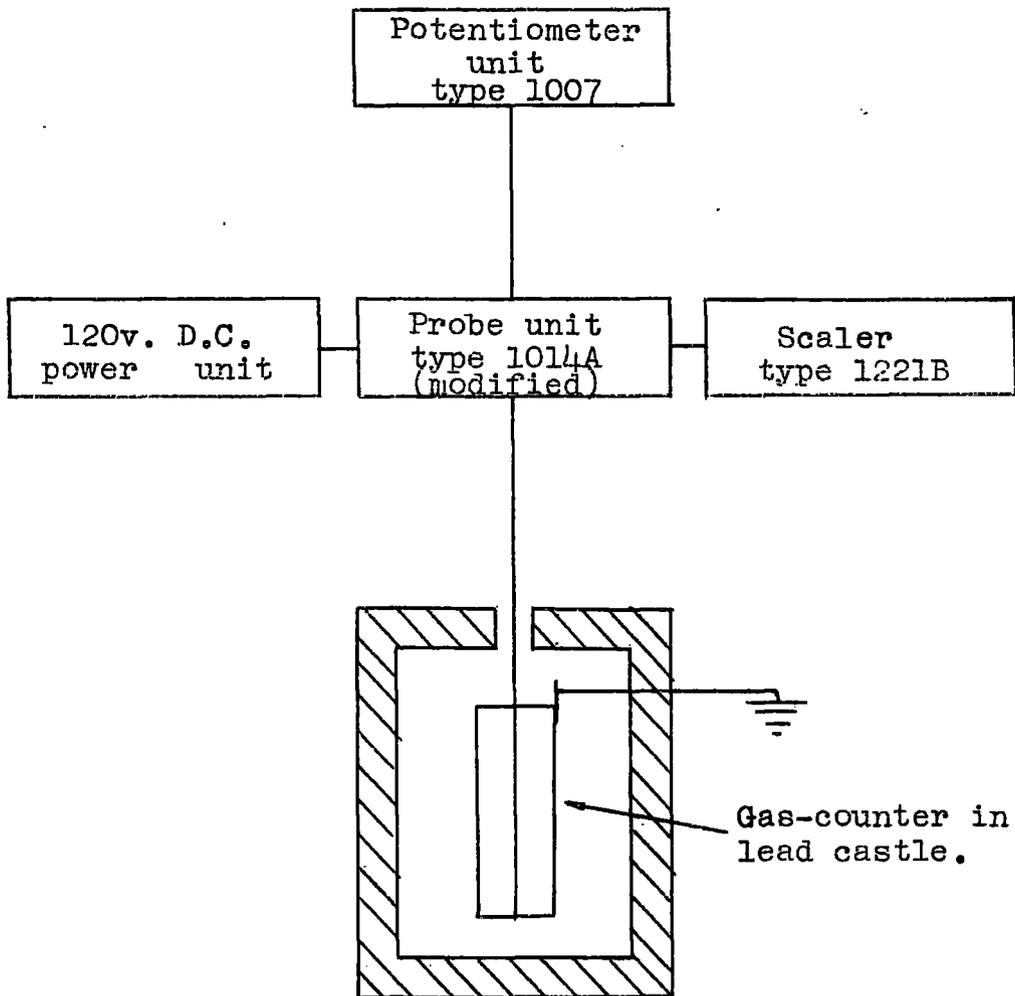
FIG. 2.17. Electronic equipment associated with
gas-counters.

Probe unit type 1014A was modified to increase
the quenching pulse by 120v and the paralysis
time to 1000 μsecs.
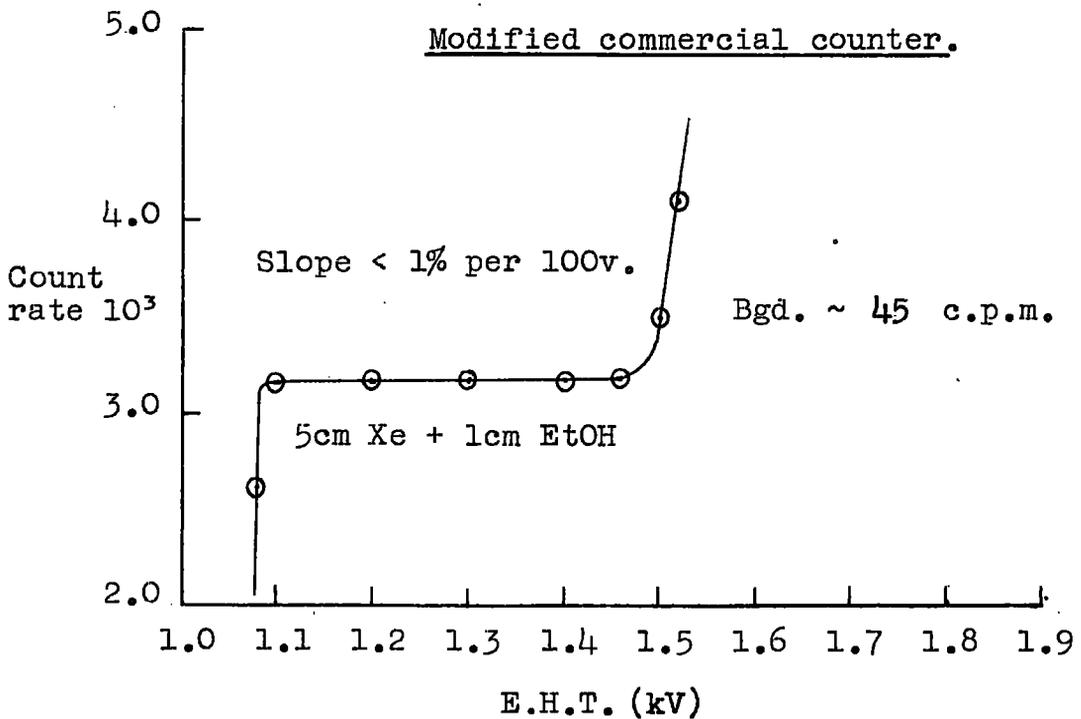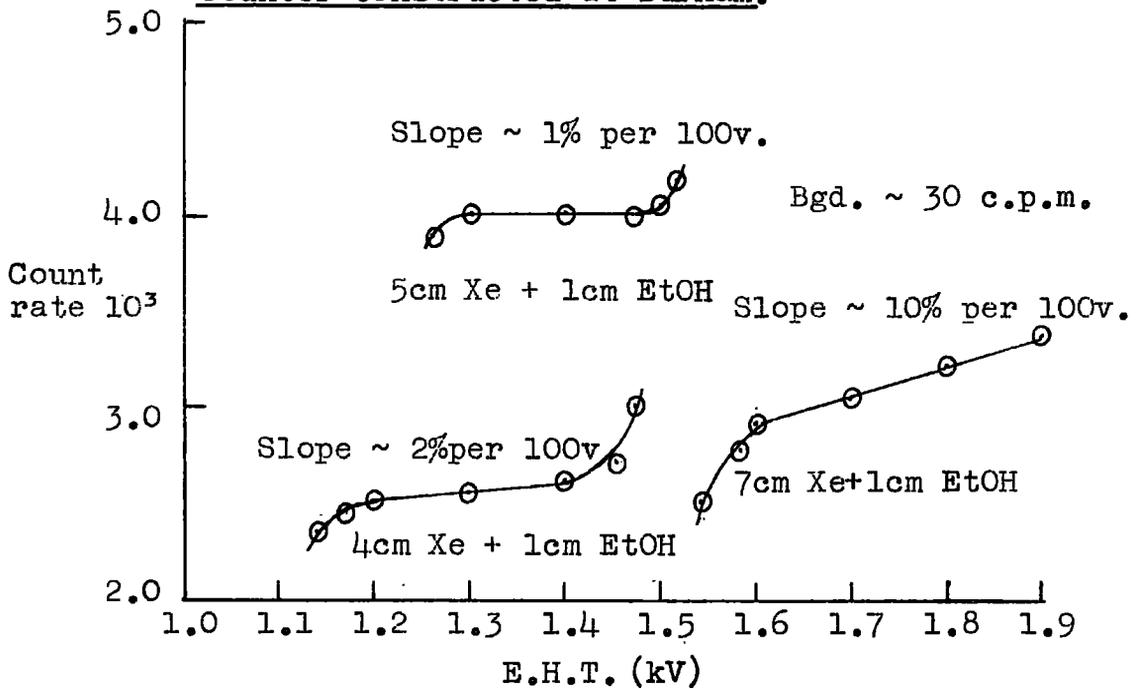
FIG. 2.18. Counter characteristics of gas-counters.

2.5(e). Calibration of gas Geiger-counters

The gas Geiger-counters were calibrated relative to the β-proportional counter by conducting control experiments on samples of uranium of natural isotopic composition irradiated with thermal neutrons; under these irradiation conditions the absolute yields of masses 97, 99, 133 and 135 are known[23-28].Calibration of the counters by this method also served to reduce systematic errors in the general procedure devised in this work for determining the xenon isotopes.

Several calibrations were attempted at Durham by irradiation of a sealed solution of uranyl nitrate according to the method described by Silvester[1]. The neutron flux from a small Sb-Be source immersed in a water tank was low and induced activities were too low to enable accurate calibration. An alternative method was devised whereby a nuclear reactor at Harwell provided a comparitively high flux of thermal neutrons.

Uranium oxide was prepared by thermal decomposition of purified uranyl nitrate of natural isotopic composition. The oxide was contained either in a nickel tube (internal diameter about 1 mm, length about 50 mm) sealed at both ends with silver solder or in a silica tube (internal diameter about 3 mm, length about 15 mm) closed at both ends with copper foil held to the silica by

"Araldite"; five irradiations were carried out using the first type of container and two using the second type. The activities, induced in a sample of about 20 mg uranium oxide after an irradiation in a thermal column at pile factor 0.1 for thirty minutes, were comparable to the activities resulting from a normal run.

The operations performed on an irradiated sample on its return to the laboratory at Canterbury were similar to those of a normal run. The sample was introduced into the dissolver vessel and dissolution of the uranium oxide was effected after removal of the seals from the sample tube with nitric acid; the presence of silver in the solder necessitated the absence of chloride ions from the carrier solutions. The fissiogenic nuclides were recovered in an identical method to that used for recovery of nuclides from samples induced to undergo fission at higher neutron energies as described previously.

Calculation of the counter efficiency depended fundamentally on accurate values for the absolute cumulative fission yields for masses 97, 99, 133 and 135 from thermal neutron-induced fission of uranium-235. The values available to date are listed in Table 2.2. The values adopted for this work were those claimed by Farrar [23,24] et al to be precise to about 1%.

Table 2.2.

Absolute cumulative fission yield (%)

Fragment mass	Katcoff and Rubinson (19)	Farrar et al (23,24)	Walker (25)	Katcoff (25)	Steinberg and Glendenin (27)	Petruska et al (28)
97	–	6.33	6.2	6.09	6.1	–
99	–	6.25	6.3	6.06	6.1	–
133	6.62	6.62	6.5	6.62	6.5	6.59
135	–	6.45	6.4	6.41	6.3	6.41

The neutron beam in the thermal column of the reactor at pile factor 0.1 was estimated by Harwell personnel to contain neutrons of energies higher than thermal energy to the extent of<10%. Corrections to allow for fission of uranium-238 by fission-spectrum neutrons could not be estimated; the corrections are considered to be very small as the fission cross-section of uranium-238 for fission-spectrum neutrons is several orders of magnitudes less than that of uranium-235 for thermal neutrons.

REFERENCES - CHAPTER 2

1. D.J. Silvester, Ph.D. Thesis (Durham University, 1958).

2. J.P. Conner, T.W. Bonner and J.R. Smith, Phys. Rev., **88**, 468 (1952).

3. D.L. Allan and M.J. Poole, Proc. Roy. Soc., **204A**, 500 (1951).

4. J.L. Tuck, Nuclear Fusion, **1**, 201 (1961).

5. G. Preston, P.F.D. Shaw and S.A. Young, Proc. Roy. Soc., **226A**, 206 (1954).

6. M.G. Brown, S.J. Lyle and G.R. Martin, Radiochimica Acta, **6**, 16 (1966).

7. Md. M. Rahman, Ph.D. Thesis (Durham University, 1965).

8. G. Herrmann, Radiochimica Acta, **3**, 169 (1964).

9. R. Belcher, A. Sykes and J.C. Tatlow, Analytica Chimica Acta, **10**(1), 34 (1954).

10. R.B. Hahn and R.F. Stromieczny, Nucleonics, **14**(2), 56 (1956).

11. A.I. Vogel, Quantitative Inorganic Analysis, p.508, (Longmans, Green and Co., London, 1961).

12. E.M. Scadden, Nucleonics, **15**(4), 102 (1957).

13. S. Katcoff, C.R. Dillard, H. Finston, B. Finkle, J.A. Seiler and N. Sugarman, Radiochemical Studies: The Fission Products, Book 2, P/141 (McGraw-Hill Co., New York, 1951).

14. W.W. Meinke, AECD Report-2738 (1949).

15. A.N. Murin, I.S. Kirin, V.D. Nefedov, S.A. Grachev, Yu. K. Gusev, N.V. Ivannikova and V.S. Gusel'nikov, Radiokhimiya, **8**, 449 (1966).

16. G.N. Walton, Quart. Rev., **15**, 95 (1961).

17. Handbook of Chemistry and Physics, p.D-102
    (The Chemical Rubber Co., 1965).

18. W.J. Arrol, K.F. Chackett and S. Epstein,
    Can. J. Res., 27B, 757 (1949).

19. S. Katcoff and W. Rubinson, Phys. Rev.,
    91, 1458 (1953).

20. B.P. Bayhurst and R.J. Prestwood, Nucleonics,
    17(3), 82 (1959).

21. C.G.B. Williams, Ph.D. Thesis (Durham University,
    1966).

22. Nuclear Data Sheets, National Academy of Sciences,
    National Research Council, Washington.

23. H. Farrar and R.H. Tomlinson, Nuclear Physics,
    34, 367 (1962).

24. H. Farrar, H.R. Fickel and R.H. Tomlinson,
    Can. J. Phys., 40, 1017 (1962).

25. W.H. Walker, Chalk River Report CRRP-913 (1960).

26. S. Katcoff, Nucleonics, 18(11), 201 (1960).

27. E.P. Steinberg and L.E. Glendenin, Proceedings of
    the U.N. International Conference on the Peaceful
    Uses of Atomic Energy, 7, P/614 (1956).

28. J.A. Petruska, H.G. Thode and R.H. Tomlinson,
    Can. J. Phys., 33, 693 (1955).

CHAPTER 3

Analyses of Decay Curves

3.1. Introduction

The Elliott 803B computer at the University of Kent at Canterbury was used to effect objective resolution of the experimental decay curves. A computer program, based on the paper by Wentworth[1], was written so that decay curves containing several components could be resolved provided the half-lives and decay schemes of the components were known.

The Wentworth treatment depends on the assumption that random errors resulting from a series of observations of a given quantity have a Gaussian distribution. This treatment may be applied to any number of unknown parameters for any function.

Consider a function relating two variables ξ, η and three parameters α, β, γ

$$F(\xi, \eta, \alpha, \beta, \gamma)$$

and consider a series of n pairs of values of the variables designated by (x_i, y_i), where $i = 1, 2, \ldots n$.

An estimate of the parameters (α, β, γ), which will be designated a, b, c, can then be made based on the criteria of least-squares of the observations (x_i, y_i). The adjusted values of the variables can be calculated

from the estimated values of the parameters; these
will be designated $(\bar{x}_i, \bar{y}_i)$, where $i = 1, 2, \ldots \ldots n$.
The residuals of the observed and adjusted values of
the variables can then be calculated and represented by

$$Vx_i = (x_i - \bar{x}_i)$$
$$V_{yi} = (y_i - \bar{y}_i)$$

An application of a least-squares treatment results
in values for the unknown parameters for which the sum
of the squares of the weighted residuals is a minimum
given by

$$S = \Sigma(Wx_i \cdot Vx_i{}^2 + Wy_i \cdot Vy_i{}^2) = minimum$$

where Wx_i, Wy_i are the weighting factors of the
observations of x_i and y_i. (The weighting factor is
defined as a quantity inversely proportional to the
variance.)

The restriction imposed on the least-squares
treatment is that the expressions

$$F_i(\bar{x}_i, \bar{y}_i, a, b, c) = o \text{ for } i = 1, 2, \ldots \ldots n,$$

be satisfied.

Expanding the function in a Taylor's Series about
the point $(x_i, y_i, a^o, b^o, c^o)$ and truncating the series after
the first-order terms gives

$$F_i(\bar{x}_i, \bar{y}_i, a, b, c) = F_i{}^o(x_i, y_i, a^o, b^o, c^o) - Fx_i \cdot Vx_i - Fy_i \cdot Vy_i - Fa_i \cdot$$
$$\Delta a - Fb_i \cdot \Delta b - Fc_i \cdot \Delta c = o \qquad i = 1, 2, \ldots \ldots n \qquad \ldots \ldots \ldots \ldots (1)$$

(a^o, b^o, c^o are values of the parameters estimated by
graphical means.)

where Δa, Δb, Δc represent the difference between a first approximation of the parameters (a^o, b^o, c^o) and a least-squares estimate (a, b, c), so that

$$\Delta a = (a^o - a)$$

$$\Delta b = (b^o - b)$$

$$\Delta c = (c^o - c)$$

$Fx_i, Fa_i, \ldots$ represent the partial derivatives of the function, so that

$$Fx_i = (\frac{\partial F_i}{\partial x}) (x_i, y_i, a^o, b^o, c^o,)$$

$$Fa_i = (\frac{\partial F_i}{\partial a}) (x_i, y_i, a^o, b^o, c^o,)$$

A solution of equations (1) may be effected by solving the following equations

$$\sum_{i=1}^{i=n} \frac{Fa_i \cdot Fa_i \cdot \Delta a}{L_i} + \sum_{i=1}^{i=n} \frac{Fa_i \cdot Fb_i \cdot \Delta b}{L_i} + \sum_{i=1}^{i=n} \frac{Fa_i \cdot Fc_i \cdot \Delta c}{L_i} = \sum_{i=1}^{i=n} \frac{Fa_i \cdot F_i^o}{L_i}$$

$$\sum_{i=1}^{i=n} \frac{Fb_i \cdot Fa_i \cdot \Delta a}{L_i} + \sum_{i=1}^{i=n} \frac{Fb_i \cdot Fb_i \cdot \Delta b}{L_i} + \sum_{i=1}^{i=n} \frac{Fb_i \cdot Fc_i \cdot \Delta c}{L_i} = \sum_{i=1}^{i=n} \frac{Fb_i \cdot F_i^o}{L_i}$$

$$\sum_{i=1}^{i=n} \frac{Fc_i \cdot Fa_i \cdot \Delta a}{L_i} + \sum_{i=1}^{i=n} \frac{Fc_i \cdot Fb_i \cdot \Delta b}{L_i} + \sum_{i=1}^{i=n} \frac{Fc_i \cdot Fc_i \cdot \Delta c}{L_i} = \sum_{i=1}^{i=n} \frac{Fc_i \cdot F_i^o}{L_i}$$

where $L_i = \dfrac{Fx_i^2}{Wx_i} + \dfrac{Fy_i^2}{Wy_i}$

The proof of the validity of the above set of equations is comprehensively described in Wentworth's paper[1].

The linear equations may be solved for Δa, Δb, Δc, by use of matrix algebra[1] if the above equations are simplified to

$$B11.\Delta a \;+\; B12.\Delta b \;+\; B13.\Delta c \;=\; C1$$
$$B21.\Delta a \;+\; B22.\Delta b \;+\; B23.\Delta c \;=\; C2$$
$$B31.\Delta a \;+\; B32.\Delta b \;+\; B33.\Delta c \;=\; C3$$

where $B21 = B12$, etc.

Let $\overline{B}$ represent the matrix of the coefficients

$$\overline{B} \;=\; \begin{bmatrix} B11 & B12 & B13 \\ B21 & B22 & B23 \\ B31 & B32 & B33 \end{bmatrix}$$

The inverse of the matrix $\overline{B}^{-1}$ is then given by $\overline{B}^{-1}.\overline{B} = 1$ or, if Dkl represents the elements of the inverse matrix,

$$\begin{bmatrix} D11 & D12 & D13 \\ D21 & D22 & D23 \\ D31 & D32 & D33 \end{bmatrix} \begin{bmatrix} B11 & B12 & B13 \\ B21 & B22 & B23 \\ B31 & B32 & B33 \end{bmatrix} = \begin{bmatrix} 1 & 0 & 0 \\ 0 & 1 & 0 \\ 0 & 0 & 1 \end{bmatrix}$$

From the inverse matrix, the change in the coefficients may be computed

$$\Delta a \;=\; D11.C1 \;+\; D12.C2 \;+\; D13.C3$$
$$\Delta b \;=\; D21.C1 \;+\; D22.C2 \;+\; D23.C3$$
$$\Delta c \;=\; D31.C1 \;+\; D32.C2 \;+\; D33.C3$$

If a^O, b^O, c^O are sufficiently good estimates of the parameters, then the least-squares estimates of the parameters are

$$a = a^O - \Delta a$$

$$b = b^O - \Delta b$$

$$c = c^O - \Delta c$$

If a^O, b^O, c^O are not sufficiently good, then the computations may be repeated with the new values of a,b,c as the first approximations.

Further, the standard errors[5] of the new set of parameters are given by

$$\sigma a = \sqrt{D11 \cdot \frac{S}{n-m}}$$

$$\sigma b = \sqrt{D22 \cdot \frac{S}{n-m}}$$

$$\sigma c = \sqrt{D33 \cdot \frac{S}{n-m}}$$

where S is the sum of the squares of the weighted residuals; m is the number of parameters for which the data are being solved; in this example m is equal to 3.

3.2. Computer techniques

A computer program reproduced in the next section in Elliott-Algol Code was written to analyse data from radioactive decay of several components so that the initial activity of each component could be estimated.

Radioactive decay may be represented by the equation

$$F_1(t_1, A_1, A_1, A_2 \ldots A_N) = A_1 - \sum_{j=1}^{j=N} A_j \cdot f_j(t_1) = 0$$

where A_1 is the total activity at time t_1; A_j is the activity of the jth component at zero time; N is the number of components; $f_j(t_1)$ is the decay-function of the jth component at time t_1.

By analogy with Wentworth's general treatment[1], the equations obtained after expanding the function F_1 about the point $(t_1^!, A_1^!, A_1^0, A_2^0, \ldots A_N^0)$ are

$$F_1(\overline{t}_1^!, \overline{A}_1^!, A_1^{\prime\prime}, A_2^{\prime\prime}, \ldots A_N^{\prime\prime}) = F_1^0(t_1^!, A_1^!, A_1^0, A_2^0, \ldots A_N^0)$$

$$-Ft_1 \cdot Vt_1 - FA_1 \cdot VA_1 - \sum_{j=1}^{j=N} FA_{j1} \cdot \Delta A_j = 0 \text{ for } i=1,2,\ldots n$$

where $t_1^!, A_1^!$ are the experimental values of t_1, A_1; $\overline{t}_1^!, \overline{A}_1^!$ are the adjusted values of t_1, A_1 after a least-squares estimate of the parameters $A_1, A_2 \ldots A_N$ commencing the computations with the estimated values $A_1^0, A_2^0, \ldots A_N^0$; Ft_1, FA_{j1}, FA_1 are the partial derivatives of the function F_1; Vt_1, VA_1 are the residuals in t_1, A_1 after a least-squares treatment; ΔA_j is the difference between the first estimate of the parameter A_j and the least-squares estimate; n is the number of data pairs; $A_1^{\prime\prime}, A_2^{\prime\prime}, \ldots A_N^{\prime\prime}$ are the least-squares estimates of $A_1, A_2, \ldots A_N$.

A matrix of N^2 elements is set up to solve the equations. The element Bjk of the matrix to be inverted is given by

$$Bjk = \sum_{i=1}^{i=n} FA_{ji} \cdot FA_{ki} / L_i$$

where $L_i \propto Ft_i^2 \cdot \sigma t_i'^2 + FA_i^2 \cdot \sigma A_i'^2$

$\sigma t_i', \sigma A_i'$ are the standard deviations of the experimental values of t_i, A_i; $FA_{ji}, FA_{ki}, Ft_i, FA_i$ are the partial differentials of the function so that

$$FA_{ji} = -f_j(t_i')$$
$$FA_{ki} = -f_k(t_i')$$

The experimental data were considered to result from nuclides decaying to radioactive daughters which in turn decay to stable nuclides so that the decay-function $f_j(t_i)$ is given by

$$f_j(t_i) = \exp(-\lambda_{jD} t_i') + \frac{\lambda_{jP}}{\lambda_{jD} - \lambda_{jP}} \cdot \frac{C_{jP}}{C_{jD}} \cdot$$

$$(\exp(-\lambda_{jP} \cdot t_i) - \exp(-\lambda_{jD} \cdot t_i))$$

$\lambda_{jP}, \lambda_{jD}$ are the decay-constants for the parent and daughter nuclide; C_{jP}, C_{jD} are the counter-efficiencies for the parent and daughter nuclide.

There is a similar expression for $f_k(t_i)$.

$$Ft_i = (\frac{\partial F_i}{\partial t})(t_i', A_i', A_1^O, A_2^O, \ldots \ldots A_N^O)$$

$$FA_i = 1$$

It was assumed for this work that the standard deviations of the time observations were negligible so that

$$L_i \propto FA_i^2 \cdot \sigma A_i'^2$$

$$FA_i = 1$$

therefore $\quad L_i \propto \sigma A_i'^2$

The data should be weighted therefore by factors inversely proportional to the square of the standard deviation of the experimental value of the activity A_i'.

The difference between the first estimate of A_j and that of the least-squares treatment is given by

$$\Delta A_j = \sum_{k=1}^{k=N} Djk \cdot Ck$$

where Djk is an element of the inverse matrix

$$Ck = \sum_{i=1}^{i=n} \frac{FA_{ki} \cdot F_i^0}{L_i}$$

where $\quad F_i^0 = A_i' - \sum_{j=1}^{j=N} A_j^0 \cdot f_j(t_i')$

The program was written so that, prior to a least-squares treatment, the data can be corrected for the background count if it is known. Several distinct operations are carried out by the computer.

(i) A least-squares treatment is carried out with equal weighting given to all data pairs. The treatment is repeated until the corrections in the computed values of the initial activities are less than 1%.

(ii) Data values are eliminated from the computations if the residual between the least-squares value of the total activity and the experimental value is greater than a set

standard; for this work, the set standard was three standard deviations of the experimental value of the total activity.
(iii) A least-squares treatment is carried out with each data pair not previously eliminated weighted by a factor Z given by

$$Z = (DA/DT - BG)^2/(DA/DT^2 + SDBG^2).100 \quad \ldots\ldots\ldots(2)$$

where DA, DT are the gross count and duration of the count; BG, SDBG are the background count and the standard deviation of the background count. When the correction due to the dead-time of the counter is small, then

$$Z \simeq AX^2/\sigma^2_{AX}.100$$

where AX is the experimental value of the activity (i.e. the observed activity corrected for dead-time and background); σ_{AX} is the standard deviation of the experimental value of the activity.

(iv) The residuals are again compared with the set standard; any data pair not previously eliminated are rejected if the residual exceeds the set standard; data previously eliminated are re-introduced into the computations with the appropriate weighting factor if the residual is less than the set standard.

(v) The computations are repeated until there are no further changes in the data values in the least-squares treatment. The final estimate of the initial activity of each component is then printed out together with the standard error.

   The program is reproduced in Section 3.3. with explanatory notes in parentheses.

3.3. Computer program

LEAST SQUARES PROGRAM;

```
BEGIN
    INTEGER E,H,G,M,N,P;
    PROCEDURE MXINVERT(A,R,C,EPS,L);VALUE EPS;
    REAL ARRAY A; INTEGER ARRAY R,C; REAL EPS;
    LABEL L; ELLIOTT (6,7,440,0,4,5,6853);
```
(E,H,G identify the experiment, normally by the date
of the experiment; M is the number of components in
the decay-curve; N is the total number of pairs of
data values; P is the number of standard deviations
for the reject criterion; the procedure is a matrix
inversion program[2] from the Algol Program Library.)

```
    READ E,H,G,M,N,P;
    BEGIN
        INTEGER X,Y,I,J,K,Q,V; REAL C5,BG,SDBG,S1,S2;
        ARRAY A(1:N),T(1:N),DA(1:N),DT(1:N),W(1:N),
        Z(1:N),FO(1:N),F(1:M,1:N),B(1:M,1:M),L1(1:M),
        L2(1:M),E1(1:M),E2(1:M),AO(1:M),AC(1:M),D(1:M),
        SD(1:M),C(1:M),AX(1:N);
        INTEGER ARRAY R(1:M),R1(1:M);
        SWITCH SS:= MESS,FIN,ERR;
        PRINT £RUN ON?,SAMELINE,E,H,G,££L??;
        READ BG,SDBG;
```

(BG is the background count; SDBG is the standard
deviation of the background count.)

```
        FOR J:=1 STEP 1 UNTIL M DO
        READ L1(J),E1(J),L2(J),E2(J),AO(J);
```

(L1(J),E1(J),L2(J),E2(J) are the half-lives and
efficiencies of the counter for a parent-daughter
relationship of the Jth component as shown below

$$1(J) \xrightarrow{t_{\frac{1}{2}}=L1(J)} 2(J) \xrightarrow{t_{\frac{1}{2}}=L2(J)} \text{stable}$$

If the daughter nuclide is stable, or decays by a
mechanism so that the counter does not respond, then
the value of the counter efficiency for the daughter
nuclide was set at zero. AO(J) is the first estimate
of the initial activity of the Jth component.)

```
      FOR I:=1 STEP 1 UNTIL N DO
      READ T(I),A(I),DA(I),DT(I);
```

(T(I),A(I),DA(I),DT(I) are the mean time of an
activity observation from zero time, the observed
activity corrected for the dead-time of the counter,
the gross count and the duration of the count for the
Ith reading.)

```
      Q:=0;
      X:=N;
      FOR I:=1 STEP 1 UNTIL N DO
      BEGIN
          Z(I):=((DA(I)-BG*DT(I))**2/(DA(I)+SDBG**
          2*DT(I)**2))/100;
          W(I):=1;
      END;
```

(Z(I) is the weighting factor of the Ith data pair
as defined in equation (2); W(I) is the weighting
factor for the first least-squares estimate.)

```
      MESS:
      FOR K:=1 STEP 1 UNTIL M DO
      BEGIN
          FOR J:=1 STEP 1 UNTIL M DO
          BEGIN
              B(K,J):=0;
              C(J):=0;
          END;
      END;
      FOR I:=1 STEP 1 UNTIL N DO
      BEGIN
          AX(I):=A(I)-BG;
          FOR J:=1 STEP 1 UNTIL M DO
          BEGIN
              AX(I):=AX(I)-AO(J)*(EXP(-0.69315*T(I)/
              L1(J))+L1(J)/(L2(J)-L1(J))*E2(J)/E1(J)*
              (EXP(-0.69315*T(I)/L2(J))-EXP(-0.69315*
              T(I)/L1(J))));
              FO(I):=AX(I);
              F(J,I):=-(EXP(-0.69315*T(I)/L1(J))+L1(J)/
              (L2(J)-L1(J))*E2(J)/E1(J)*(EXP(-0.69315*
              T(I)/L2(J))-EXP(-0.69315*T(I)/L1(J))));
          END;
      END;
```

```
C5:=0;
FOR I:=1 STEP 1 UNTIL N DO
BEGIN
    C5:=C5+FO(I)*FO(I)*W(I);
    FOR J:=1 STEP 1 UNTIL M DO
    BEGIN
        C(J):=C(J)+F(J,I)*FO(I)*W(I);
        FOR K:=1 STEP 1 UNTIL M DO
        BEGIN
            B(K,J):=B(K,J)+F(K,I)*F(J,I)*W(I);
```

(B(K,J) is the element Bkj of the matrix to be inverted.)

```
        END;
    END;
END;
MXINVERT (B,R,R1,1@-4,ERR);
```

(The matrix is inverted using the Gauss-Jordan method[2] with complete matrix pivoting. The suffices of the successive pivots are stored in R and R1. If any pivot is less than EPS(0) in absolute value then the procedure exits to ERR. For greater values of EPS, greater accuracy can be quoted for the matrix inversion.)

```
FOR K:=1 STEP 1 UNTIL M DO
BEGIN
    S1:=0;
    FOR J:=1 STEP 1 UNTIL M DO
    BEGIN
        S1:=S1+B(K,J)* C(J);
        D(K):=S1;
    END;
END;
FOR K:=1 STEP 1 UNTIL M DO
AC(K):=AO(K)-D(K);
Y:=X;
S2:=0;
FOR K:=1 STEP 1 UNTIL M DO
S2:=S2-C(K)*D(K);
S2:=S2+C5;
FOR K:=1 STEP 1 UNTIL M DO
SD(K):=SQRT(B(K,K)*S2/(Y-M));
```

(SD(K) is the standard   error   of the Kth component.)

```
FOR K:=1 STEP 1 UNTIL M DO
BEGIN
    IF ABS(D(K)) GR ABS (AO(K)/100)
    THEN
    BEGIN
        FOR K:=1 STEP 1 UNTIL M DO
        AO(K):=AC(K);
        GOTO MESS
    END
    ELSE
    PRINT £A?,SAMELINE,SPECIAL(1),DIGITS(1),
    SCALED(4),K,£1S?,SPECIAL(2),AC(K),£ST.ERR.1S?,
    SD(K),££L??;
END;
IF P GR O
THEN
BEGIN
    Q:=Q+1;
    FOR I:=1 STEP 1 UNTIL N DO
    BEGIN
        IF (FO(I)*FO(I)) GR ((DA(I)+SDBG**2*DT(I)**2)/
        DT(I)**2)*P**2
```

(This is the criterion for elimination of data values
from calculation.)

```
                    THEN
                    BEGIN
                        IF W(I) LESSEQ O
                        THEN
                        X:=X
                        ELSE
                        BEGIN
                            W(I):=O;
                                X:=X-1;
                        END;
                    END
                    ELSE
                    BEGIN
                        V:=O;
                        IF W(I) LESSEQ O
                        THEN
                        BEGIN
                            W(I):=Z(I);
                                X:=X+1;
                                V:=V+1;
                        END
                        ELSE
```

```
            BEGIN
                W(I):=Z(I);
                    X:=X;
            END;
        END;
    END;
    IF Q LESSEQ 1 THEN GOTO MESS;
    IF X NOTEQ Y THEN GOTO MESS;
    IF V GR O THEN GOTO MESS
    ELSE
    FOR K:=1 STEP 1 UNTIL M DO
    PRINT £FINAL A?,SAMELINE,SPECIAL(1),
    DIGITS(1),SCALED(4),K,£1S?,SPECIAL(2),
    AC(K),£ST.ERR.1S?,SD(K),££L??;
    END;
FOR I:=1 STEP 1 UNTIL N DO
BEGIN
    IF W(I) GR O
    THEN
    PRINT SCALED (5),T(I),SAMELINE,££S1??,
    A(I),££S1??,FO(I),££L??
    ELSE
    PRINT £ REJECT POINT?,SAMELINE,££S1??,
    SCALED(5),T(I),££S1??,A(I),££S1??,FO(I),
    ££L??;
END;
GOTO FIN;
ERR: PRINT £MATRIX INVERSION-NO SOLUTION?;
FIN: PRINT £END?;
    END;
END;
```

3.4. Treatment of Experimental Data

Prior to a least-squares analysis of decay data, the background count of the counting equipment was subtracted from the observed activities. The analysis was made on the assumption that chemical purification procedures reduced contamination to a negligible extent.

3.4(a) Zirconium

Decay data for zirconium sources were not normally recorded until after a state of transient equilibrium had been attained between zirconium-97 and niobium-97. The data also contained contributions from zirconium-95 and its radioactive daughter products. However, analyses based on the assumption that the observed activity was caused solely by decay of zirconium-97 and -95 and their daughter products, proved unsatisfactory. This was attributed to poor statistics in the activity readings recorded after ten half-lives of zirconium-97 had elapsed. The data were therefore analysed assuming the activity to be caused by a single component with a constant background; the error introduced was considered to be negligible as the half-life of zirconium-95 is several times greater than that of zirconium-97 and the computed background activity was about 1% of the initial activity attributed to zirconium-97 and its daughters.

3.4(b) Molybdenum

Decay data for molybdenum sources were recorded after a state of transient equilibrium had been reached between molybdenum-99 and technetium-99m. The data were analysed assuming the observed activity to be caused by decay of molybdenum-99 and technetium-99m with a constant background. The computed background activities were very small thus showing the sources to be free of contamination.

3.4(c) Xenon

It was noticed that analyses of decay data for xenon samples, based on the assumption that only xenon-133 and -135 caused the observed activities, were unsatisfactory particularly for data recorded soon after the isolation of the xenon. This was attributed to traces of short-lived krypton isotopes (4.4 hr krypton-85m, 1.96 hr krypton-83m), which remained in the gas-stream after purification in the gas-solid chromatography section. The contamination was small but caused erroneous results from least squares analyses although it was not observed in analyses performed by the subtraction method.

To minimize contributions from short-lived krypton isotopes, only data recorded later than forty-eight hours after the end of the irradiation were used in the analyses.

It has been suggested[3] that there will be
appreciable contributions from xenon-133m in the decay
curves. This was not considered to be a serious source
of error because of the low calculated independent yields
of xenon-133 and -133m and also because of the small
branching ratio of xenon-133m to xenon-133 from iodine-133.
However, several sets of decay data were tested for a
contribution from xenon-133m.

The decay data were considered to result from the
following decay schemes.
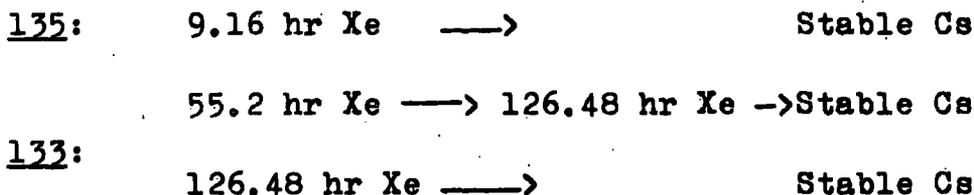
135:     9.16 hr Xe   ——>   Stable Cs

         55.2 hr Xe ——> 126.48 hr Xe ->Stable Cs
133:
         126.48 hr Xe ——>   Stable Cs

To minimize contributions from short-lived krypton
isotopes, only data recorded later than forty-eight hours
after the end of irradiation were used in the analyses;
the counter efficiency for xenon-133m was estimated with
the aid of information from the Nuclear Data Sheets[4]
to be about 0.8 times that of xenon-133.

The calculated activity of xenon-133m was very low
relative to that of xenon-133 and normally within one
standard   error   of its computed activity; the

contribution from xenon-133m was therefore ignored in analysing the decay data of xenon samples.

Xenon samples recovered from irradiated uranium were analysed for xenon-133 and -135 only; those recovered from irradiated thorium were analysed for xenon-133, -135 and radon-222 and its daughters.

3.4(d) Iodine

Decay data for samples recovered after a long "cooling" period (4 days) were analysed for contributions from iodine-131, -132 and -133. Contributions from xenon-131m and -133m were shown by calculation to be negligible. The decay schemes were hence simplified to the following:

<u>131</u>: 193.44 hr I $\longrightarrow$ Stable Xe

<u>132</u>: 2.28 hr I $\longrightarrow$ Stable Xe

<u>133</u>: 20.8 hr I $\longrightarrow$ 126.48 hr Xe $\longrightarrow$ Stable Cs

Analyses based on the above assumptions were satisfactory and in good agreement with those carried out by a graphical method. The graphical method is outlined below.

After sufficient time has elapsed so that contributions from iodine-132 can be ignored (i.e. after ten half-lives of iodine-132), the observed activity is caused by iodine-131, -133 and xenon-133.

The decay may be represented by the following equation.

$$A(t) = A_{I131}^{o} \cdot \exp(-\lambda_{I131} \cdot t)$$

$$+ A_{I133}^{o} \cdot (\exp(-\lambda_{I133} \cdot t) + \frac{\lambda_{Xe133}}{\lambda_{I133} - \lambda_{Xe133}} \cdot \frac{C_{Xe133}}{C_{I133}} \cdot$$

$$(\exp(-\lambda_{Xe133} \cdot t) - \exp(-\lambda_{I133} \cdot t)))$$

where $A(t)$ is the total activity at time t; $A^{o}, \lambda, C,$ are the activity at the time of precipitation of the palladium iodide sample, the decay constant and the counting efficiency for the nuclide indicated by the subcript.

The equation may be rearranged by dividing throughout by $\exp(-\lambda_{I131} \cdot t)$.

$$\frac{A(t)}{\exp(-\lambda_{I131} \cdot t)} = A_{I131}^{o} +$$

$$A_{I133}^{o} (\frac{\exp(-\lambda_{I133} \cdot t)}{\exp(-\lambda_{I131} \cdot t)} + \frac{\lambda_{Xe133}}{\lambda_{I133} - \lambda_{Xe133}} \cdot \frac{C_{Xe133}}{C_{I133}} \cdot$$

$$\frac{1}{\exp(-\lambda_{I131} \cdot t)} \cdot (\exp(-\lambda_{Xe133} \cdot t) - \exp(-\lambda_{I133} \cdot t)))$$

A straight line of slope A_{I133}^{o} and intercept A_{I131}^{o} should be obtained when

$$\frac{A(t)}{\exp(-\lambda_{I131} \cdot t)}$$

is plotted against

$$\left(\frac{\exp(-\lambda_{I133} \cdot t)}{\exp(-\lambda_{I131} \cdot t)} + \frac{\lambda_{Xe133}}{\lambda_{I133} - \lambda_{Xe133}} \cdot \frac{C_{Xe133}}{C_{I133}} \cdot \frac{1}{\exp(-\lambda_{I131} \cdot t)} \cdot\right.$$

$$\left(\exp(-\lambda_{Xe133} \cdot t) - \exp(-\lambda_{I133} \cdot t))\right).$$

After calculating A^o_{I131} and A^o_{I133} by this method, the initial activity of iodine-132 was determined, after subtracting calculated contributions of iodine-131 and -133 from the observed activity readings, by extrapolation of the residual activity values to the iodine separation time.

Decay data for iodine samples isolated after a short "cooling" period (5-30 minutes) were impossible to analyse completely when the analysis was based on the following decay schemes.

<u>133</u>: 20.8 hr I ⟶ 126.48 hr Xe ⟶ Stable

<u>134</u>: 0.88 hr I ⟶ Stable

<u>135</u>: 6.75 hr I ⟶ 0.26 hr Xe ⟶ 9.16 hr Xe ⟶ Stable
6.75 hr I ⟶ 9.16 hr Xe ⟶ Stable

The contribution from the 0.26 hr xenon-135m in transient equilibrium with iodine-135 was calculated to increase the counter efficiency for iodine-135 by about 4%. The decay scheme for mass-135 was therefore simplified to the following form:

6.75 hr I ⟶ 9.16 hr Xe ⟶ Stable

Only data, recorded after a state of transient equilibrium between iodine-135 and xenon-135m had been reached, were used in the analyses.

The anomalies observed in this system are discussed in detail in chapter 5.

<u>REFERENCES - CHAPTER 3</u>

1. W.E. Wentworth, Journal of Chemical Education, <u>42</u>(2), 96 (1965).

2. J.K. Brookhouse, Algol paper tape library scheme, Dept. of Applied Statistics, University of Reading.

3. J.H. Forster, N.T. Porile and L. Yaffe, Can. J. Chem., <u>44</u>, 2951 (1966).

4. Nuclear Data Sheets, National Academy of Sciences, National Research Council, Washington.

5. W.E. Deming, Statistical Adjustment of Data, 168 (Dover Publications, Inc. New York, 1964).

CHAPTER 4

Treatment of Results

4.1. Introduction

Radiochemical data, obtained experimentally by the methods outlined in the previous chapters, require the application of certain corrections.

(i) Corrections are made to account for variation in the neutron flux during the irradiation.

(ii) Allowance is made for decay of the precursors of the nuclide under observation during the irradiation and during the period between the end of the irradiation and the time when the nuclide is isolated.

(iii) Corrections are applied to allow for the independent yields of members of the decay chain under investigation.

4.2. Variation in neutron flux

Consider an irradiation of duration T, after which the nuclide is isolated at time t' after the end of the irradiation. At time t', the amount of the separated nuclide will depend on the fraction of its precursors that have decayed to the nuclide and also on the fraction of the nuclide that has not decayed.

4.2(a). Short-lived precursors

In the simplest example, the half-lives of the precursors are so short relative to the separation time (t') that the decay-chain may be considered to begin at the separated nuclide. In this instance, the nuclide may be considered to be produced throughout the irradiation at an irregular rate, dependent only on the neutron flux.

At time t after the beginning of the irradiation, the number of nuclei of nuclide 1'produced in the time interval dt is given by

$$dN_1 = B.Y_1.Z_1.\phi(t).dt$$

where B is an irradiation constant and contains such factors as the number of target nuclei and the total fission cross-section of the target. Y_1 is the cumulative fission yield of the mass-chain of which the separated nuclide is a member. Z_1 is a correction term to allow for the independent yields of the isobaric members following the separated nuclide in the decay chain; $\phi(t)$ is the neutron flux at time t.

If the neutron flux is monitored with an instrument of efficiency η, then the relationship between the absolute neutron flux and the monitored reading , I(t), is given by

$$\phi(t) = I(t)/\eta$$

Hence

$$dN_1 = \frac{B}{\eta} \cdot Y_1 \cdot Z_1 \cdot I(t) \cdot dt$$

which reduces to

$$dN_1 = K \cdot Y_1 \cdot Z_1 \cdot I(t) \cdot dt$$

where K is a constant peculiar to the irradiation.

The nuclei produced during the irradiation will decay with a characteristic half-life so that the number of nuclei originally produced at time t and remaining at the end of the irradiation is given by

$$dN_1 = K \cdot Y_1 \cdot Z_1 \cdot I(t) \cdot \exp(-\lambda_1 \cdot (T-t)) \cdot dt$$

The total number of nuclei remaining at the end of the irradiation will then be

$$N_1 = \int_{t=o}^{t=T} K \cdot Y_1 \cdot Z_1 \cdot I(t) \cdot \exp(-\lambda_1 \cdot (T-t)) \cdot dt \quad \ldots(1)$$

and, at time t' after the end of the irradiation, the number is given by

$$N_1(t') = \exp(-\lambda_1 \cdot t') \cdot \int_{t=o}^{t=T} K \cdot Y_1 \cdot Z_1 \cdot I(t) \cdot \exp(-\lambda_1 \cdot (T-t)) \cdot dt \quad \ldots(2)$$

When the neutron flux is constant, as it may be assumed to be within a nuclear reactor, the expressions (1) and (2) may be solved so that

$$N_1 = K.Y_1.Z_1.I.(1-\exp(-\lambda_1.T))/\lambda_1$$

at the end of the irradiation, and

$$N_1(t') = K.Y_1.Z_1.I.(1-\exp(-\lambda_1.T)).\exp(-\lambda_1.t')/\lambda_1$$

at time t' after the end of the irradiation.

When the neutron flux is varying, the variation in fissioning rate can be corrected for by the summation

$$\sum_{t=o}^{t=T} I(t).\exp(-\lambda_1.(T-t)).\delta t$$

provided the time interval δt, at which the neutron flux is monitored, is short relative to the half-life of the nuclide under observation.

Then,

$$N_1 = K.Y_1.Z_1.\sum_{t=o}^{t=T} I(t).\exp(-\lambda_1.(T-t)).\delta t$$

at the end of the irradiation, and

$$N_1(t') = K.Y_1.Z_1.\exp(-\lambda_1.t').\sum_{t=o}^{t=T} I(t).\exp(-\lambda_1.(T-t)).\delta t$$

at time t'.

If the nuclide 1 is isolated at time t' and quantitatively determined, the number of atoms at the end of the irradiation may be obtained by extrapolation.

When the quantity of the isolated nuclide is compared with that of the reference nuclide, the relative yield, Y_1/Y_R is given by

$$\frac{Y_1}{Y_R} = \frac{N_1}{N_R} \cdot \frac{Z_R}{Z_1} \cdot \frac{(1-\exp(-\lambda_R \cdot T))/\lambda_R}{(1-\exp(-\lambda_1 \cdot T))/\lambda_1}$$

for a constant flux, and by

$$\frac{Y_1}{Y_R} = \frac{N_1}{N_R} \cdot \frac{Z_R}{Z_1} \cdot \frac{\sum\limits_{t=o}^{t=T} I(t) \cdot \exp(-\lambda_R \cdot (T-t)) \cdot \delta t}{\sum\limits_{t=o}^{t=T} I(t) \cdot \exp(-\lambda_1 \cdot (T-t)) \cdot \delta t}$$

for a varying flux.

The summations to correct for variation in the fissioning rate will be denoted by the symbol S in the following sections of this chapter.

4.2(b). One long-lived precursor

When one of the precursors has a long half-life relative to the separation time (t'), the number of nuclide 1 isolated at time t' is dependent on the half-life of the precursor. $N_1(t')$ then is given by

$$N_1(t')= \frac{\lambda_2}{-\lambda_2+\lambda_1} \cdot K.Y_1.Z_1.I. \left(\exp(-\lambda_2 \cdot t') \cdot (1-\exp(-\lambda_2 \cdot T))/\lambda_2 \right.$$

$$\left. -\exp(-\lambda_1 \cdot t') \cdot (1-\exp(-\lambda_1 \cdot T))/\lambda_1 \right)$$

for a constant flux, and

$$N_1(t')= \frac{\lambda_2}{-\lambda_2+\lambda_1} \cdot K.Y_1.Z_1.(\exp(-\lambda_2 \cdot t').S_2-\exp(-\lambda_1 \cdot t').S_1)$$

for a varying flux.

Subscripts 1 and 2 refer to the isolated nuclide and long-lived precursor in the decay chain; this may be represented by

$$2 \xrightarrow{\lambda_2} 1 \xrightarrow{\lambda_1}$$
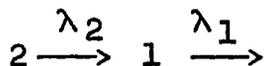
The fission yield relative to that of the reference nuclide is then given by

$$\frac{Y_1}{Y_R} = \frac{N_1(t').Z_R.(1-\exp(-\lambda_R.T))}{N_R.Z_1.(\exp(-\lambda_2.t').(1-\exp(-\lambda_2.T))/\lambda_2 - \exp(-\lambda_1 t').(1-\exp(-\lambda_1.T))/\lambda_1) \lambda_2/(\lambda_1+\lambda_2)}$$

for a constant flux, and

$$\frac{Y_1}{Y_R} = \frac{N_1(t')}{N_R}.\frac{Z_R}{Z_1}.\frac{S_R}{(\exp(-\lambda_2 t').S_2 - \exp(-\lambda_1 t').S_1) \lambda_2/(\lambda_1+\lambda_2)}$$

for a varying flux.

4.2(c). Two long-lived precursors

When two of the precursors of the isolated nuclide have relatively long half-lives, $N_1(t')$ is given by

$$N_1(t') = K.Y_1.Z_1.I.(C_3.\exp(-\lambda_3 t').(1-\exp(-\lambda_3.T))/\lambda_3 + C_2.\exp(-\lambda_2.t')(1-\exp(-\lambda_2.T))/\lambda_2 + C_1.\exp(-\lambda_1.t').(1-\exp(-\lambda_1.T))/\lambda_1)$$

for a constant flux, and

$$N_1(t') = K.Y_1.Z_1.(C_3.\exp(-\lambda_3.t').S_3 + C_2.\exp(-\lambda_2.t').S_2 + C_1.\exp(-\lambda_1.t').S_1)$$

for a varying flux. Subscripts 1, 2 and 3 refer
to the isolated nuclide and its long-lived precursors
as represented below.

$$3 \xrightarrow{\lambda_3} 2 \xrightarrow{\lambda_2} 1 \xrightarrow{\lambda_1}$$
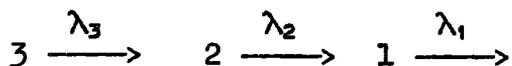
C_1, C_2, C_3 are the Bateman coefficients for the
decay scheme, given by

$$C_3 = \frac{\lambda_3 \cdot \lambda_2}{(\lambda_2 - \lambda_3)(\lambda_1 - \lambda_3)}$$

$$C_2 = \frac{\lambda_2 \cdot \lambda_3}{(\lambda_3 - \lambda_2)(\lambda_1 - \lambda_2)}$$

$$C_1 = \frac{\lambda_2 \cdot \lambda_3}{(\lambda_3 - \lambda_1)(\lambda_2 - \lambda_1)}$$

The fission yield for the mass-chain containing
nuclide 1 relative to that for the reference nuclide
is then given by

$$\frac{Y_1}{Y_R} = \frac{N_1(t')}{N_R} \cdot \frac{Z_R}{Z_1} \cdot \frac{(1-\exp(-\lambda_R \cdot T))}{\begin{array}{l}(C_3 \cdot \exp(-\lambda_3 \cdot t') \cdot (1-\exp(-\lambda_3 \cdot T))/\lambda_3 + \\ C_2 \cdot \exp(-\lambda_2 \cdot t') \cdot (1-\exp(-\lambda_2 \cdot T))/\lambda_2 + \\ C_1 \cdot \exp(-\lambda_1 \cdot t') \cdot (1-\exp(-\lambda_1 \cdot T))/\lambda_1)\end{array}}$$

for a constant flux, and

$$\frac{Y_1}{Y_R} = \frac{N_1(t')}{N_R} \cdot \frac{Z_R}{Z_1} \cdot \frac{S_R}{(C_3 \cdot S_3 \cdot \exp(-\lambda_3 \cdot t') + C_2 \cdot S_2 \cdot \exp(-\lambda_2 \cdot t') + C_1 \cdot S_1 \cdot \exp(-\lambda_1 \cdot t'))}$$

for a varying flux.

The expressions hold for relatively simple decay-schemes in which the isolated nuclide is formed by only one mechanism. If the nuclide is formed from several sources, the expression for correcting the experimental data becomes more complex.

The nuclide may be formed from several sources as illustrated below.

Fission $\xrightarrow{\quad x \quad\quad\quad\quad\quad\quad\quad\quad}$ Nuclide 1

Fission $\xrightarrow{\quad y \quad}$ Nuclide 2 $\longrightarrow$ Nuclide 1

Fission $\xrightarrow{\quad z \quad}$ Nuclide 3 $\longrightarrow$ Nuclide 2 $\longrightarrow$ Nuclide 1

where x, y, z are the fraction of fission events for the mass-chain that may be considered to give rise to nuclides 1, 2, 3 respectively. Factor x will be determined by the independent yield of nuclide 1 and any short-lived precursors that decay to nuclide 1 by a route that bypasses nuclides 2 and 3; y is determined by the independent yields of nuclide 2 and any short-lived precursors that decay to nuclide 2 by a route that bypasses nuclide 3; z is determined by the independent

yields of nuclide 3 and any short-lived precursors
that decay directly to nuclide 3.

For the decay scheme as illustrated, the number
of atoms of nuclide 1 isolated at time t', is given by

$$N_1(t') = K.Y_1.Z_1.I.[x.\exp(-\lambda_1.t')(1-\exp(-\lambda_1.T))/\lambda_1 +$$

$$y. \frac{\lambda_2}{-\lambda_1+\lambda_2} .(\exp(-\lambda_2.t')(1-\exp(-\lambda_2.T))/\lambda_2 - \exp(-\lambda_1.t')(1-\exp(-\lambda_1.T))/\lambda_1) +$$

$$z.(C_3.\exp(-\lambda_3.t')(1-\exp(-\lambda_3.T))/\lambda_3 + C_2.\exp(-\lambda_2.t')(1-\exp(-\lambda_2.T))/\lambda_2$$

$$+ C_1.\exp(-\lambda_1.t')(1-\exp(-\lambda_1.T))/\lambda_1)]$$

for a constant flux. An analogous expression can be deduced
for a varying flux.

The equations for calculating relative yields are also
modified to allow for the independent yields of the precursors
of the isolated nuclide. The correction factors in the
calculations to allow for the independent yields of the
precursors, the variation in the neutron flux and the
independent yields of the members of the decay chain following
the isolated nuclide have been collected together into one
correction factor("Irradiation factor" in Chapter 6).

The number of nuclei of the reference nuclide and of
the nuclide under observation were calculated from the activity
attributed to the relevant nuclide. The number of nuclei of
nuclide 1 is given by

$$N_1 = \frac{A_1}{\lambda_1.C_1}$$

where A_1 is the activity; λ_1 is the decay-constant;
C_1 is the efficiency of the detecting equipment for
nuclide 1.

4.3. Estimation of independent yields

It has been found that the Equal Charge
Displacement Hypothesis of Glendenin, Coryell and
Edwards[1] is in good agreement with observed charge
distributions resulting from fission induced at low to
moderate excitation energies. Steinberg and Glendenin[2]
found evidence from the thermal neutron fission of
uranium-235, uranium-233, plutonium-239 and the
spontaneous fission of curium-242 and californium-252
in agreement with the predictions of the hypothesis.
The results of Wahl[3] for the yields from neutron-
induced fission of uranium-235 at 14-MeV and those of
Alexander and Coryell[4] for the yields from fission
induced in thorium-232 by 13.6-MeV deuterons and neutrons
of moderate energy also show agreement.

It is only at excitation energies in excess of
about 30-MeV that deviations from the predictions of the
hypothesis have been observed. Therefore, this hypothesis
can with reasonable accuracy be expected to predict the
independent yields resulting from 3- and 14-MeV neutron-
induced fission of uranium-238 and thorium-232.

The Equal Charge Displacement Hypothesis may be written as

$$Z_A - Z_p = Z_A^* - Z_p^*$$

where Z_A, Z_A^* are the most stable charges for complementary fission-product chains and Z_p, Z_p^* are the most probable charges for the primary fission fragments A and A^*. The sum of the primary charges must be equal to the charge of the fissioning nucleus, Z_f, so that

$$Z_p + Z_p^* = Z_f$$

and the complementary fission-fragment masses are related by

$$A + A^* = A_f - \bar{\nu}$$

where A_f is the mass of the fissioning nucleus and $\bar{\nu}$ is the average number of neutrons emitted per fission event leading to these products.

In the treatment of Glendenin, Coryell and Edwards[1], the most probable charge is calculated on the assumption that the distribution rule holds for the fission fragments after emission of prompt-neutrons. The most probable charge is then given by

$$Z_p = Z_A - \tfrac{1}{2}(Z_A + Z_A^* - Z_f)$$

Values of Z_A are calculated using the Bohr-Wheeler Mass-Equation[5] which does not take account of shell-effects.

Pappas[6] has introduced modifications into the original theory; in his treatment, the most probable charge is calculated on the assumption that the distribution rule holds for the fission fragments before prompt-neutron emission. The most probable charge is then given by

$$Z_p = Z_{(A+n)} - \tfrac{1}{2}(Z_{(f-A-n)} + Z_{(A+n)} - Z_f)$$

where $Z_{(A+n)}$ is the most probable charge for any mass chain A, $Z_{(f-A-n)}$ is the most probable charge for the complementary fragment, n is the average number of neutrons emitted by the ~~heavy~~ fragment.

The method by which Pappas estimates the most probable charge is based on the treatment of β-stability by Coryell[7]. The resulting charge functions show discontinuities near shell edges; for mass numbers near to shell edges two possible values of Z_A occur. Steinberg and Glendenin[2] suggest that the average value be used.

It has been suggested[8] that corrections should be made to Z_p for shell effects. The resulting function does not completely agree with the empirical Z_p function determined by Wahl[9].

The method of Pappas[6] has been applied throughout in this work. The treatment requires a knowledge of the average number of prompt neutrons emitted by each primary fragment. Such data are available for only a few fissioning systems[10]. However, the average total number of prompt neutrons has been measured for the systems under investigation; values of 2.86[11] and 4.75[12] for 3.1-MeV and 14.8-MeV neutron-induced fission of uranium-238, and 2.42[12] and 4.43[12] for 3.6-MeV and 14.9-MeV neutron-induced fission of thorium-232 have been reported.

Since the data for thorium-232 correspond closely to those for uranium-238 at each neutron energy, it has been assumed that the average number of neutrons emitted by the heavy fragment for thorium-232 is the same as that for uranium-238 at each neutron energy. Cuninghame[13] and Ames et al[14] have shown that the average number of neutrons emitted by the heavy fragment during neutron-induced fission of uranium-238 at 14-MeV is approximately three; this value has been adopted for the fission of thorium-232 at this neutron energy. Information has not been found relating to the number of prompt neutrons emitted by the heavy fragment for either nuclide at 3-MeV; a value of one has been assumed.

The values for $Z_A^{(6)}$ given by Pappas have been used. After calculating the most probable charge, the independent yields were found from the charge distribution curve of Pappas[6].

The estimated independent yields for the members of the mass-chains investigated in this work are given in Table 4.1. The simplified decay schemes for the mass-chains and the fraction of chain considered to originate at each nuclide are shown in Figure 4.1; mass-chain 133 has been simplified in the manner of Katcoff and Rubinson[15], and the fractions quoted for the fission of uranium-235 induced by thermal neutrons are the values either calculated (for mass-chain 133) or experimentally determined (for independent yield of xenon-135) by them.

	(i)	(0.82)	(0.18)
<u>131</u>:	23minSb ⟶	25 min Te⟶	193.44hr I ⟶ Stable

	(i)	(0.95)	(0.05)
<u>132</u>:	77.7hr Te ⟶	2.28hr I ⟶	Stable

	(v)	(0.75)	(0.25)
	(iv)	(0.80)	(0.20)
	(iii)	(0.70)	(0.30)
	(ii)	(0.82)	(0.18)
	(i)	(0.74)	(0.26)
<u>133</u>:	52min Te ⟶	20.8hr I ⟶	126.48hr Xe ⟶ Stable

	(i)	(.76)	(.22)	(.02)
<u>134</u>:	43.2minTe ⟶	52.8min I⟶	Stable

	(v)	(0.96)	(0.04)
	(iv)	(1.00)	(0)
	(iii)	(0.85)	(0.15)
	(ii)	(1.00)	(0)
	(i)	(0.93)	(0.07)
<u>135</u>:	6.75hr I ⟶	9.16 hr Xe ⟶	Stable

(i) Uranium-238 (14-MeV neutron fission).

(ii) Uranium-238 (3-MeV neutron fission).

(iii) Thorium-232 (14-MeV neutron fission).

(iv) Thorium-232 (3-MeV neutron fission).

(v) Uranium-235[15] (thermal neutron fission).

FIG. 4.1. Simplified decay-schemes.

Table 4.1.

Independent yields calculated by Pappas' method[6]

Mass A	Charge Z	Fraction of chain			
		Uranium-238		Thorium-232	
		3-MeV	14-MeV	14-MeV	3-MeV
131	49	–	0.05	–	–
	50	–	0.31	–	–
	51	–	0.46	–	–
	52	–	0.18	–	–
132	50	–	0.18	–	–
	51	–	0.46	–	–
	52	–	0.31	–	–
	53	–	0.05	–	–
133	50	0.30	0.10	0.06	0.24
	51	0.46	0.40	0.34	0.47
	52	0.18	0.40	0.44	0.24
	53	0	0.10	0.15	0.02
134	51	–	0.26	–	–
	52	–	0.48	–	–
	53	–	0.22	–	–
	54	–	0.02	–	–
135	51	0.40	0.15	0.06	0.34
	52	0.40	0.44	0.34	0.44
	53	0.10	0.34	0.44	0.15
	54	0	0.07	0.15	0
97	⩽ 40	1.00	1.00	1.00	0.99
	41	0	0	0	0.01
99	⩽ 42	1.00	1.00	1.00	1.00

REFERENCES – CHAPTER 4

1.	L.E. Glendenin, C.D. Coryell and R.R. Edwards,
	Phys. Rev., 75, 337 (1949).

2.	E.P. Steinberg and L.E. Glendenin, Proceedings of
	the U.N. International Conference on the
	Peaceful Uses of Atomic Energy, 7, P/614 (1956).

3.	A.C. Wahl, Phys. Rev., 99, 730 (1955).

4.	J.M. Alexander and C.D. Coryell, Phys. Rev.,
	108, 1274 (1957).

5.	N. Bohr and J.A. Wheeler, Phys. Rev., 56, 426 (1939).

6.	A.C. Pappas, Proceedings of the U.N. International
	Conference on the Peaceful Uses of Atomic Energy
	7, P/881 (1956).

7.	C.D. Coryell, Ann. Rev. Nuc. Sci., 2, 305 (1953).

8.	T.J. Kennett and H.G. Thode, Phys. Rev.,
	103, 323 (1956).

9.	A.C. Wahl, J. inorg. nucl. Chem., 6, 263 (1958).

10.	J. Terrell, Phys. Rev., 127, 880 (1962).

11.	R. Sher and J. Leroy, Reactor Science, J. Nucl. Energ.
	Part A, 12, 101 (1960).

12.	H. Condé and N. Starfelt, Nucl. Sci. Eng., 11, 397
	(1961).

13.	J.G. Cuninghame, J. inorg. nucl. Chem., 5, 1 (1957).

14.	D.P. Ames, J.P. Balagna, J.W. Barnes, A.A. Comstock,
	G.A. Cowan, P.B. Elkin, G.P. Ford, J.S. Gilmore,
	D.C. Hoffman, G.W. Knobeloch, E.J. Lang,
	M.A. Melnick, C.O. Minkkinen, B.D. Pollock,
	J.E. Sattizah, C.W. Stanley and B. Warren,
	Los Alamos Scientific Lab. Report LA-1997 (1956).

15.	S. Katcoff and W. Rubinson, Phys. Rev., 91, 1458
	(1953).

CHAPTER 5

An Investigation of the Decay Chain of Mass-135

5.1. Introduction

Because of the difficulties encountered during resolution of the decay data from iodine samples recovered after short "cooling" periods, several experiments were devised and implemented to ascertain the cause of the anomalies.

(It is interesting to note that other workers[1] have obtained low values for the cumulative fission yield of mass-135 when basing their measurements on iodine isotopes.)

Close inspection of the experimental data indicated that perhaps the decay systematics of decay chain 135 could be in error. Resolution of experimental data recorded later than sixty hours after zero time and subtraction of the computed activities of iodine-133 and -135 from the total decay data, revealed a component with a half-life of 5 to 7 hours. This component was observed in the decay data of every iodine sample prepared from iodine isolated after a short "cooling" period even when the most stringent precautions were taken in the purification procedures.

Further, it was found that the cumulative fission yield of mass-135 calculated from the computed activity of iodine-135 was about 30% lower than that calculated from xenon measurements.

Experiments were therefore performed to check the decay scheme of mass chain 135.

5.2. Half-life of precursor of xenon-135

To test the proposition that xenon-135 may be produced by a circuitous route and not directly from 6.75 hr iodine-135, an experiment was devised whereby the radioactive xenon daughters were removed periodically from a solution containing iodine isotopes and quantitatively determined. This allowed the half-life of the precursor of xenon-135 to be calculated; an internal check was provided by the decay of iodine-133 to xenon-133.

Experimental Procedure

1. An iodine sample was separated from irradiated uranyl nitrate and purified as described previously in Chapter 2; the final form of the iodine sample was chosen as sodium iodide in sodium sulphite solution, thus minimizing retention of xenon as oxygenated compounds.

2. The iodine sample was placed in the dissolver vessel (see section 2.4(d)) and air passed through the solution for three minutes. A carrier amount of inactive xenon was measured out and condensed in the dissolver vessel.

3. Xenon was quantitatively removed from the vessel eleven hours after the zero time for growth of xenon isotopes. This was effected by passing a stream of air through the liquid for two minutes. The xenon sample was purified and

quantitatively determined in a gas Geiger-counter.

4. A second carrier amount of xenon was added to the vessel and step 3 was repeated.

5. A third carrier amount of xenon was added after removal of the second sample and step 3 was repeated.

The results of the above experiment are shown in Table 5.1. Within experimental error the half-lives of the precursors of xenon-133 and -135 were found to agree with the accepted values of 20.8 hr and 6.75 hr respectively (see Figure 5.1.).

The results suggest that xenon-135 is produced only by decay of 6.75 hr iodine-135 with the possibility of a short-lived intermediate.

5.3. Short-lived Xenon-135m

An experiment was devised to check the half-life and decay-systematics of short-lived xenon isotopes of mass-135.

An iodine solution was prepared as described in section 5.2. The solution was placed in the apparatus illustrated in Figure 5.2 and allowed to stand for about one hour.

A stream of argon was then passed through the solution, through the cold-trap at -90°C where iodine and water vapour were retained, and into the charcoal chamber. The charcoal previously outgassed in vacuo at 200°C, was cooled by means

Table 5.1. Results of xenon "milking" experiment.

Separation time (hrs)*	Counter number	Recovery yield	Computed activity at sepn. time		Counter efficiency rel. to counter 1		Activity (corrected for recovery yield)		Activity (corrected for efficiency for relative to counter 1)	
			133	135	133	135	133	135	133	135
11.00	2	0.575	9.31×10^2	1.96×10^4	0.919	0.937	1.62×10^3	3.41×10^4	1.76×10^3	3.64×10^4
22.00	3	0.548	6.11×10^2	5.86×10^3	0.928	0.931	1.11×10^3	1.07×10^4	1.20×10^3	1.15×10^4
33.00	1	0.568	4.84×10^2	2.04×10^3	1.000	1.000	8.52×10^2	3.59×10^3	8.52×10^2	3.59×10^3

* The separation time is measured from the zero time for growth of xenon isotopes for the first "milking".

Activity

$t_{\frac{1}{2}} = 6.8$ hr.

$t_{\frac{1}{2}} = 20.9$ hr.

Separation Time (hrs)

FIG. 5.1.   Half-lives of precursors of Xenon-133 and
           -135.

Argon in

Iodine solution

1 mg/cm² Mylar window

Cold trap (-90°C)

Proportional counter

Screw clips

Activated charcoal

Polythene

Brass rod
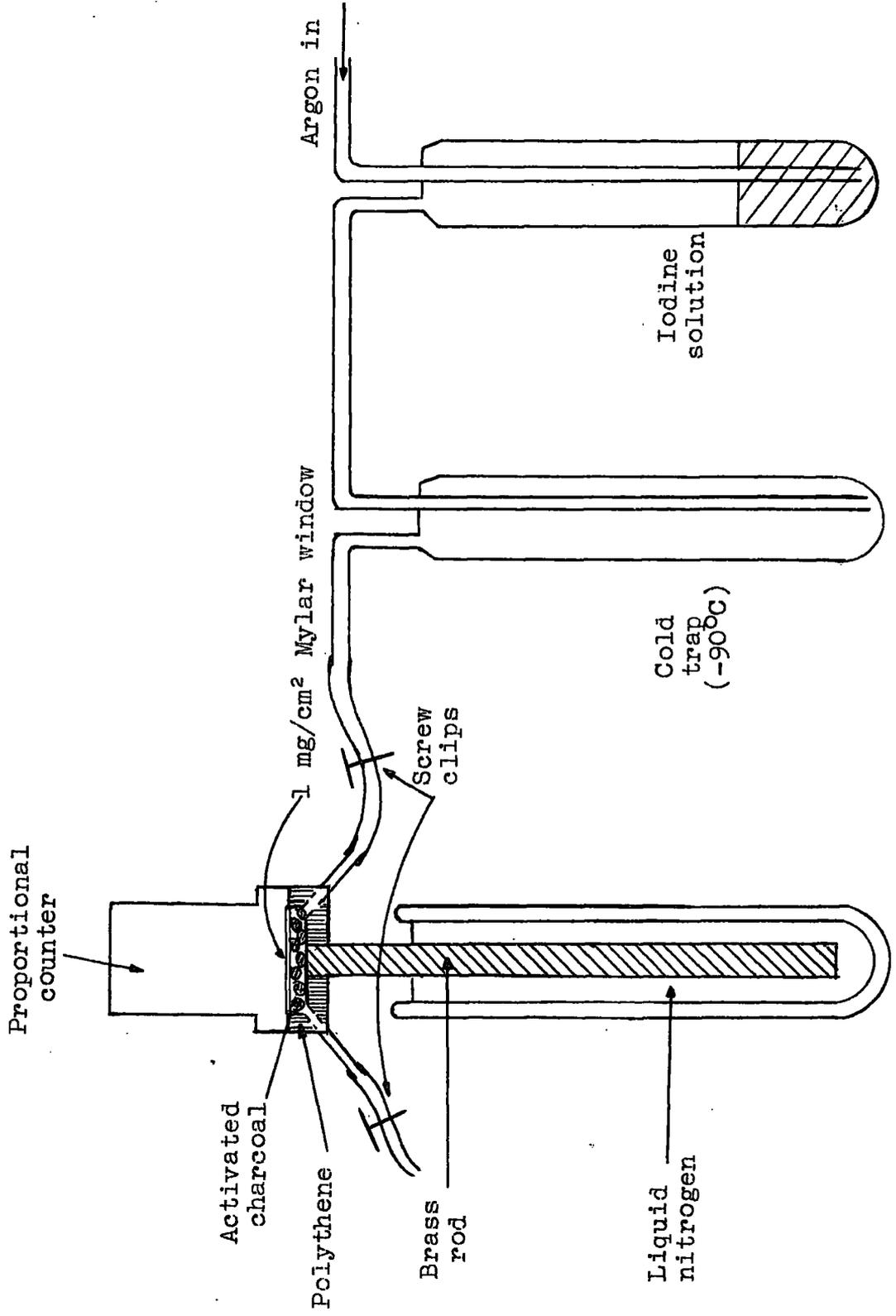
Liquid nitrogen

FIG. 5.2. Apparatus to study short-lived xenon isotopes.

of a brass rod cooled in liquid nitrogen. The xenon

isotopes, adsorbed on the charcoal, were detected by an

end-window gas-flow β-proportional counter. The amplifier

of the counting equipment was connected to a multi-channel

analyser (Laben 512) and to a scaler so that both the

spectrum of the pulses from the counter and the decay of

the xenon sample could be observed.

The experiment did not reveal any isotopes other than

those reported in the literature. Figure 5.3 shows a

typical decay curve. It was not possible to obtain information

about the decay-systematics of xenon-135m from the spectrum

of the pulses from the counter. (A pulse from a counter of the

type used is not always proportional to the energy of the

β-particle causing the pulse).

5.4. Diffusion of Xenon from Palladium Iodide Sources

Other workers[2] showed that diffusion of xenon from

palladium iodide and silver iodide sources was negligible

even at elevated temperatures and in vacuo.

Because an explanation for the anomalous experimental

results had not been found, it was decided to check that

diffusion was in fact negligible. A simple experiment was

carried out whereby a palladium iodide source was prepared

and placed in a closed system containing air at atmospheric

pressure and at room temperature. Several hours later

carrier xenon was added to the system, removed after five
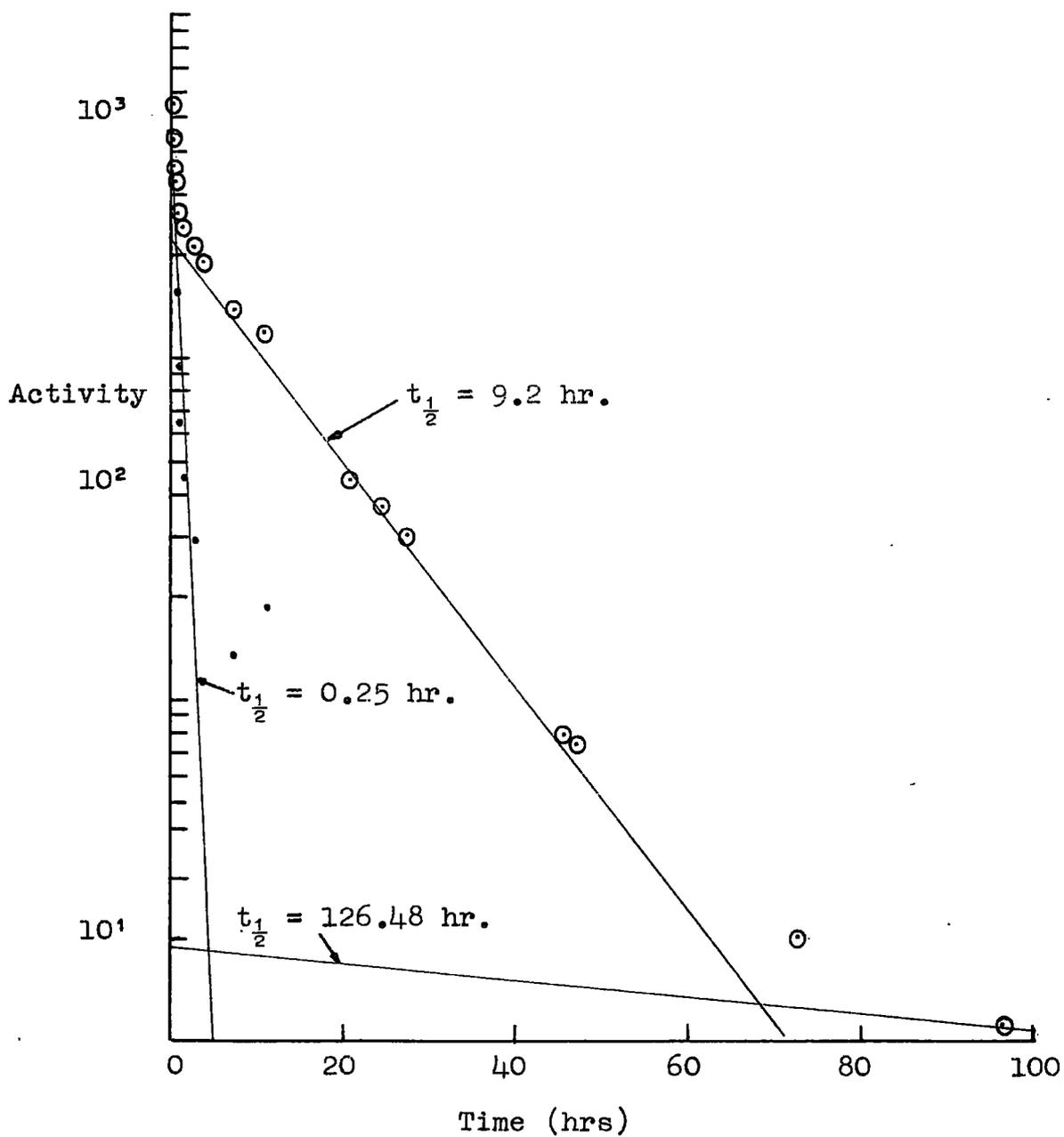
FIG. 5.3. Xenon decay-curve.

minutes, purified and counted. Appreciable activity
was found in the recovered xenon sample although an
estimate of the rate of diffusion could not be made.

A second experiment was effected whereby a
palladium iodide source was dissolved in a closed system
several hours after its preparation and the xenon in the
sample was quantitatively determined. It was found that
the cumulative fission-yield of mass-135 calculated from
the results of the above experiment was about 20% lower
than that calculated from direct xenon measurements.

Hence, it appears that there is appreciable diffusion
of xenon from palladium iodide sources. (The diffusion of
xenon-133 will not critically affect the resolution of data
from iodine samples recovered after long "cooling" periods
as the contribution from xenon-133 is small because of its
low β-energy and long half-life.) Although this may not be
the full explanation for the anomalous results, it will
cause erroneous resolution of experimental data.

Time did not allow further investigations to be
carried out and hence no attempt has been made to calculate
the cumulative fission yield of mass-135 from iodine
measurements. Data, recorded immediately after preparation
of the sources from iodine isolated after a short "cooling"
period, were analysed for contributions from iodine-134 and
a component of half-life of ten hours; it was then possible

to obtain a value for the initial activity of iodine-134. Inspection of data for sources containing iodine-133 and -135 showed that, for data recorded up to fifteen hours after the precipitation of palladium iodide, the activity decreased with an apparent half-life of about ten hours. The uncertainty in the computed activity of iodine-134 was therefore estimated to be only about 10%.

REFERENCES - CHAPTER 5

1. R. Ganapathy, Tin Mo and J.L. Meason, J. inorg. nucl. Chem., $\underline{29}$, 257 (1967).

2. S. Katcoff, C.R. Dillard, H. Finston, B. Finkle, J.A. Seiler and N. Sugarman, Radiochemical Studies: The Fission Products Book 2, P/141 (McGraw-Hill Co., New York, 1951).

CHAPTER 6

Collected Results

6.1. Introduction

The results obtained during the course of the present work are reported in this chapter. Where an error is quoted, it is the standard deviation given by

$$\sigma = \sqrt{\frac{\sum_{i=1}^{n} d_i^2}{(n-1)}}$$

where d_i is the residual between the mean value and the actual value of the ith result; n is the total number of results.

6.2. Calibration of gas Geiger-counters

Normally two counters were calibrated from any one irradiated sample of uranium oxide so that, even when absolute calibration could not be made, the efficiencies of the counters were intercompared.

Three counters were calibrated; the results are set out in Tables 6.1, 6.2 and 6.3. The value obtained for the cumulative fission yield of mass-97 is in good agreement with the values of other workers[1,3,4,5], thus giving confidence in the Bayhurst method of calculating the counter efficiency for zirconium-97 and molybdenum-99.

TABLE 6.1. Fission of uranium-235 induced by Thermal neutrons.

Xenon

Irradn. number	Separation time (hrs)	Irradn. factor 133	Irradn. factor 135	Counter number	Recovery yield	Computed at sepn. 133	activity time 135	Counter efficiency relative to counter 1 — 133	Counter efficiency relative to counter 1 — 135	c_{133}/c_{135}
1	23.75	0.171	0.101	1	0.401	6.40×10^2	4.64×10^3	1.000	1.000	1.096
				2	0.384	5.81×10^2	4.27×10^3	0.949	0.961	1.081
2	24.02	0.173	0.100	1	0.563	9.67×10^2	6.91×10^3	1.000	1.000	1.088
				2	0.108	1.68×10^2	1.21×10^3	0.906	0.913	1.080
3	29.33	0.193	0.080	1	0.340	1.29×10^3	6.12×10^3	1.000	1.000	1.175
				3	0.091	3.21×10^2	1.51×10^3	0.930	0.922	1.185
4	29.00	0.192	0.077	1	0.507	1.42×10^3	7.01×10^3	1.000	1.000	1.093
				3	0.273	7.07×10^2	3.55×10^3	0.925	0.940	1.074
5	35.00	0.210	–	1	0.407	6.20×10^4	–	1.000	–	–
				2	0.200	2.75×10^4	–	0.903	–	–
6	20.80	0.157	0.115	3	0.432	6.80×10^2	6.07×10^3	–	–	1.104

Table 6.2. - Calibration of counter 1.

Reference nuclides (zirconium-97, molybdenum-99).

Irradiation number	Irradiation factor		Recovery yield		Computed activity at zero time		Counter efficiency		Y97/Y99	$\frac{Y133 \times C133}{Y99}$
	97	99	97	99	97	99	97	99		
1	0.343	0.346	0.361	0.434	7.90×10^3	1.25×10^3	0.719	0.357	0.970	0.759
2	"	"	0.561	0.403	1.39×10^4	1.33×10^3	0.706	0.358	0.979	0.706
3	"	"	0.398	0.291	6.52×10^5	6.20×10^4	0.716	0.356	0.983	0.795
Mean Values:									0.977 ± 0.005	0.754 ± 0.037

From the literature: $Y99 = 6.25 (1)$, $Y133 = 6.62 (2)$,

$Y135 = 6.45 (2)$; therefore $Y97 = 6.11 \pm 0.03$ and

$C133 = 0.712 \pm 0.035$.

TABLE 6.3.

Counter number	C133/C135 (Mean Value)	Counter efficiency relative to counter 1 (Mean Values)		Counter efficiency	
		133	135	133	135
1	1.113	1.000	1.000	0.712	0.640
2	1.080	0.919	0.937	0.654	0.600
3	1.121	0.928	0.931	0.661	0.596

Table 6.4.

3-MeV neutron-induced fission of uranium-238

Reference nuclides (zirconium-97, molybdenum-99).

Irradiation number	Irradiation factor		Recovery yield		Computed activity at zero time		Counter efficiency		$\frac{Y97}{Y99}$
	97	99	97	99	97	99	97	99	
1	0.903	0.917	0.394	0.505	4.05×10^3	6.74×10^2	0.717	0.342	0.951
2	1.176	1.194	0.423	0.272	5.35×10^3	4.93×10^2	0.715	0.357	0.902
3	1.857	1.885	0.518	0.424	7.07×10^3	7.78×10^2	0.708	0.347	0.943

Xenon

Irradn. number	Sepn. time (hrs.)	Irradiation factor		Counter number	Recovery yield	Computed activity at sepn. time		Counter efficiency		$\frac{Y133}{Y135}$	$\frac{Y133}{Y99}$	$\frac{Y135}{Y99}$
		133	135			133	135	133	135			
1	20.03	0.411	0.316	(1 3	0.513 0.190	4.43×10^2 1.58×10^2	4.25×10^3 1.48×10^3	0.712 0.661	0.640 0.596	0.995 1.022	1.315 1.364	1.322 1.335
2	18.00	0.496	0.442	(1 2	0.104 0.293	1.04×10^2 2.77×10^2	1.30×10^3 3.10×10^3	0.712 0.654	0.640 0.600	0.885 1.009	1.263 1.300	1.427 1.288
3	17.83	0.776	0.703	3	0.505	4.73×10^2	5.50×10^3	0.661	0.596	0.970	1.234	1.272
4	18.67	0.684	0.584	1	-	3.9×10^1	4.47×10^2	0.712	0.640	0.925	-	-

Mean values: $Y97/Y99 = 0.932 \pm 0.026$, $Y133/Y99 = 1.295 \pm 0.050$,

$Y135/Y99 = 1.329 \pm 0.060$, $Y133/Y135 = 0.968 \pm 0.053$.

Table 6.6.

14-MeV neutron-induced fission of uranium-238

Reference nuclide (molybdenum-99)

Irradiation number	Irradiation factor	Recovery yield	Computed activity at zero time	Counter efficiency
1	24.57	0.512	3.49×10^4	0.342
2	89.44	0.584	2.56×10^4	0.337
3	67.00	0.230 0.178	1.03×10^4 8.21×10^3	0.361 0.365

Iodine

Irradiation number	Sepn. time (hrs)	Pptn. time (hrs)	Recovery yield	Irradiation factor			Computed activity at pptn. time			Counter efficiency			$\frac{Y131}{Y99}$	$\frac{Y132}{Y99}$	$\frac{Y133}{Y99}$
				131	132	133	131	132	133	131	132	133			
1	72.85	1.00	0.215	19.01	0.368	2.255	$.42 \times 10^3$	4.79×10^3	4.93×10^3	0.310	0.357	0.357	0.685	0.968	1.132
2	90.93	0.75	0.633	64.84	1.140	4.480	$.37 \times 10^3$	7.78×10^3	4.94×10^3	0.263	0.352	0.354	0.624	0.904	1.082
3	89.42	1.50	0.164	48.84	0.867	3.509	$.87 \times 10^2$	1.44×10^3	1.32×10^3	0.318	0.357	0.357	0.610	0.892	1.147

Mean values: Y131/Y99 = 0.640 ± 0.040, Y132/Y99 = 0.921 ± 0.041,

Y133/Y99 = 1.120 ± 0.034.

Table 6.7.

14-MeV neutron-induced fission of uranium-238

Reference nuclide (molybdenum-99)

Irradiation number	Irradiation factor	Recovery yield	Computed Activity at zero time	Counter efficiency
1	1.000	0.370	3.54×10^2	0.350
2	1.000	0.342	6.86×10^2	0.352
3	1.000	0.413	1.94×10^2	0.348

Iodine-134

Irradiation number	Sepn. time (hrs)	Pptn. time (hrs)	Irradiation factor	Recovery yield	Computed activity at pptn. time	Counter efficiency	$\dfrac{Y134}{Y99}$
1	0.23	0.40	0.324	0.599	1.24×10^4	0.353	1.282
2	0.13	0.87	0.275	0.283	6.94×10^3	0.355	1.154
3	0.18	0.40	0.299	0.494	4.91×10^3	0.354	1.258

Mean value: $Y134/Y99 = 1.231 \pm 0.068$.

Table 6.8.

3-MeV neutron-induced fission of thorium-232

Reference nuclide (zirconium-97, molybdenum-99)

Irradiation number	Irradiation factor		Recovery yield		Computed activity at zero time		Counter efficiency		$\frac{Y97}{Y99}$
	97	99	97	99	97	99	97	99	
1	0.306	0.313	0.594	0.648	3.31×10^3	2.69×10^2	0.704	0.334	1.660
2	0.458	0.473	0.338	0.443	1.25×10^3	1.25×10^4	0.720	0.346	1.658
3 ‡	0.744	–	0.563	–	2.63×10^2	–	0.706	–	–
4	0.654	0.673	0.284	0.468	3.54×10^2	4.5×10^1	0.724	0.344	1.615

Xenon

Irradiation number	Sepn. time (hrs)	Irradiation factor		Recovery yield	Counter number	Counter efficiency		Computed activity at sepn. time		(Radon 222)	$\frac{Y133}{Y135}$	$\frac{Y133}{Y99}$	$\frac{Y135}{Y99}$
		133	135			133	135	133	135				
1	20.07	0.143	0.107	0.631	3	0.661	0.596	1.66×10^2	2.75×10^3	6.06×10^2	0.562	1.329	2.365
2	20.50	0.220	0.157	0.536	3	0.661	0.596	1.27×10^2	1.38×10^3	1.8×10^1	0.818	1.792	2.191
3 ‡	18.33	–	0.277	0.731	2	0.654	0.600	–	2.58×10^3	–	–	–	2.115
4	20.28	0.310	0.226	0.622	3	0.661	0.596	5.2×10^1	5.67×10^2	7.5×10^1	0.832	1.863	2.239

Mean values: $Y97/Y99 = 1.644 \pm 0.026$, $Y133/Y99 = 1.661 \pm 0.290$, $Y135/Y99 = 2.228 \pm 0.105$; $Y133/Y135 = 0.737 \pm 0.152$.

‡ The cumulative fission yield of mass-135 relative to that of mass-99 has been calculated using the mean value of $Y97/Y99$ (1.644). Because of deterioration of the Geiger-action of the gas counter, it was not possible to collect sufficient data to allow analysis for radon-222, xenon-133 and -135 to be made. The data were therefore analysed for xenon-135 and a component with a half-life of 110 hours; this value for the half-life was chosen after inspection of other decay curves.

Table 6.9.

14-MeV neutron-induced fission of thorium-232

Reference nuclides (zirconium-97, molybdenum-99)

Irradiation number	Irradiation factor		Recovery yield		Computed activity at zero time		Counter efficiency		$\frac{Y97}{Y99}$
	97	99	97	99	97	99	97	99	
1‡	1.257	-	0.621	-	1.58×10^4	-	0.702	-	-
2	2.220	2.203	0.493	0.384	7.24×10^3	4.88×10^2	0.710	0.350	1.469
3	0.958	0.951	0.452	0.195	7.44×10^3	3.14×10^2	0.713	0.363	1.344
4	1.239	1.232	0.558	0.661	1.01×10^4	9.69×10^2	0.706	0.333	1.504
5	1.415	1.404	0.453	0.243	3.02×10^4	1.45×10^3	0.713	0.360	1.455
6	0.560	0.558	0.580	0.229	5.64×10^3	2.21×10^2	0.705	0.367	1.361
7	0.711	0.709	0.396	0.527	1.59×10^3	1.98×10^2	0.717	0.341	1.317

Xenon

Irradn. number	Sepn. time (hrs)	Irradiation factor		Recovery yield	Counter number	Computed activity at sepn. time			Counter efficiency		$\frac{Y133}{Y135}$	$\frac{Y133}{Y99}$	$\frac{Y135}{Y99}$
		133	135			133	135	(Radon) 222	133	135			
1‡	19.25	0.554	0.424	0.670	3	1.47×10^3	1.73×10^4	2.5×10^1	0.661	0.596	0.810	2.134‡	2.635‡
2	20.42	0.986	0.711	0.344	2	4.37×10^2	4.82×10^3	3.79×10^2	0.654	0.600	0.828	2.266	2.737
3	20.70	0.431	0.304	0.181	2	3.05×10^2	2.91×10^3	1.23×10^3	0.654	0.600	0.936	2.429	2.595
4	21.13	0.567	0.386	0.635	1	1.18×10^3	1.15×10^4	1.0×10^1	0.712	0.640	0.867	2.443	2.817
5	18.52	0.588	0.490	0.177 / 0.198	{ 1 / 2 }	1.10×10^3 / 1.12×10^3	1.33×10^4 / 1.37×10^4	-3.3×10^1 / 8.0×10^0	0.712 / 0.654	0.640 / 0.600	0.855 / 0.863	2.383 / 2.363	2.787 / 2.738

‡ The cumulative fission yields of mass-133 and -135 relative to that of mass-99 have been calculated using the mean value of Y97/Y99 (1.408).

Mean values: Y97/Y99 = 1.408 ± 0.077, Y133/Y99 = 2.336 ± 0.117, Y135/Y99 = 2.718 ± 0.087, Y133/Y135 = 0.860 ± 0.043.

6.3. Fission of uranium-238 induced by 3-MeV neutrons

Uranyl nitrate hexahydrate targets of six grams weight were irradiated for one hour, using the S.A.M.E.S. machine at Canterbury. Four experiments were carried out; three allowed absolute cumulative fission yields for mass-133 and -135 to be calculated and the fourth gave the cumulative fission yield of mass-133 relative to that of mass-135.

The results are set out in Table 6.4.

6.4. Fission of uranium-238 induced by 14-MeV neutrons

Samples, from which xenon-133 and -135 were determined, were prepared from a purified uranyl nitrate solution. The targets irradiated using the accelerator at Canterbury consisted of two grams of uranyl nitrate hexahydrate; the length of each irradiation was ten minutes. At Durham, sodium or ammonium polyuranate targets of six grams weight were irradiated for one hour.

Seven experiments were carried out to measure the xenon isotopes. The results are set out in Table 6.5; irradiations 1 to 5 were effected at Canterbury; the remaining two were carried out at Durham.

The targets, from which iodine isotopes were recovered, were prepared from analytical grade uranyl nitrate hexahydrate without purification. For

experiments carried out to determine the cumulative fission yields of mass-131, -132 and -133, compressed pellets of five grams of uranyl nitrate hexahydrate were irradiated for twenty minutes. For experiments carried out so that iodine isotopes could be recovered after a short "cooling" period, the target sample consisted of three grams of uranyl nitrate hexahydrate crystals contained in a polythene bag; the length of each irradiation was two minutes.

The results obtained are set out in Tables 6.6 and 6.7.

6.5. Fission of thorium-232 induced by 3-MeV neutrons

After partial purification of the thorium sample by repeated precipitation of barium sulphate from a thorium nitrate solution, thorium hydroxide was precipitated by the addition of aqueous ammonia. The precipitate was filtered, washed and dried.

Targets, each of four grams of purified thorium hydroxide, were irradiated for two hours using the S.A.M.E.S. machine. The recovered xenon samples always showed contamination attributed to radon-222 and its daughters.

Four irradiations were carried out; the results are set out in Table 6.8.

6.6. <u>Fission of thorium-232 induced by 14-MeV neutrons</u>

Thorium nitrate pellets were irradiated at Canterbury for ten minutes; the weight of the target was normally four grams. Results are set out in Table 6.9.

The data, recorded for recovered xenon samples, were analysed for contamination attributable to radon-222 and its daughters. Contamination was most noticeable in data recorded for irradiations 2 and 3. The target material for irradiations 1, 2 and 3 were prepared from unpurified thorium nitrate samples; the sample from which target 1 was made was different to that used in preparation of targets 2 and 3. Irradiations 4 and 5 were carried out using thorium nitrate targets prepared by evaporation of purified thorium nitrate solution; contamination was found to be very small in such samples.

REFERENCES - CHAPTER 6

1.   H. Farrar, H.R. Fickel and R.H. Tomlinson,
     Can. J. Phys., 40, 1017 (1962).

2.   H. Farrar and R.H. Tomlinson, Nuclear Physics,
     34, 367 (1962).

3.   W.H. Walker, Chalk River Report CRRP-913 (1960).

4.   S. Katcoff, Nucleonics, 18(11), 201 (1960).

5.   E.P. Steinberg and L.E. Glendenin, Proceedings of
     the U.N. International Conference on the
     Peaceful Uses of Atomic Energy, 7, P/614 (1956).

CHAPTER 7

Discussion

The results obtained during the course of this work are set out in Tables 7.1, 7.2, 7.3 and 7.4 together with those of other workers; all results have been adjusted using selected published values for absolute cumulative fission yield of mass-99[5,12,15] for the systems investigated.

As is seen from the tables, reasonable agreement between the data of other workers and of this work has been reached for the fission yields of mass-97. However, severe discrepancies exist for the fission yields of masses 131 - 135.

James, Martin and Silvester[7] obtained values for the fission yields of mass-131, -133 and -135 for 14-MeV neutron-induced fission of uranium-238. The values for mass-133 and -135 were obtained by determination of the xenon isobars of these mass-chains. It is interesting to note that their calculations are based on the assumptions that the decay chains for mass-133 and -135 begin at iodine-133 and -135 (i.e. the independent yield of the xenon isobar is assumed negligible) and that the counter efficiency of their gas Geiger-counter for xenon-135 is the same as that for xenon-133. If the experimental results obtained in this work are subjected to the treatment

Table 7.1. Neutron-induced fission of uranium-238 at 3-MeV

Cumulative fission yield (%)

Fragment mass	This work	Bunney et al[1]	Keller et al[2]	Levy et al[3]	Bonyushkin et al[4]
91	-	-	-	4.4	-
95	-	-	4.65	-	4.51
97	5.89	-	-	-	4.69
99*	6.32*	6.32*	6.32*	6.32*	6.32*
103	-	-	6.2	-	3.52
106	-	-	2.9	-	2.57
132	-	-	4.65	-	3.70
133	8.18	-	-	-	-
135	8.40	-	-	-	-
137	-	-	7.0	5.4	5.51
140	-	-	5.6	5.8	5.24
144	-	4.3	4.85	-	-
147	-	2.8	-	2.9	-
149	-	2.1	-	-	-

*Normalization point, $Y_{99} = 6.32\%$ [5]. (Interpolated)

Table 7.2.   Neutron-induced fission of uranium-238 at 14-MeV

Cumulative fission yield (%)

Fragment mass	This work	Bonyushkin et al(4)	Broom(6)	James et al(7)	Cuninghame(8)	Ames et al(9)	Protopopov et al(10)	Ganapathy and Ihochi(11)
90	–	–	3.55	–	–	–	–	–
91	–	–	2.71	–	2.83	–	3.7	–
93	–	4.15	–	3.61	–	–	–	–
95	–	–	–	–	–	–	5.3	–
97	5.40	4.42	–	5.24	–	4.8	5.8	–
99*	5.68*	5.68*	–	5.68*	5.68*	5.7	5.68*	5.68*
101	–	–	–	–	–	–	5.6	6.44
102	–	–	–	–	–	–	4.0	2.89
105	–	2.98	–	2.33	–	3.4	?	–
129	–	1.10	–	1.04	–	–	–	–
131	3.64	–	2.82	4.04	–	–	5.2	–
132	5.23	3.97	4.70	–	–	4.7	–	–
133	6.56	–	2.71	5.84	–	–	–	–
134	6.99	–	4.91	–	–	–	–	–
135	7.16	–	5.22	4.91	–	–	–	–
137	–	5.96	–	–	–	–	–	–
139	–	–	4.59	4.32	–	–	–	–
140	–	4.42	4.48‡	4.10	4.48	4.6	4.5	–
141	–	5.24	–	–	–	–	–	–
143	–	–	–	3.08	3.60	–	–	–
144	–	–	–	–	2.73	3.4	–	–
147	–	–	–	–	2.03	–	–	–

* Normalization point, Y99 = 5.68%(5).

‡ Normalization based on ratio Y99/Y140 = 1.265(8).

Table 7.3. Neutron-induced fission of thorium-232 at

3-MeV

Cumulative fission yield (%)

Fragment mass	This work	Iyer et al[12]	Wyttenbach et al[13]	Rahman[14]	Broom[15]	Kennett & Thode[16]
90	–	7.41	6.99	–	–	–
91	–	6.80	–	–	5.74	–
92	–	–	–	–	5.92	–
95	–	5.15	–	–	–	–
97	4.57	4.22	–	4.98	–	–
99*	2.78*	2.78*	2.78*	2.78*	2.78*	–
103	–	0.15	–	–	–	–
127	–	0.09	–	–	–	–
129	–	–	–	1.48	–	–
131	–	1.73	2.13	–	1.03	1.62
132	–	–	–	3.13	2.24	2.87
133	4.62	–	–	–	2.92	–
134	–	–	–	–	7.31	5.38
135	6.19	–	–	–	5.00	–
136	–	–	–	–	–	5.65
137	–	4.46	6.59	–	–	–
139	–	6.64	–	–	6.08	–
140	–	8.50	7.72	–	–	–
141	–	7.87	7.26	–	–	–
143	–	7.32	–	6.23	–	–
144	–	7.93	7.98	–	–	–
145	–	–	–	4.92	–	–
147	–	3.82	–	–	–	–
149	–	0.95	–	–	–	–

*Normalization point, Y99 = 2.78%[12].

Table 7.4. Neutron-induced fission of thorium-232 at

14-MeV

Cumulative fission yield (%)

Fragment mass	This work	Rahman[14]	Broom[15]	Vlasov et al[17]	Ganapathy and Kuroda[18]	Ganapathy and Ihochi[11]
90	–	–	5.72	–	–	–
91	–	–	5.52	5.10	–	–
92	–	–	5.58	–	–	–
95	–	–	–	6.57	–	–
97	2.76	2.92	–	–	–	–
99*	1.96*	1.96*	1.96*	1.96*	1.96*	1.96*
101	–	–	–	–	–	1.57
102	–	–	–	–	–	0.69
103	–	–	–	–	0.74	–
129	–	0.927	–	–	–	–
131	–	2.44	1.59	–	–	–
132	–	–	3.10	2.74	–	–
133	4.58	–	3.78	–	–	–
134	–	–	6.69	–	–	–
135	5.33	–	4.74	–	–	–
139	–	–	5.34	–	–	–
140	–	–	5.97	–	–	–
141	–	–	–	5.78	–	–
145	–	2.38	–	–	–	–

*Normalization point, Y_{99} = 1.96%[15].

of James et al.[7], the value for the fission yield of mass-133 relative to that of mass-135 is in good agreement with their value. The calibration of the gas-counter used by James et al. was based on the results of one experiment only; this may be the reason for their absolute fission yields being lower than those obtained from this work.

The agreement between the two sets of results lends confidence to the experimental method; the earlier work[7] was based on the irradiation of sealed solutions of uranyl nitrate, thus preventing loss of fissiogenic xenon, whereas the present work was based on the irradiation of solid samples with subsequent dissolution. Additional confidence is provided by the good agreement obtained between the value for the fission yield of mass-133 from xenon measurements and that from iodine measurements also carried out during the course of this work (see Table 7.5.).

The disagreement between the results of Broom[6,15] and those of this work is difficult to rationalize. However, it is interesting to note that values obtained by several other workers[7,10,12-14] for the fission yields of mass-131 and -132 are different to those of Broom, the results of the latter being appreciably the lower. Details are not given concerning the method employed by Broom to analyse his experimental data and, hence no explanation for the disparities can be suggested.

Table 7.5.

Cumulative fission yield relative to that of mass-99

Mass number	Nuclide measured	Uranium-238		Thorium-232	
		3-MeV	14-MeV	3-MeV	14-MeV
97	Zirconium-97	0.93±0.03	0.95±0.02	1.64±0.03	1.41±0.08
131	Iodine-131	–	0.64±0.04	–	–
132	Iodine-132	–	0.92±0.04	–	–
133	Iodine-133	–	1.12±0.03	–	–
133	Xenon-133	1.30±0.05	1.19±0.08	1.66±0.29	2.34±0.12
134	Iodine-134	–	1.23±0.07	–	–
135	Xenon-135	1.33±0.06	1.26±0.05	2.23±0.11	2.72±0.09

The value of James et al.[7] and that of this work
for the fission yield of mass-131 agree within
experimental error. The value obtained for the fission
yield of mass-134 must be imprecise as both the method
of analysing the decay data and the method of calculating
the independent yields of the members of the mass-chain
134 are susceptible to considerable uncertainties. For
mass-chains containing nuclides with stable nucleon
configurations, it has been suggested[20] that the Equal
Charge Distribution Hypothesis[21] will not apply. If
it is the case that nuclides with stable nucleon
configurations have unusually high independent yields,
then such abnormal yields will be expected for tin-132,
antimony-133, tellurium-134, iodine-135, xenon-136 and
caesium-137. The work of Wunderlich[19] supports this
view; his results show a high value for the independent
yield of iodine-135 from fission of uranium-235 induced by
thermal neutrons. On the other hand, the results of
Strom et al.[22] do not reveal high independent yields for
tin-132 or antimony-133. If such a mechanism is operative,
then the calculations for mass-chain 134 will be in error
by a greater amount than those for the other mass-chains
investigated; this is so because of the half-lives of the
members of the mass-chains. It is considered unlikely
that the uncertainty in the value for the fission yield of
mass-134 is greater than 30% (the uncertainty in the

activity is about 10% and the uncertainty estimated for errors in the charge distribution is put at 20%).

The absolute cumulative fission yields have been plotted together with results of other workers in Figures 7.1. - 7.4. The results of Wanless and Thode[23] for neutron-induced fission of uranium-238 at 0.5-MeV have been plotted on the same figure as the data for fission at 3-MeV.

The results of this work support the suggestion[24] that the irregularities in the cumulative mass-yield curves are lessened as the excitation energy of the fissioning system is increased; the fine structure apparent in the mass-yield curve for neutron-induced fission of uranium-238 at 3-MeV is greater than at 14-MeV and, whilst there is some fine structure in the mass-yield curve of thorium-232 at 3-MeV, it is not apparent at 14-MeV (cf. Broom[15]).

Fine structure in the mass-yield curves has been reported for virtually every system undergoing low-energy fission[7,25-33]. The extent of the fine structure appears to be greater for uranium and heavier elements than for the lighter elements. The mass-yield curves of the lighter elements - data for neutron-induced fission of thorium-229 at thermal energy[25] and of thorium-232 at 3- and 14-MeV have been collected - show only small irregularities. Uranium and heavier elements show large irregularities[26-33] and the fission yields of mass-chains in the mass-region
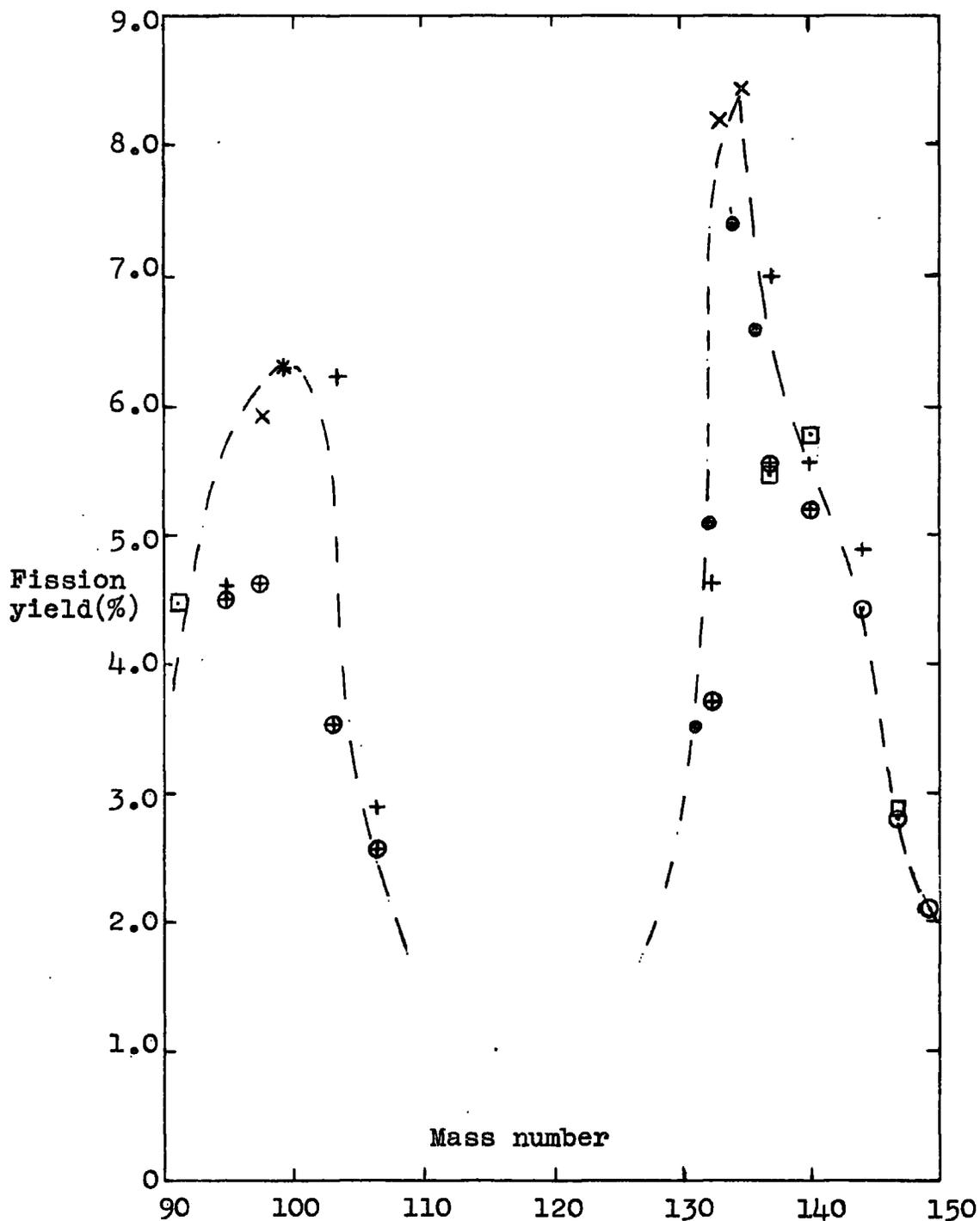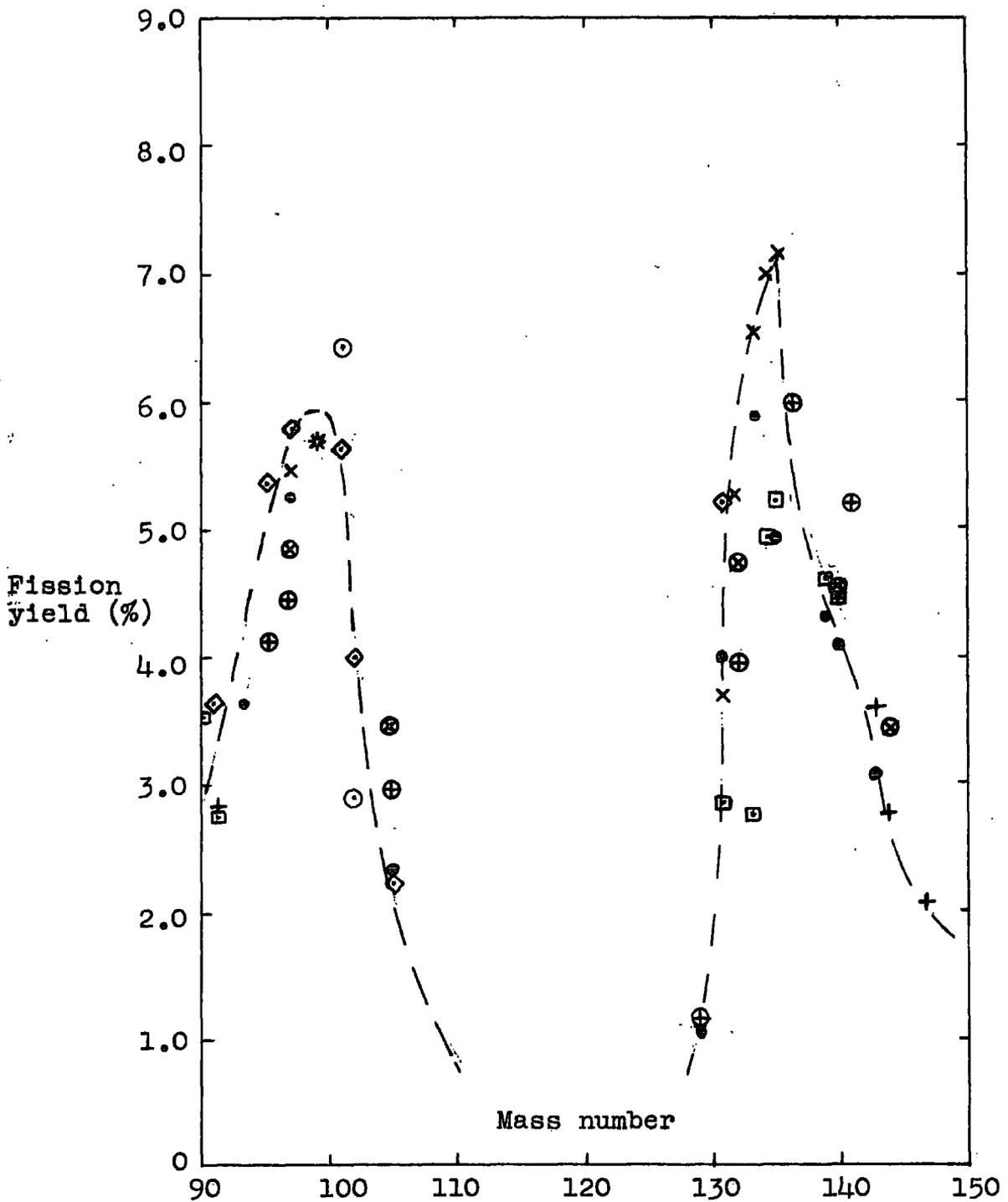
FIG. 7.1.   3-MeV neutron-induced fission of uranium-238.

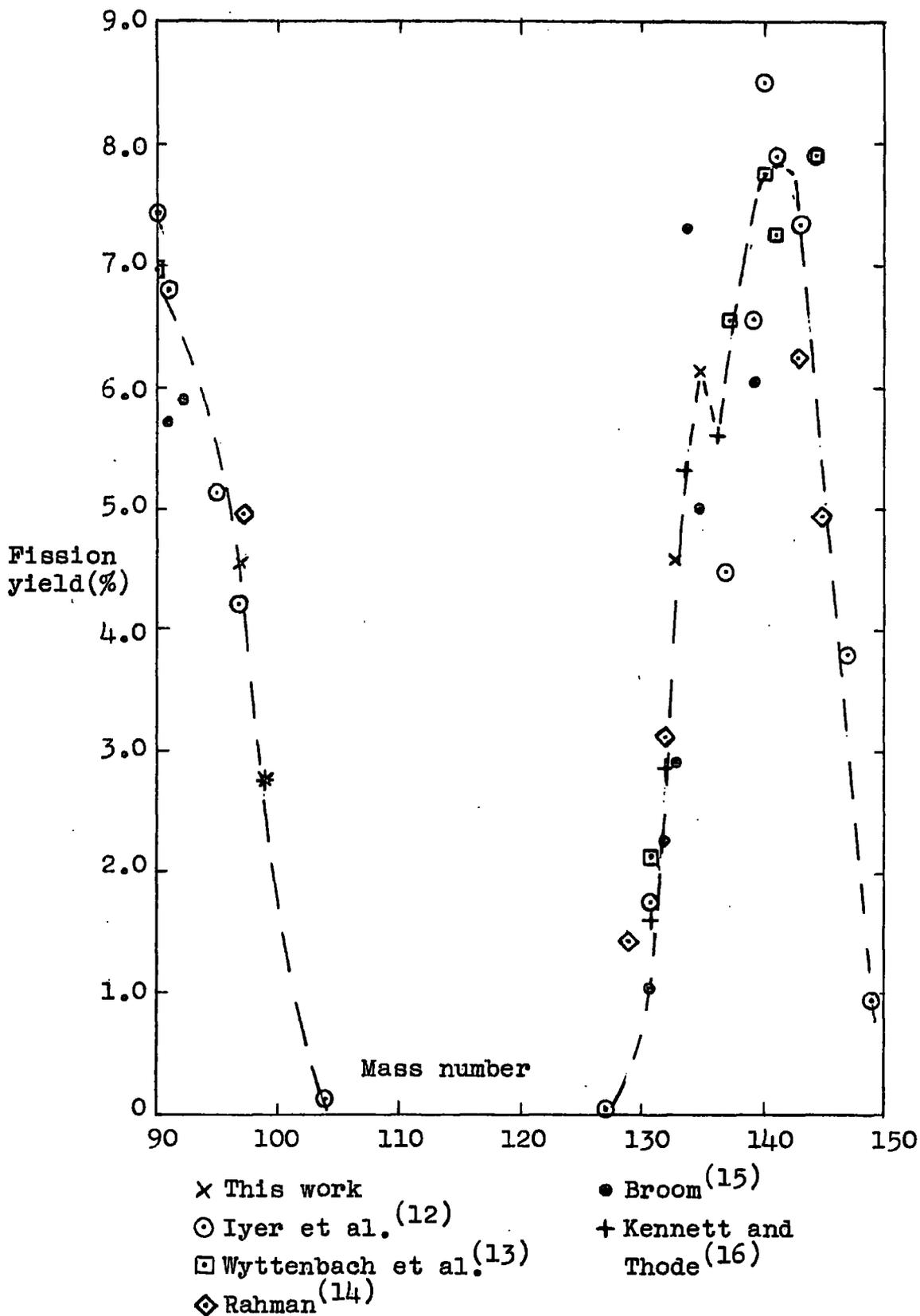FIG. 7.2.   14-MeV neutron-induced fission of
uranium-238.

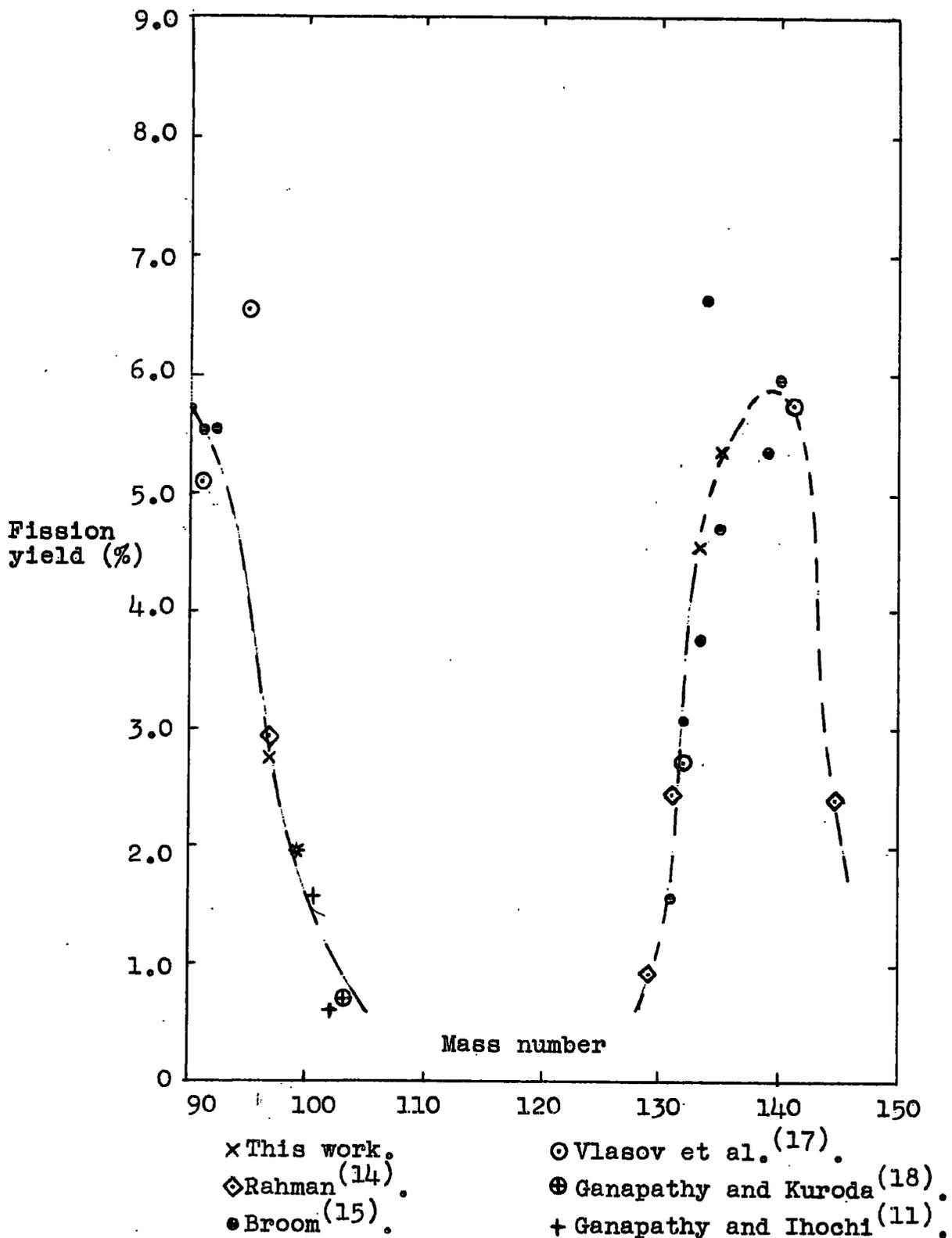FIG. 7.3. 3-MeV neutron-induced fission of thorium-232.

FIG. 7.4. 14-MeV neutron-induced fission of thorium-232.

where fine structure occurs are normally higher than those of any other mass-chain. This may be caused by a fundamental relationship between the fission processes and the mass and/or charge of the fissioning nucleus.

Why fine structure is prominent in the mass-yield curve from 14-MeV neutron-induced fission of uranium-238 and yet minimal in those of thorium-232 and uranium-235[34], again may be due to a relationship between the fission processes and the nature of the fissioning nucleus. Information relating to neutron-induced fission of other nuclides at 14-MeV is limited; data for fission of neptunium-237[35], protactinium-231[36] and plutonium-239[10] have been reported, but there is insufficient information about the fission yields of masses 131-135 to reveal the presence or absence of fine structure.

Two hypotheses have been proposed to explain the phenomenon of fine structure. That advanced by Glendenin[37], and modified by Pappas[38], suggests that it is caused by abnormal neutron-emission from fragments in which the neutron binding-energy is low due to neutron shell-effects. Such a hypothesis predicts abnormally low fission yields for mass-chains heavier than and adjacent to those exhibiting fine structure.

The hypothesis of Wiles[20] attributes fine
structure to a preferential formation during the
fissioning act of fragments with nuclei in which the
neutron binding-energy is high due to shell-effects.
A corollary of this hypothesis is the predicted presence
of fine structure in the fission yields of the complementary
fragments.

The results of this work support the latter hypothesis,
but with modifications. There is evidence[19] for the
preferential formation of fragments with stable nuclei.
There is also evidence[39] for fine structure in the
complementary fragments in the mass-yield curve for fission
induced in uranium-235 by thermal neutrons. Fine structure
at about mass-141 has been reported in the mass-yield curves
for the thermal-neutron fission of plutonium-241[28],
plutonium-239[27] and uranium-235[26]; fine structure among
the fragments complementary to mass-141 has been observed
for these systems[39-41]. Unfortunately, there is little
information relating to the fission yields of fragments
complementary to masses 131-135 for the systems investigated
in this work.

However, it is difficult to reconcile the presence of
fine structure in uranium and heavier elements and the
comparitive lack of it in lighter elements unless one
postulates that both primary fission fragments have an
effect on the extent of the fine structure. If such is the

case, fine structure would be expected to be more prominent in the mass-yield curves of nuclei, where fission can result in both primary fragments being stabilized by nuclear shell-effects, than in those where stabilization of only one fragment is possible.

The Nuclear Shell Model[42] predicts major discontinuities in nuclear properties at 2, 8, 20, 50, 82, 126 identical nucleons; it also predicts minor discontinuities at 14, 28, 40 identical nucleons. Faissner and Wildermuth[43] suggest that the completed major shell of 82 neutrons together with the completed major shell of 50 protons may be largely responsible for the high fission yields of nuclides containing these nucleon shells (i.e. around mass-132). It is interesting to speculate that the effect of a completed minor shell of forty protons may give rise to fine structure (Faissner and Wildermuth[43] also consider the completed minor shell of forty protons to have an important effect on the fission process). Fine structure would thus be expected to be particularly prominent in the mass-yield curves of nuclides where fission can result in a primary fragment containing ~82 neutrons (together with ~50 protons) and a complementary fragment containing ~40 protons. From a consideration of the Equal Charge Distribution Hypothesis[21], it is found that fragments

containing 82 neutrons normally have nuclear charges of 49 to 55. It would be expected, therefore, that nuclides with nuclear charge of 89 (49 + 40) to 95 (55 + 40) would exhibit prominent fine structure in their mass-yield curves at low excitation energy; nuclides of charge less than 89 or greater than 95 should exhibit less prominent structure. In this connection, it is interesting to note that the fine structure in the mass-yield curve for spontaneous fission of californium-252[33] (Z = 98) is less than in those of uranium-238[30] (Z = 92) and plutonium-240[31] (Z = 94).

It has been proposed[44] that the variation of neutron emission probability with fragment mass can largely account for fine structure. On the other hand, the work of Andritsopoulos[45] suggests that the major contribution to fine structure in the cumulative mass-yield curves is already present in the prompt mass-yield curves. The work of Apalin et al.[46] supports this suggestion; their results show only minor irregularities at masses 131-135 in the neutron-yield distribution from thermal fission of uranium-233, -235 and plutonium-239.

The extent of the fine structure increases as the mass of the fissioning nucleus increases, the charge remaining constant; this is noticeable for the neutron-induced fission of several elements (uranium-235[34] and

-238[7,this work] at 14-MeV, uranium-233[29] and -235[26] at thermal energies, plutonium-239[27] and -241[28] at thermal energies). The effect has been attributed[28] to the neutron to proton ratio being greater in the heavy isotope than in the light isotope thus causing the β-decay chains to be longer; hence, modification of the fine structure by emission of delayed neutrons can occur to a greater extent in the mass-yield curve of the heavy isotope[28].

In conclusion, it would appear that until more information of high precision is collected about the mass-yield curves, and about the fission process in general, one cannot reject any of the explanations that have been proposed to account for the phenomenon of fine structure. Collection of data relating to the cumulative fission yields of masses complementary to those where the effect is manifest is obviously desirable. It would also be interesting to investigate the extent of fine structure in elements lighter than uranium; protactinium appears the most interesting as the element is inter-mediate in nuclear charge between uranium and thorium.

REFERENCES - CHAPTER 7

1. L.R. Bunney, E.M. Scadden, J.O. Abriam and N.E. Ballou, Proceedings of the Second U.N. Conference on the Peaceful Uses of Atomic Energy, 15, P/643 (1958).

2. R.N. Keller, E.P. Steinberg and L.E. Glendenin, Phys. Rev., 94, 969 (1954).

3. H.B. Levy, H.G. Hicks, W.E. Nervik, P.C. Stevenson, J.B. Niday and J.C. Armstrong, Jr., Phys. Rev., 124, 544 (1961).

4. E.K. Bonyushkin, Yu. S. Zamyatin, I.S. Kirin, N.P. Martynov, E.A. Shvortsov and V.N. Ushatskii, Soviet Prog. in Neutron Physics, Part II, 164 (1961).

5. J. Terrell, W.E. Scott, J.S. Gilmore and C.O. Minkkinen, Phys. Rev., 92, 1091 (1953).

6. K.M. Broom, Phys. Rev., 126, 627 (1962).

7. R.H. James, G.R. Martin and D.J. Silvester, Radiochimica Acta, 3, 76 (1964).

8. J.G. Cuninghame, J. inorg. nucl. Chem., 5, 1 (1957).

9. D.P. Ames, J.P. Balagna, J.W. Barnes, A.A. Comstock, G.A. Cowan, P.B. Elkin, G.P. Ford, J.S. Gilmore, D.C. Hoffman, G.W. Knobeloch, E.J. Lang, M.A. Melnick, C.O. Minkkinen, B.D. Pollock, J.E. Sattizahn, C.W. Stanley and B. Warren, Los Alamos Scientific Lab. Report LA-1997 (1956).

10. A.N. Protopopov, G.M. Tolmachev, V.N. Ushatskii, R.V. Venediktova, I.S. Krisiuk, L.P. Rodionova and G.V. Iakoleva, Soviet Journal of Atomic Energy, 5, 963 (1958).

11. R. Ganapathy and H. Ihochi, J. inorg. nucl. Chem., 28, 3071 (1966).

12. R.H. Iyer, C.K. Mathews, N. Ravindran, K. Rengan, D.V. Singh, M.V. Ramaniah and H.D. Sharma, J. inorg. nucl. Chem., 25, 465 (1963).

13. A. Wyttenbach, H.R. von Gunten and H. Dulakas, Radiochimica Acta, 3, 118 (1964).

14. Md. M. Rahman, Ph.D. Thesis (Durham University, 1965).

15. K.M. Broom, Phys. Rev., 133, B874 (1964).

16. T.J. Kennett and H.G. Thode, Can. J. Phys., 35, 969 (1957).

17. V.A. Vlasov, Yu. A. Zysin, I.S. Kirin, A.A. Lbov, L.I. Osyaeva and L.I. Sel'chenkov, Soviet Prog. in Neutron Physics, Part II, 172 (1961).

18. R. Ganapathy and P.K. Kuroda, J. inorg. nucl. Chem., 28, 2071 (1966).

19. F. Wunderlich, Radiochimica Acta, 7, 105 (1967).

20. D.R. Wiles, B.W. Smith, R. Horsley and H.G. Thode, Can. J. Phys., 31, 419 (1953).

21. C.D. Coryell, L.E. Glendenin and R.R. Edwards, Phys. Rev., 75, 337 (1949).

22. P.O. Strom, D.L. Love, A.E. Greendale, A.A. Delucchi, D. Sam and N.E. Ballou, Phys. Rev., 144, 984 (1966).

23. R.K. Wanless and H.G. Thode, Can. J. Phys., 33, 541, (1955).

24. I. Halpern, Ann. Rev. Nuc. Sci., 9, 245 (1959).

25. J.W. Harvey, W.B. Clarke, H.G. Thode and R.H. Tomlinson, Can. J. Phys., 44, 1011 (1966).

26. H. Farrar and R.H. Tomlinson, Nuclear Physics, 34, 367 (1962).

27. H.R. Fickel and R.H. Tomlinson, Can. J. Phys., 37, 926 (1959).

28. H. Farrar, W.B. Clarke, H.G. Thode and R.H. Tomlinson, Can. J. Phys., 42, 2063 (1964).

29. D.R. Bidinosti, D.E. Irish and R.H. Tomlinson, Can. J. Chem., 39, 628 (1961).

30. H. Menke and G. Herrmann, Radiochimica Acta, 6, 76 (1966).

31. J.B. Laidler and F. Brown, J. inorg. nucl. Chem., 24, 1485 (1962).

32. E.P. Steinberg and L.E. Glendenin, Phys. Rev., 95, 431 (1954).

33. L.E. Glendenin and E.P. Steinberg, J. inorg. nucl. Chem., 1, 45 (1955).

34. A.C. Wahl, Phys. Rev., 99, 730 (1955).

35. R.F. Coleman, B.E. Hawker and J.L. Perkin, J. inorg. nucl. Chem., 14, 8 (1960).

36. M.G. Brown, S.J. Lyle and G.R. Martin, Radiochimica Acta, 6, 16 (1966).

37. L.E. Glendenin, Phys. Rev., 75, 337 (1949).

38. A.C. Pappas, Laboratory for Nuclear Science, M.I.T., Technical Report No. 63 (Sept. 1953).

39. H. Farrar, H.R. Fickel and R.H. Tomlinson, Can. J. Phys., 40, 1017 (1962).

40. H.R. Fickel and R.H. Tomlinson, Can. J. Phys., 37, 916 (1959).

41. H. Farrar and R.H. Tomlinson (reported in reference 28).

42. R.D. Evans, The Atomic Nucleus, 363 (McGraw-Hill Co., 1955).

43. H. Faissner and K. Wildermuth, Nuclear Physics, 58, 177 (1964).

44. H. Farrar and R.H. Tomlinson, Can. J. Phys., 40, 943 (1962).

45. G. Andritsopoulos, Nuclear Physics, A94, 537 (1967).

46. V.F. Apalin, Yu. N. Gritsyuk, I.E. Kutikov, V.I. Lebedev and L.A. Mikaelian, Nuclear Physics, 71, 553 (1965).